Interference Issues in Cognitive Radio Networks

By

Atif Elahi

Reg. No. 40-FET/PHDEE/F10

Supervised By

Prof. Dr. Ijaz Mansoor Qureshi

A dissertation submitted to I.I.U. in partial fulfillment of the requirements for the degree of

DOCTOR OF PHILOSOPHY

Department of Electrical Engineering
Faculty of Engineering and Technology
INTERNATIONAL ISLAMIC UNIVERSITY
ISLAMABAD

2017

DEDICATED TO

My Teachers,

Parents,

Wife, Kid,

Sisters and Brothers

CERTIFICATE OF APPROVAL

Title of Thesis: Interference Issues in Cognitive Radio Networks

Name of Student: Atif Elahi

Registration No: 40-FET/PHDEE/F10

Accepted by the Department of Electrical Engineering, Faculty of Engineering and Technology, International Islamic University, Islamabad, in partial fulfillment of the requirements for the Doctor of Philosophy Degree in Electronic Engineering.

Viva voce committee:

Prof. Dr. Muhammad Aamir (Dean / Chairman) ________________
Facutly of Engineering and Technology, Department of Elecctrical Engineering, International Islamic University, Islamabad.

Dr. Aamer Saleem Chaudhry (External Examiner I) ________________
Associate Professor, Hamdard institute of Engineering and Technology, Islamabad.

Dr. Muhammad Mukhtar Talha (External Examiner II) ________________
Principle Scientific Officer, Khan Research Laboratories, Kahuta.

Dr. Ihsan Ul Haq (Internal Examiner) ________________
Assistant Professor, Department of Electrical Engineering, International Islamic University, Islamabad.

Prof. Dr. Ijaz Mansoor Qureshi (Supervisor) ________________
Professor, Department of Electrical Engineering, Air University, Islamabad.

ABSTRACT

Due to the limited supply and the strict management policy of the spectrum, it is very difficult to overcome the requirements of data rates and bandwidth in communication systems. To successfully deal with this problem, the idea of random allocation of spectrum rather than fixed allocation of spectrum has come into existence which leads to the idea of cognitive radio (CR). Orthogonal frequency division multiplexing (OFDM) is a best candidate for CR. It has an ability and agility to occupy the spectral holes that are not currently in use by the licensed user and whose positions are changing randomly by simply turning on and off its subcarriers. In order to maintain the successful co-existence between the licensed and un-licensed users, the interference between them should be minimized and one such interference is due to the high sidelobes of OFDM subcarriers that should be minimized at the transmitter side of the OFDM system. Some techniques are found in literature for the suppression of the sideobes, but a need of even better techniques that suppresses the sidelobes in a better way is required.

This dissertation is a contribution towards the above mentioned area. The dissertation is mainly divided into three parts. In the first part, cancellation carriers (CC) based sidelobe reduction technique is presented. A few number of CCs are inserted on either side of used OFDM spectrum, the amplitude of the main lobe of these CCs are adjusted in such a way when it is added with the OFDM spectrum it will results in the reduction of sidelobes. For the adjustment of amplitudes of the main lobe of CCs, we have proposed different heuristic algorithms, including Genetic algorithm (GA), Firefly algorithm (FFA), Differential evolution (DE) and Cuckoo search algorithm (CSA). In the second part, we have proposed Generalized sidelobe canceller (GSC) for the reduction of sidelobes. In this proposed technique the input signal is passed through the two

branches of GSC, the upper branch and the lower branch. The upper branch consist of weight vector allows the signal to pass through it and provides the necessary gain to the desired portion of the signal satisfying the constraint. The lower branch consists of blocking matrix followed by adaptive weight vector, the blocking matrix blocks the desired portion of the signal and pass the undesired portion of the signal while the adaptive weight vector adjusts the amplitudes of the undesired portion of the signal. Finally the signal from the upper branch and lower branch are then subtracted, results in the reduction of sidelobes. In the last part, for further suppression of sidelobe, we have proposed an OFDM framework that is capable of describing any out-of-band (OOB) radiation technique, irrespective of whether one or more than one techniques are applied. Based on that framework, we proposed eight different techniques that can be viewed as two step reduction techniques and are divided into two main groups: The first group, is a combination of our proposed technique GSC with the existing techniques and in the second group is a combination of our proposed techniques GSC with GA, FFA, DE and CSA based CCs.

To show the effectiveness and reliability of all our proposed techniques, we have considered five different spectrums sharing environments. Simulation results show that our proposed techniques, get better suppression of sidelobes.

LIST OF PUBLICATIONS AND SUBMISSIONS

[1] **Elahi A**, Qureshi IM, Khan ZU, Zaman F. “Sidelobe Reduction in Non-Contiguous OFDM-Based Cognitive Radio Systems Using a Generalized Sidelobe Canceller”. *Appl. Sci. Multidisciplinary Digital Publishing Institute*; 2015;5:894–909. **(ISI Indexed & IF = 1.679)**

[2] **Elahi A**, Qureshi IM, Zaman F, Munir F. “Reduction of out of band radiation in non-contiguous OFDM based cognitive radio system using heuristic techniques”. *J. Inf. Sci. Eng*. Citeseer; 2016;32:349–64. **(ISI Indexed & IF = 0.468)**

[3] **Elahi**, **A**., Qureshi, I.M., Zaman, F., Munir, F. and Umar, A., 2016, December. Techniques for the suppression of sidelobes in a non-contiguous orthogonal frequency division multiplexing framework. In *Applied Informatics* (Vol. 3, No. 1, p. 6). Springer Berlin Heidelberg.

[4] **Elahi**, **A**., Qureshi, I.M., Zaman, F., Gul, N. and Saleem, T., 2017. Suppression of Mutual Interference in Noncontiguous Orthogonal Frequency Division Multiplexing Based Cognitive Radio Systems. *Wireless Communications and Mobile Computing, 2017*. **(ISI Indexed & IF = 1.899).**

[5] **Elahi**, **A**., Qureshi, I.M., Atif, M. and Gul, N., 2017. Sidelobe Reduction in Cognitive Radio Systems Using Hybrid Technique. *World Academy of Science, Engineering and Technology, International Journal of Electrical, Computer, Energetic, Electronic and Communication Engineering*, *11*(3), pp.203-206.

[6] **Elahi**, **A**., Qureshi, I.M., Khattak, T.S. and Gul, N., 2016, December. Application of differential and Cuckoo search algorithms in reduction of sidelobes. *In Multi-Topic Conference (INMIC), 2016 19th International (pp. 1-5)*. IEEE.

[7] **Elahi, A.**, Qureshi, I.M., Atif, M. and Gul, N., 2017, March. Interference reduction in Cognitive radio networks using Genetic and Firefly Algorithms. In *Communication, Computing and Digital Systems (C-CODE), International Conference on* (pp. 96-100). IEEE.

[8] Saleem, T., Usman, M., **Elahi**, **A**. and Gul, N., 2017. Simulation and Performance Evaluations of the New GPS L5 and L1 Signals. Wireless Communications and Mobile Computing, 2017. **(ISI Indexed & IF = 1.899)**.

[9] Gul, N., Naveed, A., **Elahi**, **A**., SaleemKhattak, T. and Qureshi, I.M., 2017, January. A combination of double sided neighbor distance and Genetic Algorithm in cooperative spectrum sensing against malicious users. In *Applied Sciences and Technology (IBCAST), 2017 14th International Bhurban Conference on* (pp. 746-753). IEEE.

[10] Khan Z, Amir M**, Elahi A,** Khan S. **"**Suppression of Side-Lobes in Orthogonal Frequency Division Multiplexing based Cognitive Radio System". *MAGNT Research Report* (ISSN. 1444-8939) Vol.2 (6): PP. 994-1002, **(ISI Indexed).**

SUBMITTED PAPERS:

[1] **Elahi A**, Qureshi IM, Khan SU, Zaman F and Gul N. "Improved Algorithms for Interference Suppression in Non-Contiguous Orthogonal Frequency Division Multiplexing-Based Cognitive Radio Systems". *Neural Computing and Applications*, Springer Journal. **(ISI Indexed & IF = 2.505)**.

[2] **Elahi A**, Qureshi IM, Zaman F, Gul N and Atif M. "Out of Band Radiation Reduction in Cognitive Radio OFDM Systems Hybridizing Firefly Algorithm with Generalized Sidelobe Canceller". *Wireless Personal Communications,* Springer Journal **(ISI Indexed**, **IF = 0.951)**

[3] **Elahi A**, Qureshi IM, Gul N, Atif M and Khattak TS. "Efficient Joint Technique for Interference Reduction in Cognitive Radio Networks", *AdHoc Networks,* Elsevier Journal. **(ISI Indexed**, **IF = 3.047)**

[4] **Elahi A**, Qureshi IM, Gul N and Khattak TS. "Interference Cancellation Technique for OFDM based Cognitive Radio Systems", *International Symposium on wireless systems and Netwroks (ISWSN 17),* IEEE.

[5] **Elahi A**, Qureshi IM, Gul N, Atif M and Khattak TS. "Efficient Sidelobe Reduction for OFDM based Cognitive radio systems", *The 2nd EAI International Conference on Future Intelligent Vehicular Technologies.* Springer

[6] Khattak TS, Usman M, Haq I, Zaman F and **Elahi A**. "Design, Characterization and Testing of LHCP Helix Antenna Array for Reception of Reflected GPS Signals". *Wireless Personal Communications,* Springer Journal. **(ISI Indexed & IF = 0.951)**

[7] Gul N, Qureshi IM, Malik AQ, and **Elahi A. "**One-to-many Relation based KL divergence in CSS against malicious user". *Radio Engineering* **(ISI Indexed & IF = 0.945)**

[8] Gul N, Qureshi IM, Malik AQ, **Elahi A**, Khan S. "Malicious Users Prevention in a Hard Fusion Scheme using Statistical Features in Cooperative Spectrum Sensing " *IETE journal of research* **(ISI Indexed & IF = 0.909**)

[9] Gul N, Qureshi IM, Umar A, Sultan K, **Elahi A, "**Malicious secondary detection in Cognitive radio network using statistical features in cooperative spectrum". *Elektronika ir Elektrotechnika* **(ISI Indexed & IF = 0.859)**

[10] Gul N, Qureshi IM, Naveed A, Umar A, **Elahi A, "**Cooperative spectrum sensing using optimal hard decision in the presence of abnormalities in cooperative spectrum sensing". *IETE journal of research* **(ISI Indexed & IF = 0.909)**

[11] Gul N, Qureshi IM, Naveed A, and **Elahi A. "**Particle Swam optimization based cooperative spectrum sensing in the presence of malicious users". *Transaction on Emerging Telecommunication Technologies.* Wiley Publishing corporation **(ISI Indexed & IF = 1.535)**

[12] Gul N, Qureshi IM, Naveed A, Umar A, and **Elahi A.** "Defense against malicious users in cooperative spectrum using Genetic algorithm". *Radio Engineering.* **(ISI Indexed & IF = 0.945)**

[13] Gul N, Qureshi IM, Naveed A and **Elahi A.** "Improved sensing against malicious users using DSNA and GA", Electrical Engineering, Springer Journal. **(ISI Indexed & IF = 0.569)**

[14] Gul N, Qureshi IM, Umar A, **Elahi A** and Khan S “History based forward and feedback mechanism in cooperative spectrum sensing including malicious users in cognitive radio network”. PLOS ONE **(ISI Indexed & IF = 2.806)**

ACKNOWLEDGEMENTS

In the name of Allah (Subhanahu Wa Ta'ala), who is the most gracious and the merciful. I would like to thank Allah for giving me strength and patience to complete this research work. Peace and blessings of Allah be upon His last Prophet Muhammad (Sallulah-o-Alaihihe-Wassalam) and all his Sahaba (Razi-Allah-o-Anhu) who dedicated their lives for Dawah and spread of Knowledge. I am truly grateful to my supervisor Dr. Ijaz Mansoor Quershi, whose inspiration, ideas and efforts make it possible for me to complete my higher studies. He has been a role model for me and many others in teaching, research and other aspects of life. I offer my sincere thanks to Dr. Zafar Ullah Khan, Dr. Fawad Zaman, Dr. Shafqat Ullah Khan, Dr. Abdul Basit, Dr. Wasim Khan, Mr. Zia-ur-Rehman and Engr. Sharjeel Abid Butt for their never ending support during last few years. I also thank Bilal Shoaib, Shah Fahad, Hayat Ullah and other PhD scholars for their useful discussions.

I would like to acknowledge the support of Higher Education commission of Pakistan for providing me Indigenous Scholarship during my MS and PhD studies. It was a great support from Higher Education commission of Pakistan. I am also thankful to administration at department as well as at university level for their kind support. I am really grateful to my father, mother, sisters and brothers for their love and support throughout my life. I am also very thankful to my wife for her patience, encouragement and prayers during every stage of my PhD degree. Finally, I am thankful to my kid, whose innocent gestures were source of inspiration for me.

(Atif Elahi)

TABLE OF CONTENTS

LIST OF FIGURES

LIST OF TABLES

LIST OF ABBREVIATIONS

ACC	Advanced cancellation carriers
ANCC	Active and null cancellation carriers
ACO	Ant colony optimization
A/D	Analog to digital converter
BAV	Binary allocation vector
BPSK	Binary phase shift keying
BSOA	Brain storm optimization algorithm
BA	Bat algorithm
BER	Bit Error Rate
CSA	Cuckoo search algorithm
CR	Cognitive radio
CP	Cyclic prefix
CC	Cancellation carriers
CSMA	Carrier sense multiple access
CS	Cyclic suffix
DSA	Dynamic spectrum access
DE	Differential evolution
DFT	Discrete Fourier transform
D/A	Digital to analog converter
EP	Evolutionary programming

FFA	Firefly algorithm
FCC	Federal communication commission
FDMA	Frequency division multiple access
FFT	Fast Fourier transform
FBF	Fixed Beamformer
FWA	Fireworks algorithm
GP	Genetic programming
GI	Guard interval
GSC	Generalized sidelobe canceller
GA	Genetic algorithm
HA	Heuristic algorithm
ISI	Intersymbol interference
ICI	Intercarriers interference
IDFT	Inverse discrete Fourier transform
IFFT	Inverse fast Fourier transform
LCMV	Linearly constraint minimum variance
LUs	Licensed Users
MSE	Mean Square Error
OFDM	Orthogonal frequency division multiplexing
OOB	Out of band
PSD	Power spectral density
P/S	Parallel to serial
PUs	Primary users

RST	Random set theory
SA	Simulated annealing
SI	Swarm intelligence
S/P	Serial to parallel
SPTF	Spectrum policy task force
SUs	Secondary users
SDR	Software defined radios
TDMA	Time division multiple access

LIST OF SYMBOLS

A list of commonly used symbol in this dissertation are given below.

$g_n(t), g_m(t)$	Complex signals on n*th* and m*th* subcarriers
f_i	Frequency of i*th* subcarrier
Δf	Subcarrier spacing
B	Total available bandwidth
N	Total number of subcarriers
$x_i(t)$	Transmitted time domain signal over i*th* subcarrier
b_i	Complex data on ith subcarrier
$I(t)$	Rectangular function
T_o	OFDM symbol duration
f_s	Sampling frequency
$x(t)$	Transmitted OFDM symbol in time domain
$x[k]$	Discrete time domain OFDM symbol
$X[n]$	Discrete frequency domin OFDM symbol
T_{CP}	Symbol duration of cyclic prefix
$\tau_{\max}$	Maximum time delay of multipath channel
T	Duration of OFDM symbol after adding cyclic prefix
N_{CP}	Length of cyclic prefix (Discrete domain)
$y[k]$	Received sequence in discrete time domain

$n[k]$	Noise sequence in discrete time domain
$h[k]$	Channel impulse response
$Y[n]$	Received sequence in discrete frequency domain
$H[n]$	Transfer function of channel impulse response
$X[n]$	Discrete frequency domain OFDM symbol
$N[n]$	Noise sequence in discrete frequency domain
N_w	Samples for transmit windowing
δ	Additional samples for receiver windowing
$Z[n]$	Sum of transfer function of channel impulse response and noise sequence in discrete frequency domain
$\mathbf{b}$	Vector consisting of complex data symbol
$\mathbf{x}$	Vector containing transmitted signal
$\mathbf{y}$	Vector containing samples of received signal
$\mathbf{h}$	Vector containing samples of channel impulse response
$\mathbf{n}$	Vector containing samples of noise
$\mathbf{x}'$	Vector containing signal transmitted on multipath channel
$\mathbf{i}$	Vector containing samples of interference from licensed system for the duration of one OFDM signal
$\mathbf{z}'$	Vector containing useful part of received signal
K_f	Total number of fireflies
$\mathbf{w}_i$	Vector containing locality of i*th* firefly

N_f	Available space to firefly
w_H^t, w_L^t	Upper and lower limit in firefly algorithm
B_i	Brightness of i*th* firefly
β_{ij}	Attractiveness of i*th* and j*th* firefly
r_{ij}	Distance between w_i and w_j
n	Number of chromosomes in differential evolution
d	Gene number in differential evolution
G	Generation number in differential evolution
H, L	Upper and lower limit in differential evolution
$\mathbf{s}_d^{n,G}$	n*th* chromosome with gene number d and generation number G
$\mathbf{s}_d^{n,G+1}$	Chromosome of next generation
$\mathbf{u}_d^{n,\mathrm{G}}$	Mutant vector
F	Mutation factor
C_r	Crossover rate
$\mathbf{W}_d^{n,G}$	Next population
x_n^k	Solution space for n*th* cuckoo
x_n^{k+1}	New solution for n*th* cuckoo
α	Step size in cuckoo search algorithm
N_s	Number of subcarriers utilized by i*th* secondary user
$x_s(t)$	Transmitted OFDM signal of i*th* secondary user

$q_{n,s}$	Modulated symbol of i*th* secondary user over n*th* subcarrier
f_n	Frequency of n*th* subcarrier
N_s	Number of subcarriers utilized by i*th* secondary user
T_g	Length of gurad interval
$X_s(f)$	Frequency domain representation of OFDM signal of i*th* secondary user
$T^{'}$	Symbol duration after adding guard interval
K	Total number of cancellation carriers
K_r, K_l	Total number of right and left sided cancellation carreirs
M_r, M_l	Total number of sample points on the left and right side of the OFDM spectrum
$c_m(\alpha)$	Spectrum of m*th* cancellation carrier
λ_m	Normalized center frequency of m*th* cancellation carrier
$\mathbf{a}$	Vector containing amplitudes of main lobes of cancellation carriers
A_{Cj}	Sum of amplitudes of m*th* left and m*th* right cancellation carrier at j*th* sample point
$A_{C(m,j)}$	Amplitude of m*th* left cancellation carrier at j*th* sample point
A_{Dj}	Sum of amplitude of n*th* data carrier at j*th* sample point
A_j	Amplitude of all data and cancellation carriers at j*th* sample point
$\mathbf{w}_q$	Quiescent weight vector
$\mathbf{B}$	Blocking matrix
$\mathbf{w}_a$	Adaptive weight vector

$\mathbf{w}_{a(opt)}$	Optimum adaptive weight vector
$\mathbf{w}$	Weight vector of generalized sidelobe canceller
$\mathbf{u}$	Vector containing samples of input signal of generalized sidelobe canceller
$\mathbf{R}_{\mathbf{u}}$	Correlation matrix
$\mathbf{I}$	Identity matrix
$\mathbf{C}$	Constraint matrix
$\mathbf{s}$	Steering vector
$\mathbf{g}$	Gain vector
Y	Output of generalized sidelobe canceller
$\mathbf{P}_c$	Projection matrix of constraint subfield
$\mathbf{P}_o$	Projection matrix of orthogonal subfield
P	Output power of generalized sidelobe canceller

Chapter 1

Introduction

1.1 Problem statement

The rapid growth in wireless communication methods and demand for high data rate in today's environment is the major reason of spectral scarcity. From the spectrum measurement done in different parts of the world and in different duration shows that most of the frequencies are idle most of the time. The above situation led to the following conclusion: First a more flexible spectrum management policy is needed and the second one, technology must be there that is compatible with the new management policy.

As to the first point, different concepts for a flexible spectrum management can be found in the literature. Several suggestions were given that include allocation of spectrum to various users functioning in the same allocated frequency range dynamically or randomly, unrestricted access of spectral resources to everyone, or spectrum auctioning which dynamically allocates spectral resources for a limited time to the most bidding user. All these suggestions have one thing in common dynamic spectrum allocation instead of fixed spectrum allocation. This is in-line with recent developments of spectrum policy. Regulatory bodies start rejecting the rigid spectrum allocation and headed towards dynamic spectrum access.

In reference to the second point J. Mitola and Gerald Q. Maguire [1] in 1999 have given the idea of cognitive radio (CR). CR is an encouraging solution to tackle such a problem and has received special attention in the research community. CR has the ability to dynamically permit secondary users (SU) to operate in those spectral domains that are not being used by the primary users (PU) at certain times and localities. Efficient techniques are needed at the transmitter side to control the shapes of the transmitted signal so that both SU and PU can share the same spectrum resources with minimum interference.

Orthogonal frequency division multiplexing (OFDM) is the best candidate for CR, with the ability to divide the available wideband channel into multiple narrow band orthogonal channels/subcarriers and to transmit those subcarriers in parallel. Some attributes of OFDM include spectral efficiency, multipath delay spread, robustness to channel fading, resilience to narrow band effects, resilience to intersymbol interference (ISI), resilience to interference and simpler channel equalization. On the other hand, due to the large sidelobes of the OFDM subcarriers, CR based on OFDM experiences high out-of-band (OOB) radiation that may result in considerable interference with the adjacent bands used by either PU or SU. To tackle the OOB radiation problem, various techniques are proposed in the literature that can be categorized into two groups: time domain techniques and frequency domain techniques.

1.2 Contribution of the dissertation

The main purpose of this dissertation is to develop some new and efficient techniques that can reduce the sidelobes in a better way, so that multiple users can access the same spectral resource at the same time with minimum level of interference. Contribution of this dissertation is summarized as follows.

1. Calculation of the amplitudes of proposed Cancellation carriers (CCs) by using different Heuristic algorithms (HA) has been presented. A few number of CCs are inserted on both

sides of OFDM spectrum, whose sidelobes can cancel out the sidelobes of the OFDM spectrum. So for the calculation of the amplitude of these CCs, we proposed different heuristic algorithms that include Genetic algorithm (GA), Differential Evolution (DE), Firefly algorithm (FFA) and Cuckoo search algorithm (CSA) by using our proposed fitness function. The effectiveness of these algorithms are checked by considering five different spectrum sharing environments with the help of simulations that shows that better suppresion of sidelobes are achieved as compared to the existing techniques. The price to pay for these results is an acceptable loss in Bit error rate (BER) performance and an increased computational complexity. But both effects can be kept at a minimum by appropriate countermeasures.

2. Next we proposed a novel technique by using generalized sidelobe canceller (GSC) for the reduction of sidelobes. In the proposed technique, the signal is passed through two branches of a GSC. The upper branch consists of the weight vector designed by multiple constraints to preserve the desired portion of the signal, while the lower branch consists of a blocking matrix followed by a weight vector. The blocking matrix blocks the desired portion and preserves the undesired portions (sidelobes). The weight vector adjusts the undesired portion (sidelobes) in such a way that when subtracted from the signal of the upper branch, it results in significant cancellation of the sidelobes of the OFDM signal. We have compared the performance of the proposed technique with already existing techniques via simulations and by considering five different spectrum sharing environments. The proposed technique achieves better suppression of the sidelobes as compared to the existing methods.

3. Finally, we have proposed a framework of an OFDM that has an ability of describing any OOB radiation reduction techniques, regardless of whether a single or multiple techniques are applied. Based on this framework, we proposed eight new different techniques that can be viewed as two level suppression techniques are proposed, which are divided into two major groups: The first one is the combination of our proposed technique GSC with four different existing CC techniques, including CC proposed by Brandes [2], [3], CC proposed by Pagadarai [4], Advanced cancellation carriers (ACC) [5] and Active and Null cancellation carriers (ANCC) [6]. The second one is the combination of our proposed techniques discussed in chapter 4 and 5 i.e. combination of GSC with GA based CC, combination of GSC with FFA based CC, combination of GSC with DE based CC and combination of GSC with CSA based CC. The purpose of combining different techniques is, to take advantages of the individual techniques for further enhancing the suppression of sidelobes. The strength and reliability of the proposed techniques are shown via computer simulations in different types of spectrum sharing scenarios, which show that the proposed techniques get far better reduction of OOB radiation as compared to the existing techniques.Our combined proposed techniques achieves better suppression of sideloes as compared with the previous techniques.

1.3 Organization of the dissertation

The organization of this dissertation is as follows.

In chapter 2, a brief survey of CR and OFDM has been given. After that some design issues when OFDM is used for CR system are discussed. In the end, an overview of some existing techniques for solving sidelobes suppression, which is one of the design issue are highlighted followed by a conclusion. In chapter 3, a detailed discussion of some proposed heuristic techniques including GA, FFA, DE and CSA are given.

In chapter 4, the application of the proposed algorithms i.e. GA, FFA, DE and CSA based on our fitness function, for the calculation of amplitudes of main lobe of CCs are given. Simulation results in term of power spectral density (PSD) and comparing it with other existing techniques are done to check the reliability and efficiency of our proposed fitness function and proposed algorithms.

In chapter 5, we proposed a new technique GSC for the reduction of sidelobes. In this chapter, we show that how an incoming signal at GSC is divided into two portions that ultimately results in the suppression of sidelobes. The performance and reliability of the proposed technique is shown with the help of simulation and comparing it with other results.

In chapter 6, we presents a framework of OFDM that has an ability of describing any OOB radiation reduction techniques, regardless of whether a single or multiple techniques are applied. Based on this framework, we proposed eight new different techniques that can be viewed as two level suppression techniques are proposed, which are divided into two major groups: First group is the combination of our proposed technique, GSC with other existing techniques including CC proposed by Brandes, CC proposed by Pagadarai, ACC and ANCC, while second group is the combination of our proposed techniques i.e GSC with GA based CC, FFA based CC, DE based CC and CSA based CC. The motive behind combination of techniques is achieving suppression of sidelobes as much as possible.

In chapter 7, we give conclusion of this dissertation along with proposed future work.

Chapter 2

Literature Review

This chapter presents necessary details about existing literature regarding CR and OFDM. It starts with a background and the motivation behind the concept of CR, then a brief discussion about the CR, its function and network architecture are given. After that the motivation behind using OFDM as a best candidate for CR system are given followed by a brief discussion about the conventional OFDM, and its working principle. Moreover, the discussion is given about the modified OFDM especially for CR system, also named as OFDM based CR system, and its working principle, followed by some design issues. In the end discussion about one of the major design issue of OFDM based CR system and the existing research for solving that issue are highlighted.

2.1 Background

The user demand for data rate and services has increased rapidly over the last few decades that results in a shortage of spectrum to new services [7]–[10]. In November 2002, spectrum policy task force (SPTF) of the federal communication commission (FCC) have shown in their report that in most of the bands, spectrum access is a more serious problem as compared to the physical inadequacy of spectrum. This is due to the traditional command and control system that restricts the potential spectrum users to obtain such access. Secondly these spectrums most of the times are either unoccupied or partially occupied. To encounter these problems, their recommendation were, to improve the flexibility of spectrum usage, to support and encourage the efficient use of the spectrum and to take all dimensions and related issues of spectrum usage into the policy. The aim were to improve both technical and economic efficiency of spectrum management. These recommendation introduces the concept of Dynamic spectrum access (DSA), where the un-licensed user also known as SU have the right to use the temporarily un-usable spectrum of the licensed user also called as PU. So CR has been proposed for the efficient use of spectrum [11]–[15].

2.2 Cognitive radio

The word cognitive is derived from the Latin word "co + gnoscere" meaning "to come to know" or to become aware of something [16]–[18]. The word CR, first used by J. Mitola, is a new way of designing a wireless communication system, whose goal is to provide wireless transmission through DSA, so that the performance of wireless transmission can be improved, as well as improving the consumption of the frequency spectrum and solving the problem of spectrum underutilization [1], [19]–[21]. It differs from the conventional radio, in that it has an ability of cognition and re-configurability. Cognition is the ability of CR to sense and to collect the information about the transmission frequency, bandwidth, allocated power, modulation scheme etc. from its surrounding environment, with the help of which the SUs are able to identify the best available spectrum. Cognitive re-configurability refers to the ability to adapt the operational environment swiftly according to the sensed information in order to attain best performance. Cognitive re-configurability is provided from a platform of software-defined radio (SDR), upon which a cognitive radio is built. SDR is now a days a practical reality, because of the convergence of digital radio, and computer software [21]–[25].

By taking the best advantage of the available spectrum opportunistically, cognitive radio empowers the SUs to sense for the spectrum holes, selecting the appropriate channel, coordinating with other users for spectrum access, and to leave the occupied channel after the reclaiming of spectrum from PUs.

2.3 Functions of Cognitive radio

The duty cycle of CR as shown in Figure. 2.1 includes detection of spectral holes, selecting the best frequency bands, coordinating the spectrum access with other users and vacating the spectral hole when the primary user appears. Such a cognitive cycle is supported by the following tasks.

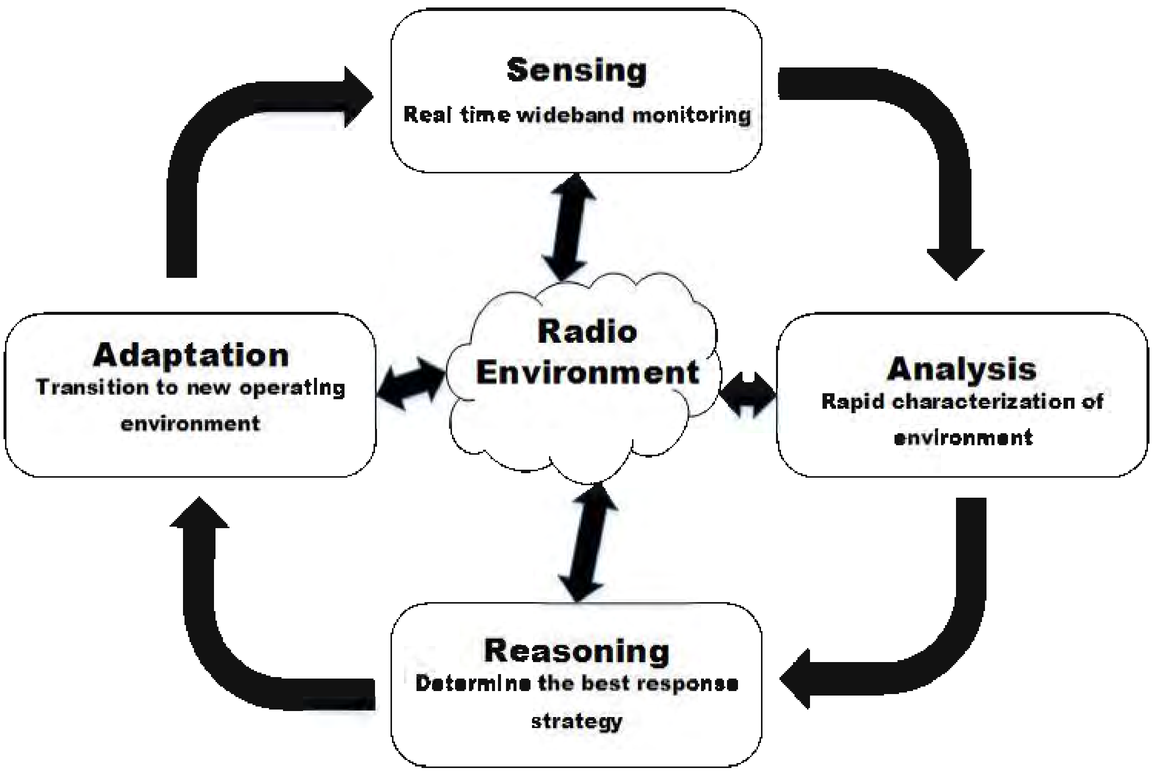

Figure 2. 1 Cognitive Radio Cycle

2.3.1 Spectrum sensing and analysis

Spectrum sensing and analysis is the first step towards the spectrum utilization dynamically. With spectrum sensing CR can gain essential information about the surrounding environment and can adjust its transmission and receiving parameters like transmission power, frequency and modulation schemes etc. in order to achieve efficient spectrum utilization. Three different aspects of spectrum sensing are interference temperature model, spectrum hole detection and cooperative sensing with multiple users.

2.3.2 Spectrum management and handoff

After knowing about the spectrum holes by sensing, spectrum management and handoff function of the CR permits the SU, also called the un-licensed user to pick the best frequency band and hop among the multiple bands according to the time varying channel characteristics to meet various quality of service requirements. For example, if the PU, also called as the licensed user, regain its frequency band, the SU will direct its transmission to the other available frequencies according to the channel capacity determined by the noise and interference levels, path loss, channel error rate and holding time etc.

2.3.3 Spectrum allocation and sharing

In DSA environment SU may share the spectrum resources with other SUs, PUs or both. A good spectrum allocation and sharing with high spectral efficiency is difficult to achieve. Since PU owns the spectrum rights, the interference level due to the SU should be limited by certain threshold. When multiple SUs share the frequency band, their access should be coordinated to alleviate collision and interference.

2.4 Network Architecture of Cognitive Radio

With the growth of CR technology, the SUs can take temporary advantage of the vacant spectral bands possessed by the PUs. So, CR network architecture consists of secondary network that contains SUs, as well as secondary base station, and primary network that contains the PUs as well as primary base station, are exhibited in Figure. 2.2 [25].

Secondary network consists of a lot of SUs, with/without a secondary base station and will only occupy the spectral hole, when it is not in use of PU. To gain the possession of a spectral hole by the SU, when it is not currently in use of PU, is usually coordinated via the secondary base station, which is a fixed infrastructure component serving as a hub of the secondary network.

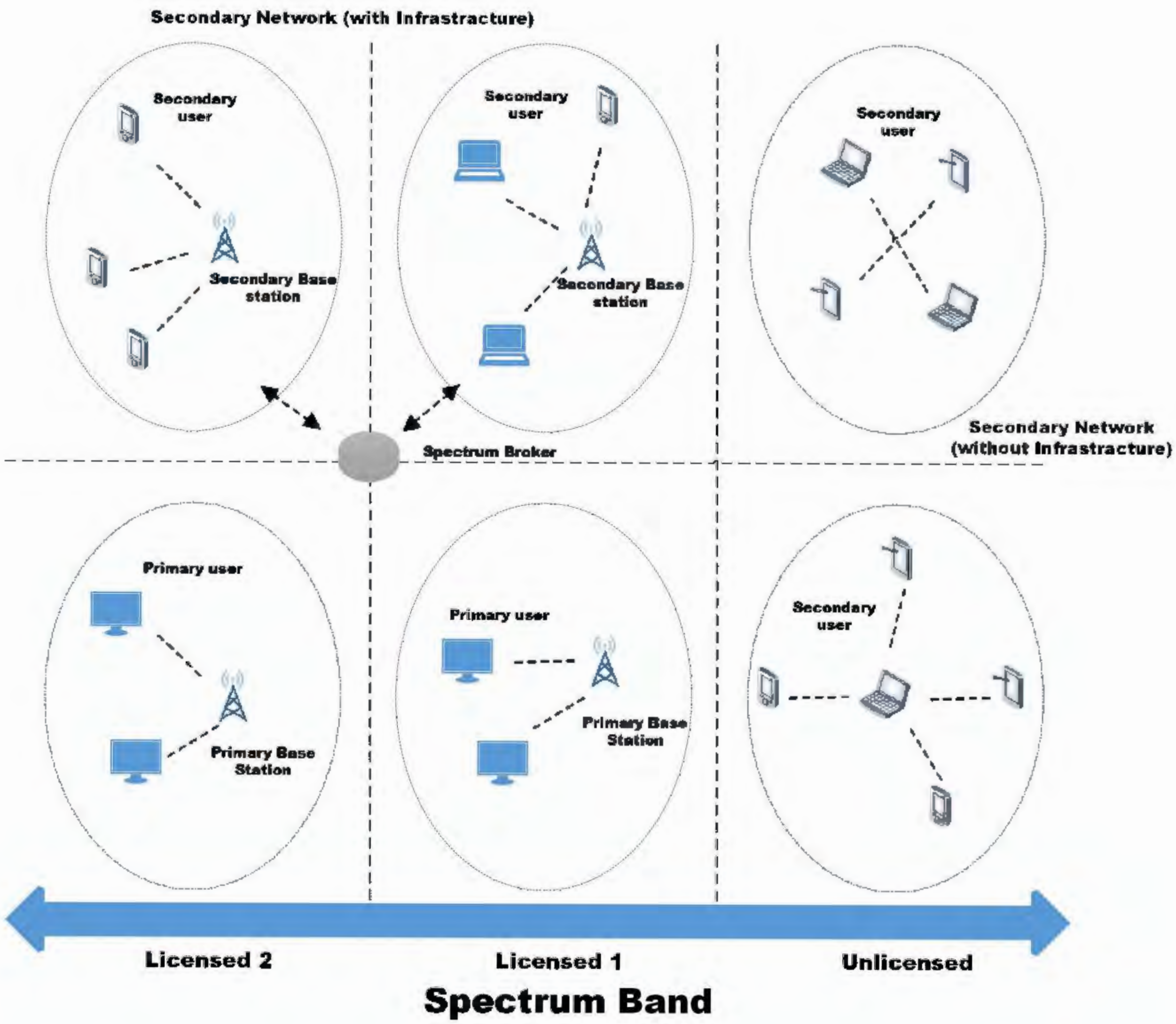

Figure 2. 2 Network Architecture of DSA

The SUs and the secondary base stations are equipped with CR functions. Whenever a lot of secondary networks are trying to utilize the same spectral band, in that situation, spectrum broker manages all the secondary networks transmission over that spectral band. This is done by collecting information from every secondary network, and assigns the network resources for efficient and fair spectrum sharing. A primary network consists of a lot of PUs and a few primary base stations. PUs are legally allowed to use defined portion of spectral band with the help of primary base stations with the insurance that their communication will not be interrupted by the secondary networks. Actually the PUs and primary base stations are not equipped with CR functions. Therefore, if a secondary network share a licensed spectrum band with a primary network, besides detecting the spectrum white space and utilizing the best spectrum band, the secondary network is required to immediately detect the presence of a primary user and direct the secondary transmission to another available band so as to avoid interfering with primary transmission [26]–[28].

2.5 Orthogonal frequency division multiplexing

Multicarrier methods are considered as the best candidates for the physical layer of CR system. By allocating the SUs to the spectral holes that can coexist with the other spectral holes used by PUs, multicarrier methods offer considerable flexibility to fill in the holes, and accordingly it utilizes the natural resources efficiently. In addition to that, OFDM is one of the best multicarrier method, has been introduced as a first candidate for this purpose.

The concept of OFDM was first given by Robert W Chang [29] in 1966. His aim was to present a new scheme of transmitting multiple signal at the same time on a narrow band channel without intercarriers interference (ICI) and ISI. The main idea of OFDM is the splitting up of frequency selective channel into multiple frequency flat fading channels that are parallel as well as orthogonal

[29]–[31]. The major drawback at that time was the implementation of bank of modulators and demodulators, until in 1971, when Weinstein and Ebert gave an idea of using discrete Fourier transformation (DFT) for performing the modulation and demodulation that reduces the implementation complexity [32]. Since early 1990's OFDM has gained increased attention and has been successfully adopted in different wireless, as well as, in wired communication systems [33]–[36].

The motivation behind adopting OFDM in CR are its advantages that are its insusceptibility to frequency selective fading and high data rate, because of its ability to divide the overall bandwidth into multiple narrow band orthogonal channels, efficient usage of spectrum by overlapping of subcarriers, removal of ISI and ICI through the use of cyclic prefix (CP), simpler channel equalization by using adaptive equalization techniques, computationally efficient by using fast Fourier transform (FFT) to implement modulation and demodulation, ability of recovering the lost symbols due to the frequency selectivity by using sufficient channel coding and maximizing the likelihood decoding etc [37], [38]. There is no need for considerable modification on the basic structure of conventional OFDM system while using OFDM in CR systems, but some parameters should be adopted to the structure defined by the PUs in advance.

2.5.1 OFDM Principle

The basic principle behind OFDM is the division of wideband channel into multiple narrow band subchannels that are transmitted parallel over number of subcarriers and these subcarriers should be orthogonal to avoid ICI. Consider subcarrier *n* and *m* carriers complex signals $g_n(t)$ and $g_m(t)$. They are orthogonal if:

$$\int_{-\infty}^{\infty} g_n(t) g_m^*(t)\, dt = \begin{cases} 0 & n \neq m \\ otherwise & n = m \end{cases} \tag{2.1}$$

Suppose these subcarriers are very close to each other, the carrier frequency of *i*th subcarrier is f_i given by:

$$f_i = i\Delta f = i\frac{B}{N}, \qquad i = 0, 1, \ldots, N \tag{2.2}$$

Here Δf represents the subcarrier spacing, B represents the total available bandwidth, while N represents the total number of subcarriers.

The transmitted time domain signal over the *i*th subcarrier is given by:

$$x_i(t) = b_i e^{j2\pi f_i t} I(t) \tag{2.3}$$

Here b_i represents the complex symbol data on *i*th subcarrier and $I(t)$ represents the rectangular function defined as:

$$I(t) = \begin{cases} 1 & 0 \leq t \leq T_0 \\ 0 & otherwise \end{cases} \tag{2.4}$$

where T_0 represents the OFDM symbol duration, the orthogonality condition in equation (2.1) can be rewritten as:

$$\int_{0}^{T_0} e^{j2\pi f_k t} e^{-j2\pi f_i t}\, dt \triangleq 0 \quad if\ i \neq k \tag{2.5}$$

Result of equation (2.5) can only be achieved, if the spacing Δf between the subcarrier is an integral multiple of inverse of duration of OFDM symbol T_0 and for spectral efficiency Δf should be as small as possible.

As there are total of *N* subcarriers, so it means that there are *N* such transmitted time domain signals. So one OFDM symbol will be the sum of all *N* time domain transmitted signals given by:

$$x(t) = \frac{1}{N}\sum_{i=0}^{N-1} x_i(t) \tag{2.6}$$

$$x(t) = \frac{1}{N}\sum_{i=0}^{N-1} b_i e^{j2\pi f_i t} I(t) \tag{2.7}$$

Taking samples of the signal given in equation (2.7) with sampling frequency $f_s = \frac{N}{T_0}$, on substituting the subcarrier frequency with discrete equivalent we get:

$$x[k] = \frac{1}{N}\sum_{i=0}^{N-1} b_i e^{j2\pi\frac{ki}{N}} \;,\; k = 0,1,\ldots,N-1 \tag{2.8}$$

where *k* denotes the number of samples. In discrete domain, the length of *N* samples are equal to the one OFDM symbol duration T_0. Sequence given in equation (2.8) is the representation of b_i $i = 0,1,\ldots,N-1$ after taking Inverse discrete Fourier transformation (IDFT) that is more generally represented by $X[n]$ $n = 0,1,\ldots,N-1$, with *n* representing the frequency domain index [31], [39], [40].

$$x[k] = IDFT\{X[n]\} = \frac{1}{N}\sum_{n=0}^{N-1} X[n] e^{j2\pi\frac{in}{N}} \;,\; k = 0,1,\ldots,N-1 \tag{2.9}$$

The main advantage of OFDM is the representation of OFDM modulation in discrete domain by using IDFT that reduces its implementation complexity.

As the transmitted radio signal is reflected from different sources resulting in multiple copies of signal that arrives at the receiver at different times can interfere with each other causing ISI. In OFDM it can be tackled by the use of CP whose time duration must exceed the maximum time delay of multipath channel given by:

$$T_{CP} \geq \tau_{\max} \tag{2.10}$$

The CP is basically the extension of each OFDM symbol with symbol duration T_{CP}. Thus the duration of OFDM symbol extends to:

$$T = T_0 + T_{CP} \tag{2.11}$$

The orthogonality between subcarriers is also maintained using CP that results in avoiding ICI. In discrete domain the length of CP is given by:

$$N_{CP} \geq \left| \frac{\tau_{\max} N}{T_0} \right| \tag{2.12}$$

After adding CP equation (2.8) will become:

$$x[k] = \frac{1}{N} \sum_{i=0}^{N-1} b_i e^{j2\pi \frac{ki}{N}},\ k = -N_{CP}, \ldots, N-1 \tag{2.13}$$

The signal in equation (2.13) is then passed through the digital to analog converter (D/A) the output of which will be $x\ (t)$ with symbol duration T. At the receiver side the signal is first converted to digital domain by using analog to digital converter (A/D). The received sequence $y[k]$,

$k = 0,1,...,N + N_{CP} - 1$ consists of transmitted sequence $x[k]$ contaminated with the multipath channel noise $n[k]$ and channel impulse response $h[k]$, $k = 0,1,...,N + N_{CP} - 1$ given by:

$$y[k] = h[k] * x[k] + n[k] \tag{2.14}$$

The CP is then removed from the signal in equation (2.14) followed by DFT, whose output is given by:

$$Y[n] = DFT\{y[k]\} = \sum_{k=0}^{N-1} y[k] e^{-j2\pi\frac{kn}{N}} \tag{2.15}$$

As ICI and ISI is completely avoided by using CP, every subchannel is completely isolated from each other. The transmitted symbol b_i, i = 0, 1… N - 1 transmitted on ith subcarrier and can be easily estimated from $Y[n]$ due to the proper adjustment of the subcarrier spacing the subchannels are experiencing frequency flat fading. The frequency domain representation of equation (2.14) can be given as:

$$Y[n] = H[n] \bullet X[n] + N[n], \; n = 0,1,...,N-1 \tag{2.16}$$

$$Y[n] = Z[n] + N[n] \text{ with } Z[n] = H[n] + X[n] \tag{2.17}$$

Here H [n] represents the transfer function of channel impulse response, X [n] represents the transmitted symbols, while N [n] represents the noise. The general schematic diagram of OFDM is shown in Figure. 2.3.

Notation:

Time domain variables are denoted by small letters, while frequency domain variables are denoted by capital letters. For continuous time domain variable t is used in parenthesis, while for discrete time domain variable k is used in square brackets. Similarly for frequency domain variable f is used in parenthesis, while for discrete frequency domain variable *n* is used in square brackets. Moreover, vectors are represented by small case bold letters, while matrices are represented by capital case bold letters.

2.6 OFDM Based CR system

As the subcarriers of OFDM are overlapping in nature, the spectral efficiency of the system

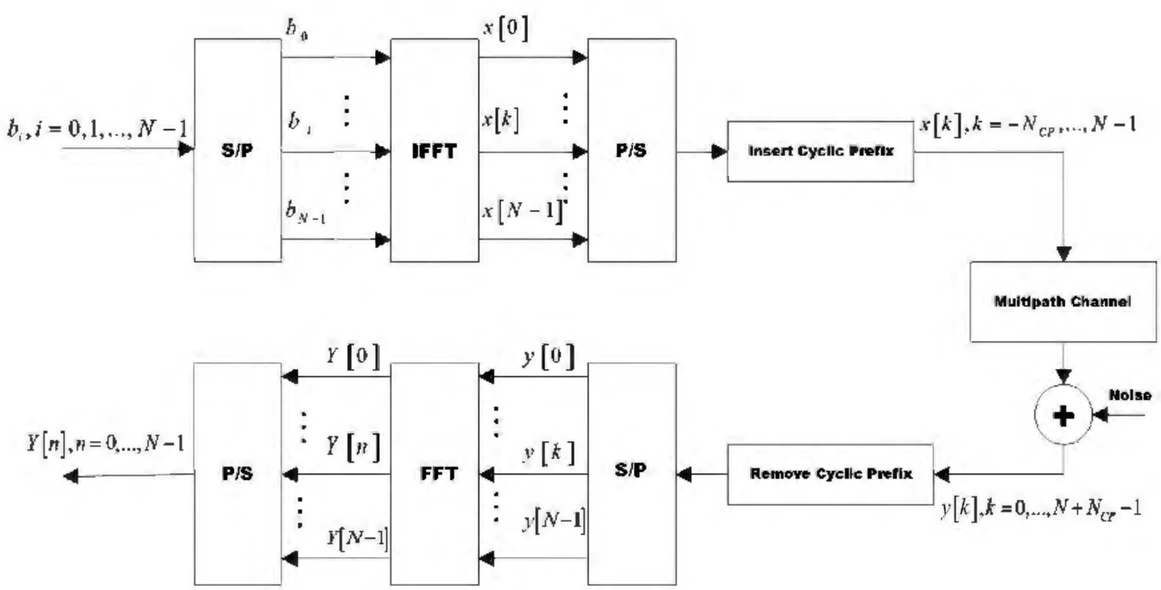

Figure 2. 3 Block Diagram of Conventional OFDM system

becomes high and achieves high rate data transmission. In the CR system framework, OFDM offers the flexibility of adjusting the transmitted spectrum to the changing spectrum allocation by simply turning on and off individual subcarriers. That is why it is considered as a perfect modulation scheme for spectrum sharing systems [41]–[44].

2.6.1 Principle of working

Before transmitting, the identification of spectrum holes has to be done with the help of spectrum sensing by CR system and then adapt its transmit signal accordingly. As the CR system and licensed system are not exchanging any information between themselves, the location of a licensed system is monitored by the CR system itself [45], [46]. This can easily be recognized when the licensed system operates on a frequency- and/or time-division multiple-access (FDMA/TDMA) basis. When the CR system is silent, then the CR receiver will receive the signal of licensed system only. In that phase, the output of the DFT/FFT operation, that is available in each OFDM receiver anyway, specifies whether or not the licensed system currently uses a channel corresponding to a set of subcarriers of the CR system. Accuracy about the existence and the location of licensed system can be improved by carrying out various DFT/FFT cycles and finally taking the average of all the results. Moreover, spatial diversity can be introduced by taking multiple stations of the CR system to monitor the licensed systems from different locations and exchange the results among them to maximize the accuracy about the location of licensed system and spectrum holes. The results are collected in the binary allocation vector (BAV) that indicates for each subcarrier whether the particular subcarriers can be used by the SU [47]. The allocation vector has to be updated and the transmitted signal has to be modified accordingly, when the licensed system changes its spectrum allocation as depicted in Figure 2.4. The optimal rate for spectral measurements and updates of the allocation vector has been investigated e.g. in [47].

Those licensed systems that uses carrier sensing technique i.e. carrier sense multiple access (CSMA) for their channel access, are not always a good idea for co-existence with CR systems, because information about the spectrum allocation cannot be suitably measured. The licensed systems scan the channel and transmit when it found that the channel is idle. The CR system would not detect the scanning function of licensed system, would also recognize that the corresponding channel as idle, and start its transmission. This will block the licensed system attempt of transmission till the CR system has ended its transmission. In this way the CR system would harm the licensed system considerably and completely block its transmission. However, a frequency range in use of licensed system using CSMA can be shared with CR system, if the licensed system has assigned a fixed channel. For that the CR system must have an information about the channel status so that it can skip all those channels that are in use of licensed system. Once the CR system has detected used subcarriers, it will adjust its transmission according to the spectrum condition.

In OFDM the spectral band is divided into a number of subchannels which are given to the licensed system. The OFDM adjusts its transmission by turning off the particular subcarriers, i.e. modulating those subcarriers with zeros, which are in use of licensed system. As the occupation of the spectrum changes with time, OFDM dynamically adjusting its transmission by turning off and on the subcarriers as shown in Figure 2.4.

Therefore, the fundamental functions of a conventional OFDM system need not to be changed to realize an OFDM based CR system and most of the blocks remain unchanged as depicted in Figure. 2.3. However, some blocks need slight modification and some additional blocks are required that are shown in Figure. 2.5.

At the transmitter side of OFDM based CR system, a complex data symbols $\mathbf{b} = [b_0, b_1, ..., b_{N-1}]^T$ is fed into the serial to parallel (S/P) block. These symbols are then allocated to the subcarriers that are not utilized by the PUs and the rest of subcarriers are filled with zeros i.e. turned off. The information about the status of subcarriers are present in BAV and as the position of spectrum holes changes the BAV updates itself as a result OFDM based CR system adjust its transmission by simply on off of the subcarriers. The symbols are modified, by using suppression techniques for reducing the sidelobes of the subcarriers, which are then converted into the time domain by using Inverse Fourier transformation (IFFT) further CP and cyclic suffix (CS) are attached to the time domain data stream. The CP contains a guard interval (GI) whose length is more than the maximum delay spread of multi-path channel. Further $N_w + \delta$ number of samples are needed for windowing functions at transmitter, as well as, on the receiver side. The CS contains N_w samples for transmit windowing. Finally the signal $\mathbf{x} = \left[x[-N_{CP} - N_w - \delta],...,x[0],...,x[N + N_w - 1]\right]^T$ is multiplied with a window function for additional suppression of sidelobes, we get the signal $\mathbf{x}'$ transmitted on multipath channel.

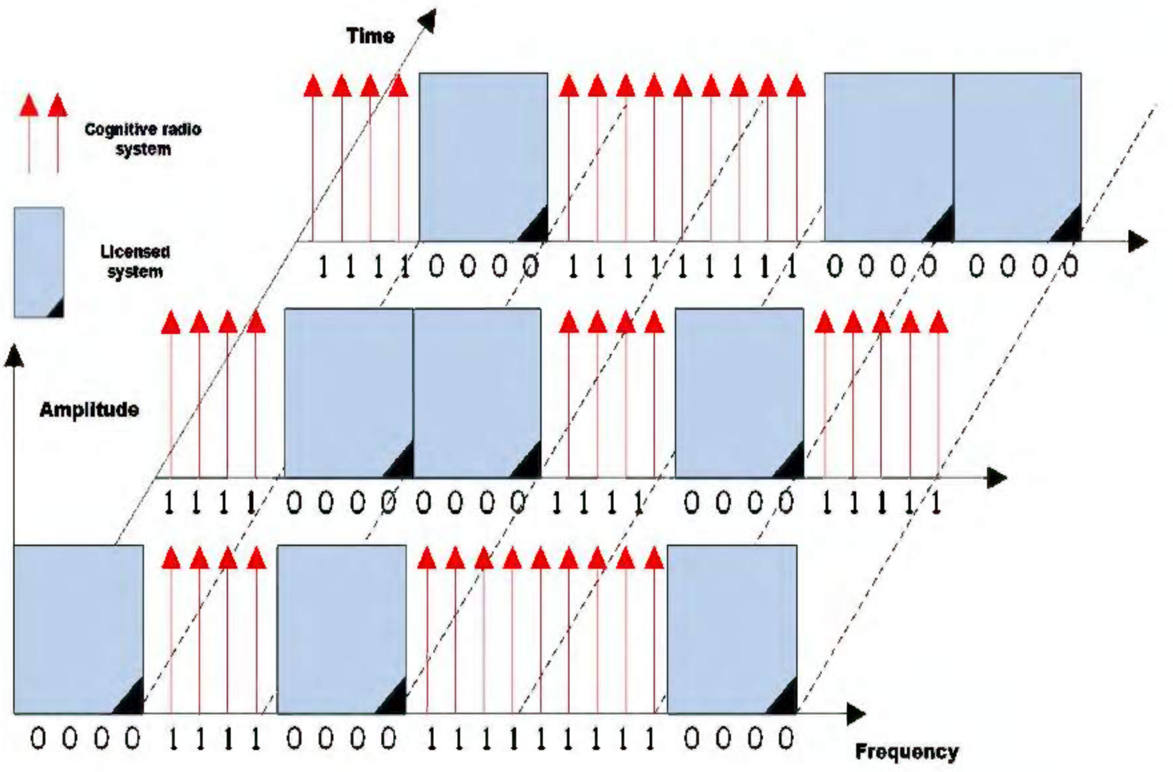

Figure 2. 4 Frequency gap utilization by OFDM based CR system

At the receive side we get the signal as given:

$$\mathbf{y} = \mathbf{h} * \mathbf{x}' + \mathbf{n} + \mathbf{i} \tag{2.18}$$

where $\mathbf{i}$ represents the samples of interference from the licensed system for the duration of one OFDM symbol.

The samples of receiver, noise and channel impulse response are collected in vectors given by:

$$\mathbf{y} = \left[y[0],...,y[k],...,y[N + N_{CP} + 2N_w + \delta - 1] \right]^T \quad (2.19)$$

$$\mathbf{n} = \left[n[0],...,n[k],...,n[N + N_{CP} + 2N_w + \delta - 1] \right]^T \quad (2.20)$$

$$\mathbf{h} = \left[h[\tau_0],...,h[\tau_{m-1}] \right]^T \quad (2.21)$$

The useful part of the received signal is $\mathbf{z}' = \mathbf{h} * \mathbf{x}'$ and so equation (2.18) becomes

$$\mathbf{y} = \mathbf{z}' + \mathbf{n} + \mathbf{i} \quad (2.22)$$

At the receiver initially the CP and $2N_w$ additional samples influenced by windowing at transmitter side are removed, after that the interference is alleviated by windowing the received signal. Finally the additional δ samples for the receiver windowing are removed. By using an appropriate choice of window algorithm the received signal becomes:

$$\mathbf{y}' = \left[y'[0],...,y'[N-1] \right]^T \quad (2.23)$$

The signal in equation (2.23) is then frequency domain by means of FFT given by:

$$\mathbf{Y}' = \left[Y'[0],...,Y'[N-1] \right]^T \quad (2.24)$$

Finally the received data symbols are extracted from frame and processed further.

2.6.2 Design Issues in OFDM based CR systems

For the design of an OFDM based CR system, different restrictions have to be considered in addition to design rules for conventional OFDM systems. The most important parameter is subcarrier spacing. In conventional OFDM systems the bandwidth of the subcarrier spacing is smaller than the coherence bandwidth of the channel and the OFDM symbol duration is smaller than the coherence time of the channel.

This is by choosing the spacing between subcarriers very small and so in conventional OFDM each subcarrier experiences flat fading. The subcarriers spacing are also monitored by licensed system and for simplicity integer multiple of subcarriers are employed in a single channel. For achieving the spectral efficiency and high throughput, number of subcarriers should be very large keeping the characteristics of the signal propagation same as conventional OFDM systems.

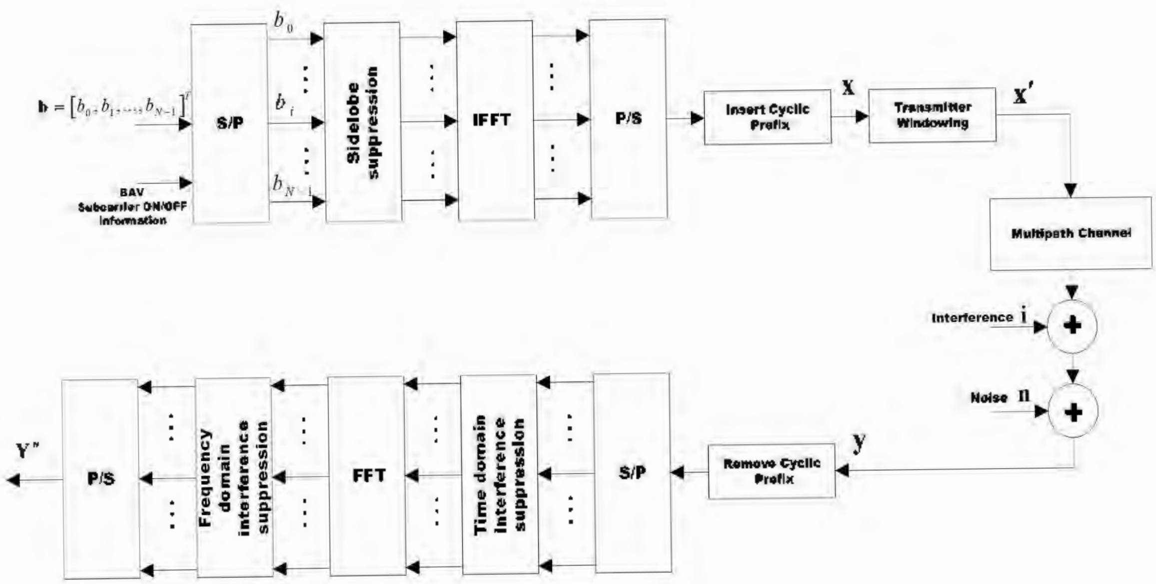

Figure 2. 5 OFDM based Cognitive radio system

From this starting point, other parameters such as the bandwidth, the FFT length, and the OFDM symbol duration are determined. In addition to the above, design constraints related to the spectrum shaping of the transmitted signal and to reduce the interference between the licensed and CR systems have to be taken into account as depicted in Figure. 2.5. In order to achieve these special requirements of CR system, the main issues that have to be considered for the design of physical layer of OFDM system are: Suppression of sidelobes, Interference mitigation, Time and frequency synchronization, channel estimation and the detection of spectrum holes.

Interference suppression from CR systems to the licensed system is very challenging task, because the licensed system transmission should not be interrupted from the transmission of CR system. In OFDM based CR system, the SUs are using those subcarriers that are not in the spectral domain of LUs. As the power of sidelobes of OFDM subcarriers decay with $\frac{1}{f^2 N^2}$, so the sidelobes of those subcarriers enters the region of LUs that results in high OOB radiation, causing a sever interference to the LUs and restricts the use of available spectrum in a well-organized way. So there is a need for some powerful techniques for its reduction in order to maintain a successful coexistence of licensed as well as OFDM based CR system and to use the spectrum efficiently. To handle that issue, different techniques are found in literature that are divided into time domain and frequency domain techniques. Time domain techniques are applied after taking the IFFT of the signal, include windowing, filtering, insertion of guard bands etc.

Vahlin, A., *et al.* [48], has proposed a special type of pulse, generated using optimization procedures, and whose duration is no longer than the duration of one OFDM symbol. Nikookar, H., *et al.* [49], designed an optimal pulse wave form using calculus of variation that leads to differential equation with boundary condition and isoperimetric constraints. Luo, J., *et al.* and Weiss, T., *et al.* [50], [51], has given the idea of using raised cosine filter. El-Saadany, *et al.* [52], proposed Hanning window with active cancellation carriers. Gudmundson, M., *et al.* [53], also proposed Hanning window but with no guard interval, Nikookar, H., *et al.* [54], in his research have compared different type of windows and came in conclusion that half sine have better suppression, Sahin, A., *et al.*[55], proposed different windows for different subcarriers for the controlling of sidelobes, heaving window for the subcarriers located at the edges, while light window for the subcarriers located in the middle of the spectrum. Mahmoud, H. A., *et al.* [56]

proposed an extension of OFDM symbol in time domain and that extension is optimized in adaptive manner based on the transmitted data.

Frequency domain techniques are those that are applied before taking the IFFT of the signal, Yamaguchi, H. [57] proposed the concept of considering the tones placed at the edges as a cancellation tone, instead of turning it off some signal should be transmitted on that edge tone to cancel out the sidelobes. Wang, Z., *et al.* and Qu, D., *et al.* [58], [59], have extended the idea of placing the cancellation tones on the edges. Cosovic, I., *et al.* [60] has given an idea of subcarrier weightings, where the amplitudes of all subcarriers in such a way to cancel out the effect of sidelobes of each other, using optimization having certain constraints, Selim, A., *et al.* [61] has also proposed the idea of subcarriers weightings but using some algorithms for the calculation of amplitudes of the subcarriers. Cosovic, I., *et al.* [62] has given an idea of replacing the actual transmitted sequence from the one that gives maximum suppression of sidelobes. Li, D., *et al.* [63] has proposed an idea of replacing the constellation point for the subcarriers placed on the edges with some other constellation that have maximum effect of sidelobe suppression. Pagadarai, S., *et al.* [4] gave an idea of expanding the constellation point of each subcarriers and chooses the one with maximum sidelobe suppression. Selim, A., *et al.* [64] gave an idea of expanding the constellation points for all subcarriers but using an algorithms to choose the one with maximum sidelobes suppression. Brandes, S., *et al.* [2], [3], [65] and Pagadarai, S., *et al.* [66] have proposed an idea of inserting few subcarriers on the edge of the spectrum, also called as cancellation carriers, whose sidelobes are used for cancellation of the sideobes of the data subcarriers. Zhou *et al* [67] have proposed an idea of calculating amplitude of cancellation carriers using genetic algorithm. Selim, A., *et al.* [5] has also given the concept of cancellation carriers but using algorithm for the adjustment of its weights. Lopes, *et al.* [6] gave an idea of active an inactive subcarriers for the suppression of sidelobes. Weiss, T., *et al.* [51] has given an idea of deactivating the subcarriers on the edges adaptively, creating a guard band between the SU and LU. Ma, M., *et al.* [68] proposed a precoding technique by treating the power leakage as a Frobenius norm minimization problem and then suggesting an optimized precoder based on singular value decomposition. Zhou, X., *et al.* [69], [70] has designed a precoder for multiple CR based users also based on singular value decomposition, Xu, R., *et al.* [71] proposed a precoder based on generalized eigen value problem. Van De Beek, J. *et al.* [72]–[74] proposed a precoder that give the emitted signal's phase and amplitudes. Pandey, A. *et al.* [75] and You, Z. *et al.* [76] have proposed a two level precoder for the suppression of sidelobes.

2.7 Conclusion

This chapter highlights that OFDM based CR system is the best solution to the problem of spectrum scarcity and spectrum underutilization. It has an ability to use the available spectrum in flexible and in efficient way, but it has some drawbacks. One of the major drawbacks is the sidelobes of its subcarriers that results in serious OOB radiation. This OOB radiation causes severe interference to the adjacent SUs and PUs that ultimately disrupts their transmission. Different techniques are found in the literature to tackle this issue but there is a need of some better techniques that reduce the sidelobes in a better way.

Chapter 3

Heuristic Algorithms

3.1 Background

The term heuristic is a Greek word meaning 'to find' or 'to discover', is a terminology used for algorithms, designed for solving a problem quickly and efficiently as compared to the traditional methods in exchange of precision and accuracy, optimality, completeness and time of execution. The advantage of heuristic algorithms (HA) are seen in optimization problems, where finding an optimal solution is impossible or impractical, HA can be used to speed up the process of finding a satisfactory solution. Researchers from almost all field have shown interest in HA, because of its simplicity in concept and in implementation, effectiveness against the variation of the environment etc [77]–[82]. HA are based on the concept of biological evolution i.e. Darwin's theory of evolution, the population based search technique uses genetic operators including crossover, mutation, inheritance and selection. The advantages of HA over traditional optimization techniques are its wide range of application, Hybridization, ease of concept, parallelism, capability of solving a problem having no solution and adaptiveness to dynamical changes etc [83]–[90]. There are many HA are found in the literature, few of them are listed below:

- Genetic algorithm
- Firefly algorithm
- Differential algorithm
- Cuckoo search algorithm

- Particle swarm optimization
- Ant colony optimization
- Bee colony optimization
- Cultural algorithm
- Pattern search algorithm
- Backtracking search algorithm
- Fire algorithm
- Bat algorithm
- Harmony search algorithm
- Evolutionary programming
- Self-organizing migration algorithm

Throughout this chapter, we will restrict our discussion to GA, FFA, DE and CSA.

3.2 Genetic Algorithm

The concept of GA was initially given by John H. Holland in 1975 in his work for presenting an easy solution of natural selection [91]–[93]. One of the main advantage of GA is that it cannot be struck in local minima, always gives a suitable result for those problems, which cannot be dealt easily by other methods, or that do not have a mathematical model, or that have a complex mathematical model, or the parameters involve in problem are huge in number. Recently, GA has been very much successful in solving different optimization problems in various field of engineering [94]–[101] .

GA is repetitive technique that initiates with the randomly generation having fixed number of individuals called population. This population represent the possible solution to the problem under consideration. The individuals in population are called as chromosomes, each chromosome contain fixed number of genes. The number of genes represents the length of each chromosomes. After the generation of population, a stochastic selection operator select the best solution through each generation. These selected solutions through selection forms a new set of individuals called parents that will now participate in the left over evolution process. For finding the best solution, the parent chromosomes will employ the process of mutation, elitism and cross over etc. whose outcome constitute a new set of individuals called children (offspring's). The process will keep on until a number of iteration has completed or best individual has been selected. The flow chat of GA is depicted in Figure. 3.1, while the procedural steps of GA are given as under.

Step I Initialization: This step is common in all HA, because every HA needs a set of individuals that contain a possible solution of a problem being solved by that algorithm. So in this step the individuals that makeup the population are generated randomly, having no constraint about the size of population.

Step II Fitness Evaluation: The fitness function is the most important part of all HA, as the performance and result of an algorithm mainly dependent on design of fitness function and is problem specific. One can get the optimum result, if it is properly designed. In this step the fitness of each individual is evaluated and is placed in order of descending order of their fitness.

Step III Parent selection and Offspring production: Individuals sorted out in previous step are now parents to the next generation. The probability of producing next generation are proportional to fitness of the parents. This production is done with cross over (single point cross over, multiple point cross over). More children will be produced by parent having higher fitness and vice versa. In this there could be two approaches.

1. Select those parents, whose probability is inversely related to their fitness and ask them produce.

2. Using roulette wheel method, whose angle of the sector is directly related to the fitness. The sector with a bigger angle has more chance to win as better parent.

Step IV Generating the new population: Children for next generation is selected by three methods that are Elitism, replacement of generation and survival of the fitness.

(a): Replacement of generation: In this process, the parents are completely replaced by their children. This process allow for a thorough mixing of genes but there is no guarantee that whether all the children or most of them will be better from their parents, will result in degradation because of losing the individual having best genes.

(b): Elitism: In this process, to tackle the handicap of the replacement of generation, some of the best individuals should be retained from the previous generation.

(c): Survival of fitness: In this process, sort out the parents and children according to descending order of their fitness.

Step V Mutation: In this process, when no improvement of fitness is noticed in the next generation, then the only solution is mutation. In mutation genes of individuals are changing randomly.

Step VI Termination criteria: The program of GA will terminate if the maximum number of iteration has reached or the required mean square error (MSE) is achieved.

else go to step II.

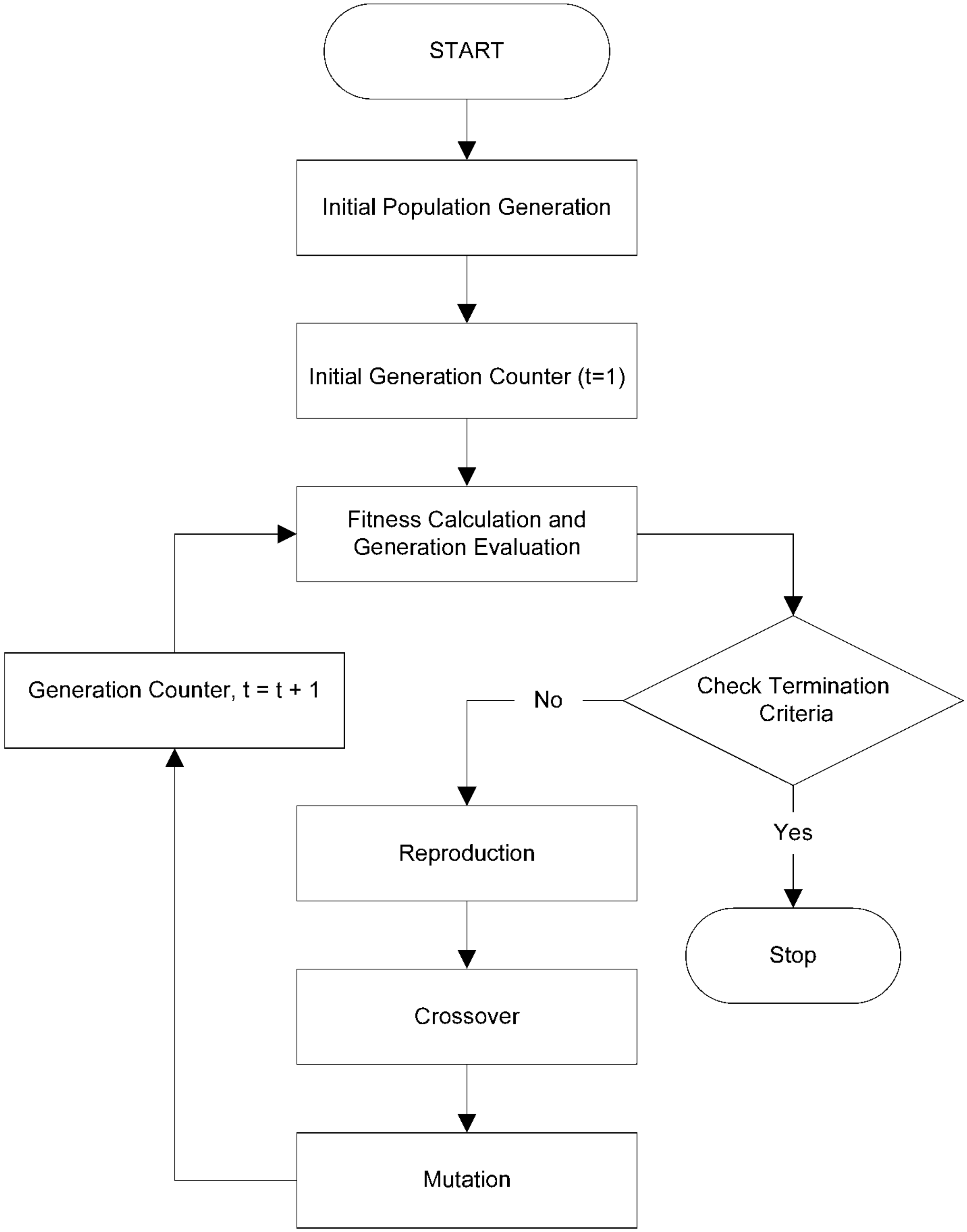

Figure 3. 1 Flow chart of GA

3.3 Firefly Algorithm

Swarm Intelligence (SI), motivated from the joint activity of collective group of ants, termites, bees, worms, flock of birds, and schools of fish and has gain attention during the last decade [102]. However these group contains rather naïve individuals that shows so much organized activity that leads them to their required destinations. Normally this results in the self-arranging activity of the entire structure, and their joint intelligence is basically the self-arrangement of such multi-agent systems that are based on simple rules of cooperation. Such an organized activity is accomplished as a result of communication among the individuals, e.g. termites and worms are capable of building complex nests etc [103].

SI related to area of research that is concerned with a joint activities with in self-organized and dispersed systems. This term was first used by Beni in the context of cellular robotic systems [104]. Now a days, swarm intelligence are used in optimization, robots controlling, routing and load balancing in new-generation mobile networks, whose demands are robustness and flexibility.

FFA, is a swarm intelligence algorithm developed by Yang in 2007 [105]. It is a population based, meta-heuristic algorithm, developed to solve the optimization problem. It resembles to other meta-heuristic algorithm like particle swarm optimization, simulated annealing and genetic algorithm etc. but the performance of FFA is found better in many cases [106]–[112]. It has attracted much attention in research community during the last decade and is applied in many fields [107], [113]–[119]. It is motivated by the flashing behavior of fireflies and is based on three rules [105], [120]: According to first, all fireflies are unisex, and they will move towards each other regardless their sex. Second their attractiveness is depending on the brightness of each firefly which is distance dependent i.e. brightness is inversely proportional to the distance. The more brightness the less distance and so more attraction and vice versa. Third the value of fitness function determined the brightness of firefly. The flow chart of FFA is shown in Figure.3.2 while the important steps are summarized as.

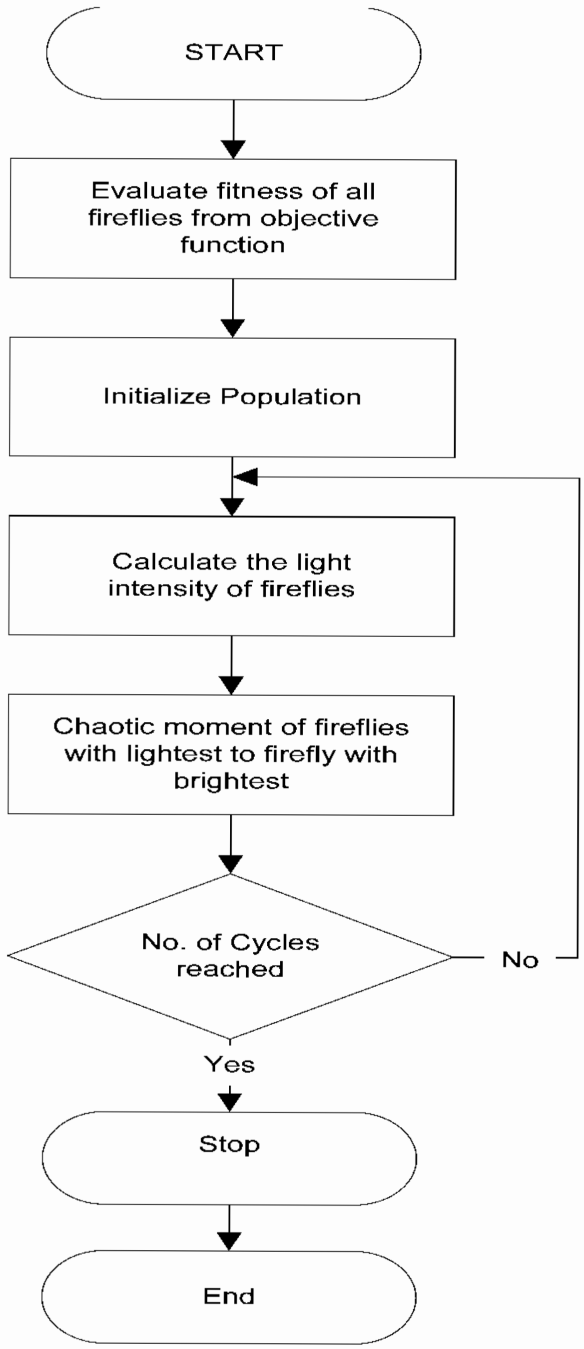

Figure 3. 2 Flow chart of FFA

Step I initialization: Consider K_f represents the total number of fireflies in a given population space, whereas $\mathbf{w}_i$ represents the locality of ith firefly.

$$\mathbf{w}_i = \left(w_i^1, w_i^2, \ldots w_i^t, \ldots w_i^{N_f} \right) \tag{3.1}$$

where $i = 1, 2\ldots K_f$ and $t = 1, 2\ldots N_f$.

$$w_i^t = w_L^t + (w_H^t - w_L^t) \times rand() \tag{3.2}$$

Equation (3.2) generates the initial localities of K_f fireflies in N_f dimensional space using uniform distribution. Where w_H^t and w_L^t represent the upper and lower limit.

Step II Fitness Function: Calculate the fitness of the locality of each firefly in the given population. Categorize the population from the brightest to lightest. The brightness of each firefly are calculated at the current generation by the fitness function at the current locality.

Step III Updation of the location of firefly: The locality of each firefly in the population depends on the attractiveness, and each firefly in the population will move toward the adjacent firefly with more light intensity and its position is updated for the next generation. The firefly i with less intensity will move toward the other fireflies j that are brighter. There are two significant concerns in the FFA, the deviation of brightness and the formation of attractiveness. The attraction of a firefly is calculated by its brightness, directly related to the cost function. The brightness of the ith firefly B_i is given by

$$B_i = f_{fitness}(w_i) \tag{3.3}$$

The attractiveness between ith and jth firefly is given by:

$$\beta_{ij} = \beta_o exp(-\gamma r_{ij}^2) \tag{3.4}$$

Here β_o = 1, and r_{ij} represents the distance between w_i and w_j as:

$$r_{ij} = \left\| w_j - w_i \right\| = \sqrt{\sum_{n=1}^{N} \left(w_j^t - w_i^t \right)^2} \quad (3.5)$$

The location of the firefly is updated at each iterative step. If the brightness of *j*th firefly is more than *i*th firefly, then the *i*th firefly will move towards the *j*th firefly, and its motion is denoted by:

$$w_n = w_n + \beta_{ij}(w_j - w_i) + \alpha\varepsilon_n \quad (3.6)$$

Step IV Ranking and computation of global best: On the basis of the brightness of fireflies, they are categorized in the current generation. The comparison of fireflies on the basis of brightness is done and the position of brightest firefly in the current population is considered as global best. In this way the brightest firefly will receive best fitness function for the next generation.

Step V Termination of Program: When the fitness function succeeds in getting the required value or when reached the maximum number of cycles stop, otherwise go to Step II.

3.4 Differential Evolution

DE, emerges as one of the most powerful and effective global search optimization algorithm during the last two decades. The first article on DE was written by Storn and Price in 1995 [121]. It has got an attention of the researchers because it is simple and easy to implement, it show much better performance as compared to the other algorithms like GA, Simulated annealing (SA) etc. it has an ability to handle unimodal, multimodal, non-linear, non-differentiable types of problems. It is accurate, has excellent convergence towards the global minimum and robust against noise [122]. Additionally, it is very effective towards the discrete, as well as, constrained problems, and is easily applied to almost every field of science and engineering [123]–[129]. DE searches for the large possible spaces having candidate solutions and using straight formulas for the creation of new and improved solutions. Now, it will keep only those candidate solutions which have best score or fitness of the under consideration optimization problem. DE is basically the combination of GA, Genetic programming (GP) [130] and evolutionary programming (EP) [131]. The main operation of DE is depending on mutation, crossover and selection operator, but their organization is different from GA. The main role of DE is with mutation, while its performance are depending on its variants. The average fitness function of DE is increasing or decreasing gradually without any use of elitism. The flow chart of DE is shown in Figure.3.3, while its steps of algorithms are given as:

Step I Initialization: The first step of DE is the initialization of randomly generated population of *N* vectors.

$$\mathbf{s}_d^{n,G} = L + rand(\mathrm{H} - L) \tag{3.7}$$

Where $1 \leq n \leq N$, $1 \leq d \leq D$, Here n = Chromosome number, d = Gene number, G = Generation number, H = Upper limit, L = Lower limit.

Step II Updating: Upgrade all the chromosomes of the current generation "*G*". Let us choose *n*th chromosome $\mathbf{s}_d^{n,G}$. The main job is to find the chromosome of the next generation $\mathbf{s}_d^{n,G+1}$ we will follow the steps given by

(a) ***Mutation:*** Select three numbers (r_1, r_2, r_3) from the population having constraint that they are all distinct and also not equal to *n*.

$$\mathbf{u}_d^{n,G} = \mathbf{s}^{r_1,G} + F(\mathbf{s}^{r_2,G} - \mathbf{s}^{r_3,G}) \tag{3.8}$$

Where F is called as mutation factor, it is problem dependent and it should be smartly placed keeping the value of genes between L and H. and $\mathbf{u}_d^{n,G}$ is called as mutant vector.

(b) ***Crossover:*** Here the mutant vector and the current generation members are allowed to cross over to create another population as:

$$\mathbf{w}_d^{n,G} = \begin{cases} \mathbf{u}_d^{n,G} & if \quad rand() \leq C_r \text{ (or) } J = J_{rand} \\ \mathbf{s}_d^{n,G} & Otherwise \end{cases} \tag{3.9}$$

Where C_r = cross over rate is normally taken near to 0.5 either above or below.

(c) ***Selection operation:*** In this the chromosomes of the next generation are generated by using the following equation:

$$\mathbf{s}^{n,G+1} = \begin{cases} \mathbf{w}^{n,G} & if \quad f(\mathbf{w}^{n,G}) < f(\mathbf{s}^{n,G}) \\ \mathbf{s}^{n,G} & Otherwise \end{cases} \tag{3.10}$$

Step III Termination Criteria: The termination of a program is depending on the following conditions given below

1. If $f\left(\mathbf{s}^{n,G+1}\right) < \varepsilon$ or
2. Required number of generation has reached

Otherwise go back to step II.

3.5 Cuckoo Search Algorithm

CSA, is a new metaheuristic algorithm, developed by Yang and Deb in 2009 [132]. It is inspired by the breeding characteristics of some specific class of cuckoo combined with the features of Levy flight of some birds and fruit flies. It is used in almost every field of science and engineering [133]–[137]. First we will discuss the breeding behavior of cuckoo and characteristics of Levy flights and then discuss the CSA.

Cuckoos birds are very attractive, because of its sound and its offensive reproductive approach.

Ani and guira, two specific class of cuckoo, can lay their eggs in a neighboring nests, and can take away other's eggs for increasing the chance of hatching of its own eggs. Actually a number of other class of cuckoos are engaged in the obligate brood parasitism, can lay eggs in the nests of other host birds (often other species).

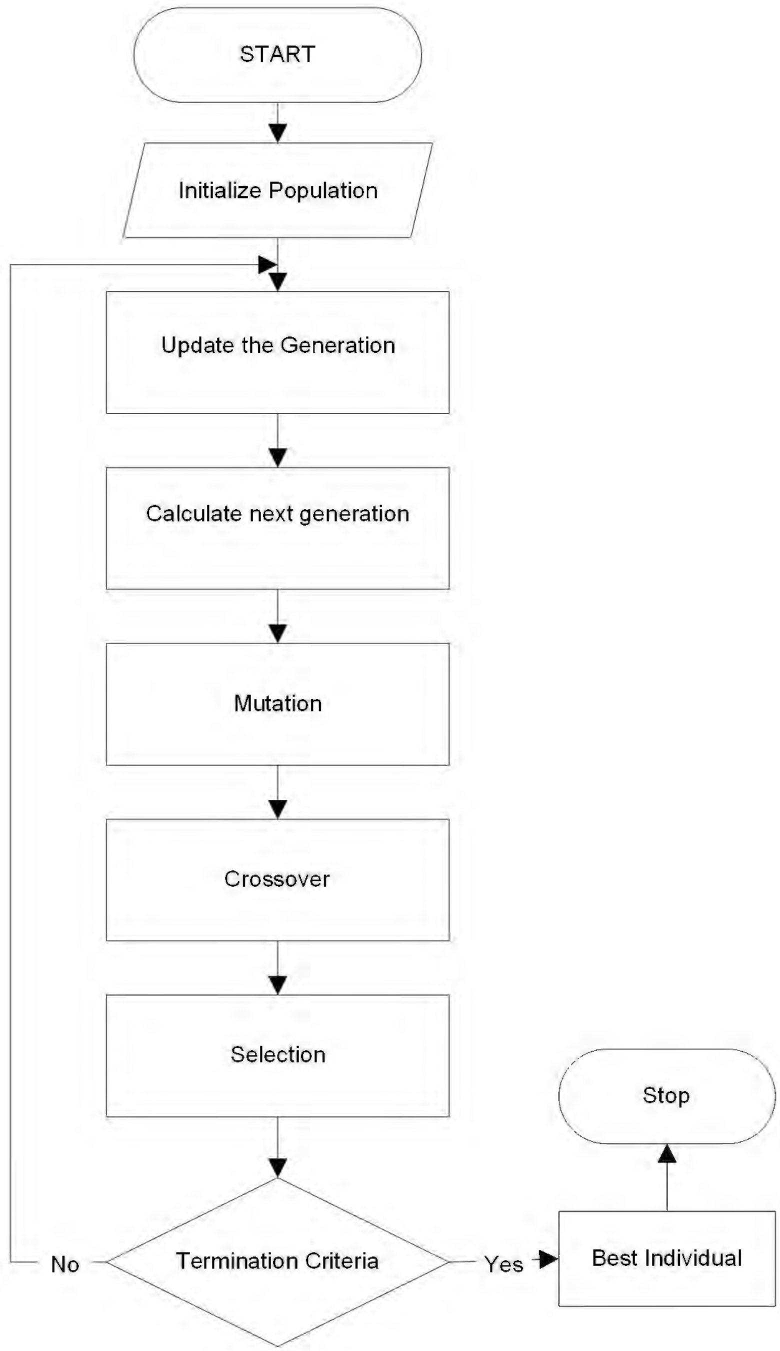

Figure 3. 3 Flow chart of DE

Intraspecific brood parasitism, cooperative breeding, and nest takeover, are the three types of brood parasitism.

Some of the other birds are in constant conflict with the cuckoos those lay eggs in their nests. If they notice an alien egg in their nest, they will either discard that egg or their nest. There are some other class of cuckoo that can lay their eggs in a host bird nest, whose eggs resembles their own egg. In this way it can save their eggs from danger of being discarded and so maximize their reproductively. The timings of some cuckoos regarding their laying eggs are very amazing, they can select a nest where the host bird just laid its own eggs. As a result the cuckoo egg will be hatched earlier than the host egg, after that it will try to remove the host eggs from the nest that maximized the cuckoo chick's share of food provided by its host bird [138].

All animals can wander unsystematically here and there in a search of food and the path in which it wander for food is effectively a random walk, because the next move is based on the current location/state and the transition probability to the next location.

Which direction it chooses depends implicitly on a probability which can be modeled mathematically. For example, various studies have shown that the flight behavior of many animals and insects has demonstrated the typical characteristics of Levy flights[139]–[144].

CSA are based on the following three rules:

1. Each cuckoo lays an egg at a time in a randomly selected nest.
2. Next generation candidates are those nests having eggs with high quality.
3. Number of host nests will be fixed and the probability of discovering the cuckoo egg by the host bird is 0 or 1. In such a situation that discovered egg will be thrown away or the nest will be discarded to make a new one.

In this work generating a new solution x_n^{k+1} for a cuckoo *n*, a Levi flight for a search capability is performed:

$$x_n^{k+1} = x_n^k + \alpha \oplus Levy(\lambda) \tag{3.11}$$

Here α represents the step size whose value is greater than 1. The Levy flight provides a random walk and a random step length is from a Levy distribution having an infinite variance:

$$Levy(\lambda) = k^{-\lambda} \tag{3.12}$$

The flow chart of CSA is given in Figure. 3.4 and its algorithmic step of cuckoo in pseudocode is given as:

Start

Objective function $f(\mathbf{s})$, $\mathbf{s} = (s_1, s_2, ..., s_d)^T$

Initiate the population of N host nests

while*(maximum no. of generation reached or stopping criteria)*

Get a cuckoo randomly by Levy flights

Evaluate the fitness F_n

Randomly select nest j

If $F_n < F_j$ *then interchange j with a new solution*

end

The least favorable nests are discarded and built new ones.

Favorable nests are kept

Rank the nests and find the best one

end while

Postprocess results and visualization

End

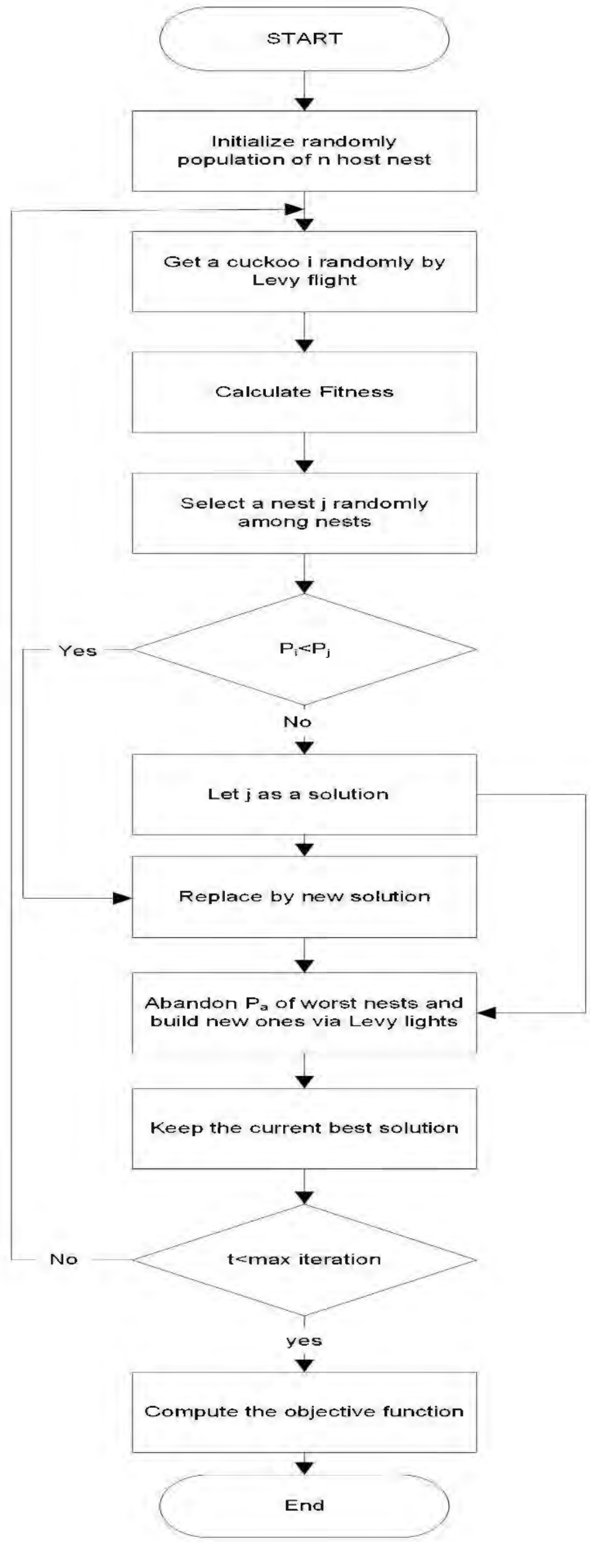

Figure 3. 4 Flow chart of CSA

3.6 Conclusion

In this chapter the comprehensive detail of some selected heuristic algorithms, used in this thesis that includes GA, FFA, DE and CSA are given.

Chapter 4

Reduction of out of Band Radiation using Heuristic Algorithms

4.1 Introduction

As concluded in chapter 2, one of the most undesirable feature of OFDM based CR system that prevents the SUs from the use of available spectrum holes efficiently and in a well-organized way and to maintain the effective coexistence between SUs and PUs are the sidelobes of their subcarriers. These sidelobes result in a high OOB radiation that is a cause of severe interference between SUs and PUs. Different techniques for the suppression of the sidelobes are found in literature, but there is a need for some more powerful techniques that reduce the sidelobes effectively.

In this chapter, CCs based sidelobe suppression technique for the reduction of sidelobes is presented. A few number of CCs are placed on the edges of the used OFDM spectrum, which are not used to carry information, but have some complex weights (amplitudes of the main lobe of the CCs), that are calculated in such a way that their sidelobes cancel the sidelobes of the transmitted OFDM spectrum in a specific defined region called as optimization range. For the calculation of those complex weights, we have proposed different heuristic algorithms: GA, DE, FFA and CSA using our proposed fitness function for achieving better suppression of sidelobes.

4.2 Data Model

Consider an OFDM system having total of M SUs that opportunistically using a spectrum not utilized by a LUs, which is identified with the help of spectrum sensing techniques. The total available spectrums are divided into N subcarriers out of which N_s subcarriers are utilized by ith SU, such that $N_s \subseteq N$. The baseband OFDM signal for ith SU is given by:

$$x_s(t) = \sum_{n=0}^{N_s-1} q_{n,s} e^{j2\pi f_n t} I(t) \tag{4.1}$$

Where $x_s(t)$ represents the OFDM signal of ith SU, $q_{n,s}$ represents the modulated symbol on nth subcarrier, $f_n = \frac{n}{T}$, $n = 0,1,...,N_s$ represents the subcarrier frequencies, while $I(t)$ represents the rectangular function defined as:

$$I(t) = \begin{cases} 1 & -T_g \le t \le T_s \\ 0 & otherwise \end{cases} \tag{4.2}$$

Where T_g represents the guard interval length for the elimination of ISI and T_s represents the symbol duration.

After taking the Fourier transformation of the signal given in equation (4.1), we get the transmitted OFDM signal for ith SU in frequency domain, whose sidelobe power in the frequency bands of the adjacent LUs decays with $\frac{1}{f^2 N_s}$ results in high OOB radiation as shown in Figure. 4.1. mathematically it is given by:

$$X_s(f) = \sum_{n=0}^{N_s-1} q_{n,s} \sin c\left(\pi\left(f - f_n\right)T^{'}\right) \quad (4.3)$$

Where $T^{'} = T_s + T_g$ represents the symbol duration, while $\sin c\left(x\right) = \frac{\sin\left(\pi x\right)}{\left(\pi x\right)}$.

To protect the LUs that may be present in the neighbouring spectrum hole of the *i*th SU, the sidelobes of the *i*th SU from both sides should be suppressed effectively.

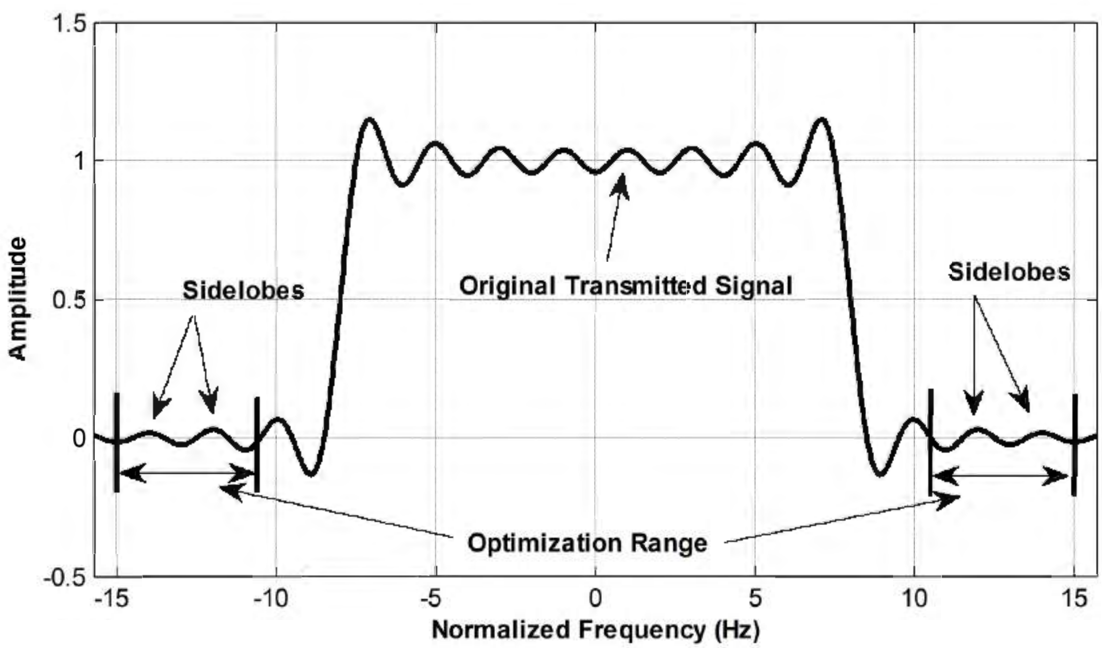

Figure 4. 1 Transmitted OFDM signal in frequency domain

4.3 Cancellation carriers based suppression of sidelobes

In this section, CCs based sidelobe suppression technique is used for the suppression of sidelobes of the original transmitted OFDM signal of *i*th SU. Consider we insert total $K = K_l + K_r$ number CC*s* on both the edges of the OFDM spectrum of the *i*th SU, where K_l and K_r represent the number of left and right sided CC*s*. As a result the total number of subcarriers is now increased to $N_s + K$. The spectrum of the m*th* CC is given by:

$$c_m(\alpha) = a_m \sin c\left(\pi\left(\alpha - \lambda_m\right)\right),\ m = 1, 2, \ldots K \tag{4.4}$$

Where $\alpha = \left(f - f_o\right)T_s$ while λ_m representing the normalized centre frequency of the m*th* CC that lies on either side of the OFDM spectrum given as:

$$\lambda_m = \begin{Bmatrix} \left(f_{1-m} - f_o\right)T_s & m = 1, 2, \ldots, K_l \\ \left(f_{N_s+m-K_l} - f_o\right)T_s & m = K_l + 1, \ldots, K \end{Bmatrix} \tag{4.5}$$

Where $a_m \in \mathbf{a} = \left[a_1, a_2 \ldots a_K\right]^T$ represents the amplitude of the main lobe of the *m*th CC that should be so adjusted that the sidelobes of these CC*s* cancel out the sidelobes of the original OFDM spectrum of *i*th SU in a certain region called as optimization range. The final signal with CCs is shown in Figure. 4.2 and mathematically it will be represented as:

$$T = \left(\sum_{m=0}^{\frac{K}{2}-1} a_m \sin c\left(\pi\left(\alpha - \lambda_m\right)\right) + \sum_{n=0}^{N_s-1} q_{n,s} \sin c\left(\pi\left(f - f_n\right)T_s\right) + \sum_{m=\frac{M}{2}}^{K-1} a_m \sin c\left(\pi\left(\alpha - \lambda_m\right)\right)\right) \tag{4.6}$$

The amplitudes of these CCs are calculated by using different heuristic algorithms: GA, DE, FFA and CSA based on our proposed fitness function.

4.4 Fitness Function:

The basic concept behind our fitness function is that, the amplitude of the main lobe of each CC is calculated by using the mean value of the sample points taken in optimization range. To decrease the computational complexity and usage of memory, these sample points are considered as the middle value of each sidelobe of the information subcarriers. The final result of our fitness function is the total OOB radiation of the sample points calculated after the insertion of all the CCs.

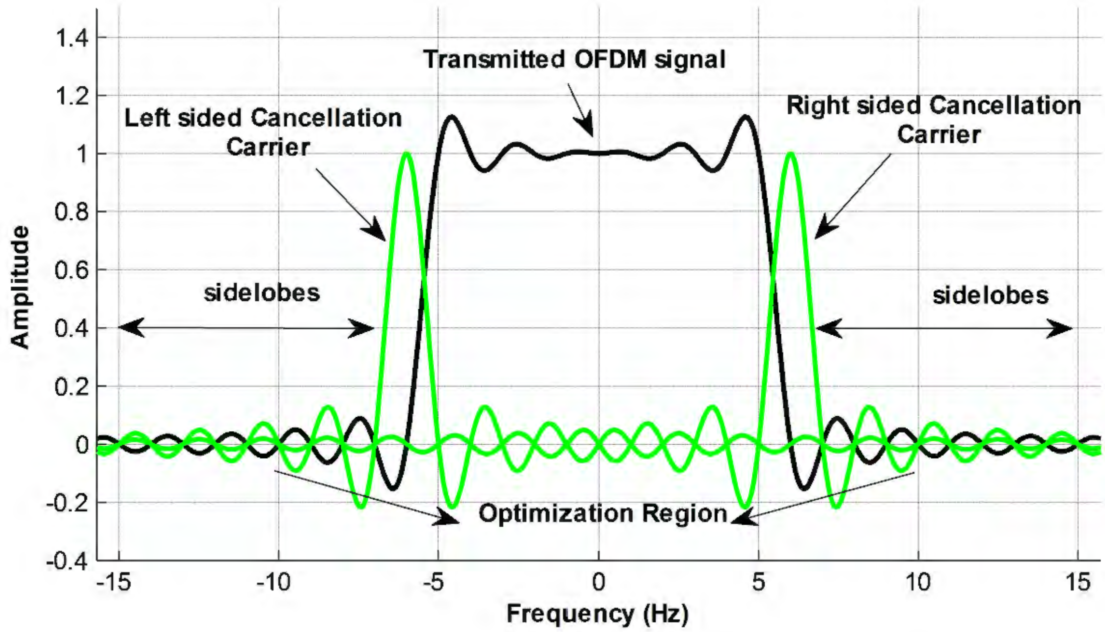

Figure 4. 2 Concept of CCs

$$A_{Cj} = \left(\sum_{m=0}^{\frac{K}{2}-1} A_{C(m,j)} a_m + \sum_{m=\frac{K}{2}}^{K-1} A_{C(m,j)} a_m \right) \tag{4.7}$$

$$A_{Dj} = \left(\sum_{n=0}^{N_s-1} A_{D(n,j)} d_n \right), \; j = 1, 2, \ldots M \tag{4.8}$$

where M represents the total number of samples taken in the optimization space. Equation (4.7) represents the sum of the amplitudes of m left and m right CC at jth sample points, while Equation (4.8) represents the sum of the amplitudes of n data carriers at jth sample point.

The resulting amplitude of the signal at *j*th sample point is due to the addition of all data carriers and CC is given by:

$$A_j = A_{Dj} + A_{Cj} \tag{4.9}$$

On putting the values of A_{Dj} and A_{Cj} from equation (4.7) and (4.8) in equation (4.9) results:

$$A_j = \left(\sum_{m=0}^{\frac{K}{2}-1} A_{C(m,j)} a_m + \sum_{n=0}^{N_s-1} A_{D(n,j)} d_n + \sum_{m=\frac{K}{2}}^{K-1} A_{C(m,j)} a_m \right) \tag{4.10}$$

The final fitness will now developed as:

$$A = \left(\frac{1}{M} \sum_{j=1}^{M} A_j \right) \tag{4.11}$$

4.5 Results and Discussion

In this section, we consider five different cases to check the efficiency and authenticity of the proposed heuristic algorithms: GA, FFA, DE and CSA discussed briefly in chapter 3. These cases are based on the number of available spectrum holes and the spacing between these holes. The performance comparison of the proposed heuristic algorithms with the existing techniques found in the literature and between them in term of PSD are discussed. The parameter settings for FFA that include initial light intensity, initial attractiveness, the light absorption and randomization parameters, while parameter settings for CSA that include population size, no. of generation, step size and discovery rate are given in Table 4.1. The parameter settings for GA that include population size, number of generations, migration direction, crossover function, crossover, function tolerance, initial range, scaling function, selection, elite count and mutation function are given in Table 4.2 respectively.

4.5.1 Case I

In this case, we have assumed that CR detects a single spectrum hole and is occupied by a single SU. Total number of subcarriers utilized by a SU in that single spectrum hole is 16, in which e.g. a 64 – point FFT is applied for OFDM modulation. Every subcarrier is modulated with a Binary phase shift keying (BPSK) symbol whose power is normalized to 1. We consider two CCs each are inserted on the left and right side of the used OFDM spectrum. Ten sidelobes are taken on both sides of the spectrum with one frequency sample taken in the middle of every sidelobe in the optimization range, result in $M_l = M_r = 10$ sample points.

Table 4. 1 Parameter settings for FFA and CSA

FFA		**CSA**	
Parameters	**Settings**	**Parameters**	**Settings**
Initial light intensity	0	Population size	80
Initial attractiveness	1	No. of generation	250
The light absorption	1	Step size	1
Randomization parameter	0.2	Discovery rate	0.25

The performance, reliability and efficiency of our proposed algorithms for this case I are shown with the help of computer simulations in terms of PSD and compared the results with each other and with different existing techniques . These simulated results show that our proposed algorithms outclass all the existing techniques.

4.5.1.1 Performance of GA

In this section, GA is used for the calculation of amplitudes of the main lobe of the CCs that uses our proposed fitness function discussed in section 4.4. The amplitudes of CCs calculated with the help of GA for case I are given in Table. 4.3. The performance of GA in term of PSD with the existing techniques found in literature is shown in Figures. 4.3 – 4.4 respectively. Simulation results shows that with the help of GA sidelobe suppression upto -55.5 dB on left and -52.5 dB on right side of spectrum is achieved which is better as compared to the existing techniques found in the literature.

Table 4. 2 Parameter settings for GA

GA	
Parameters	**Settings**
Population size	240
No. of generations	1000
Migration direction	Both way
Crossover fraction	0.2
Crossover	Heuristic
Function tolerance	1e-6
Initial range	[0,1]
Scaling function	Rank
Selection	Stochastic uniform
Elite count	2
Mutation function	Adaptive feasible

Table 4. 3 Amplitudes of CCs calculated using GA (Case I)

Amplitudes of left and right sided cancellation carriers (CC*s*)				
Technique used	**First left CC**	**Second left CC**	**First right CC**	**Second right CC**
GA	0.13009249	0.61528217	0.61528217	0.13009249

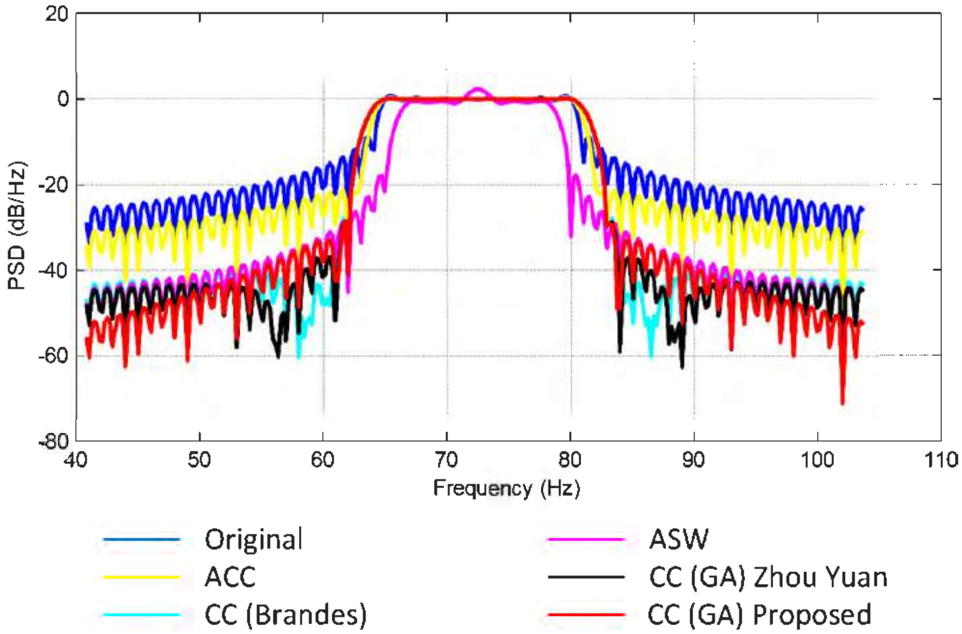

Figure 4. 3 Spectrum of OFDM signal of single SU; Comparison of GA with existing techniques; N_s = 16 data carriers; K_l = K_r = 2 CCs; $q_{n,s}$ = 1, n = 0, 1, … , N_s – 1; Case I

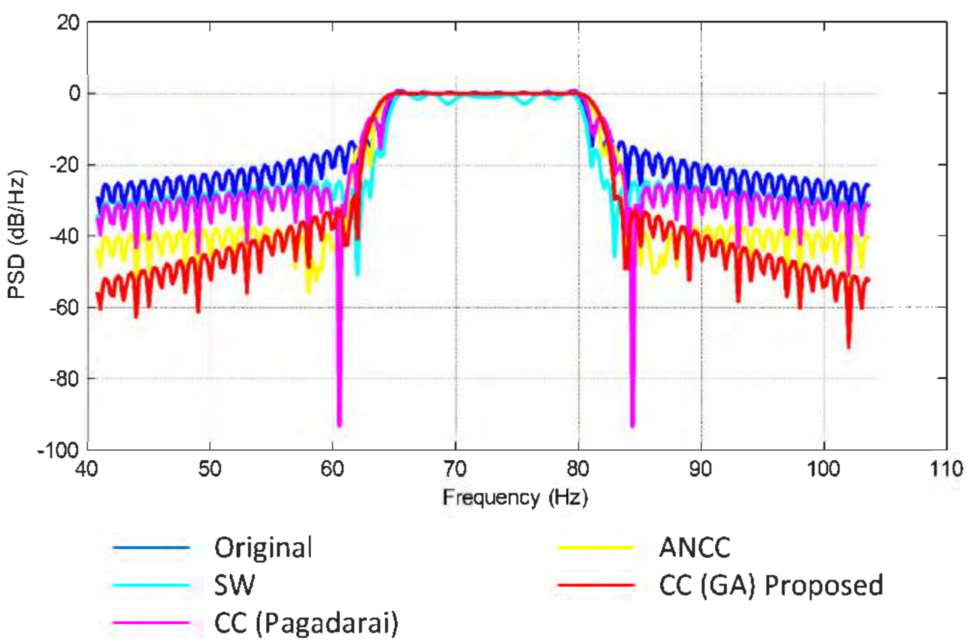

Figure 4. 4 Spectrum of OFDM signal of single SU; Comparison of GA with existing techniques; N_s = 16 data carriers; Total K = 4 CCs are used on both sides; $q_{n,s}$ = 1, n = 0, 1, … , N_s – 1; Case I

4.5.1.2 Performance of FFA

In this section, FFA is used to calculate the amplitudes of the main lobe of CCs, by using the fitness function discussed in section 4.4. Amplitudes of CCs calculated with the help of FFA are given in Table 4.4. The effectiveness and performance of FFA with the help of computer simulations are shown in Figures. 4.5 – 4.6, shows that sidelobe suppression upto -57 dB and -54 dB on left and right side of spectrum is achieved which is better as compared to the existing as well as GA.

Table 4. 4 Amplitudes of CCs calculated using FFA (Case I)

Amplitudes of left and right sided cancellation carriers (CC*s*)				
Technique used	**First left CC**	**Second left CC**	**First right CC**	**Second right CC**
FF**A**	0.12678163	0.61126778	0.61126778	0.12678163

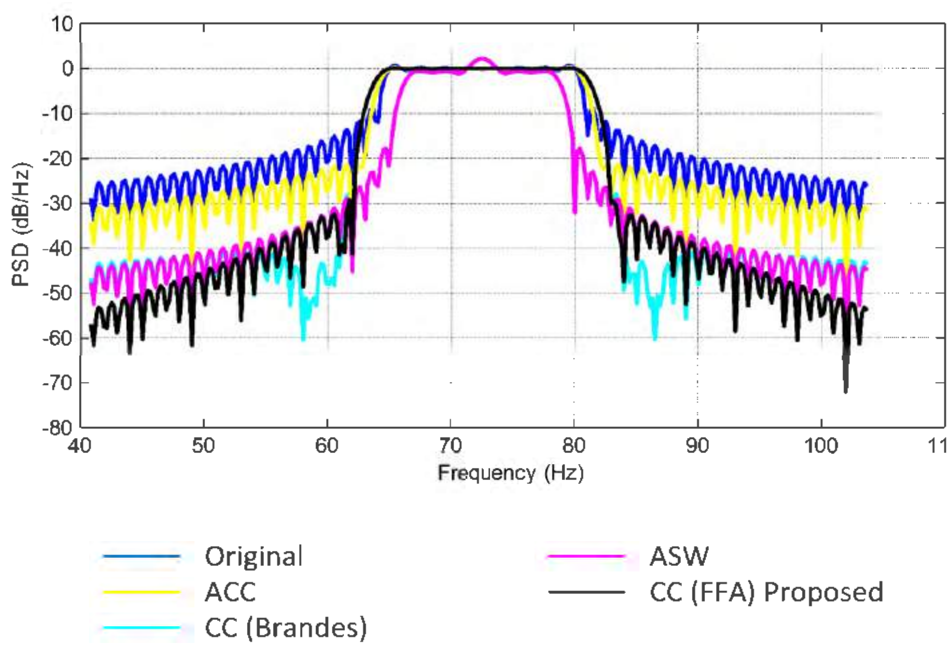

Figure 4. 5 Spectrum of OFDM signal of single SU; Comparison of FFA with existing techniques; N_s = 16 data carriers; $K_l = K_r$ = 2 CCs; $q_{n,s}$ = 1, n = 0, 1, … , N_s – 1; Case I

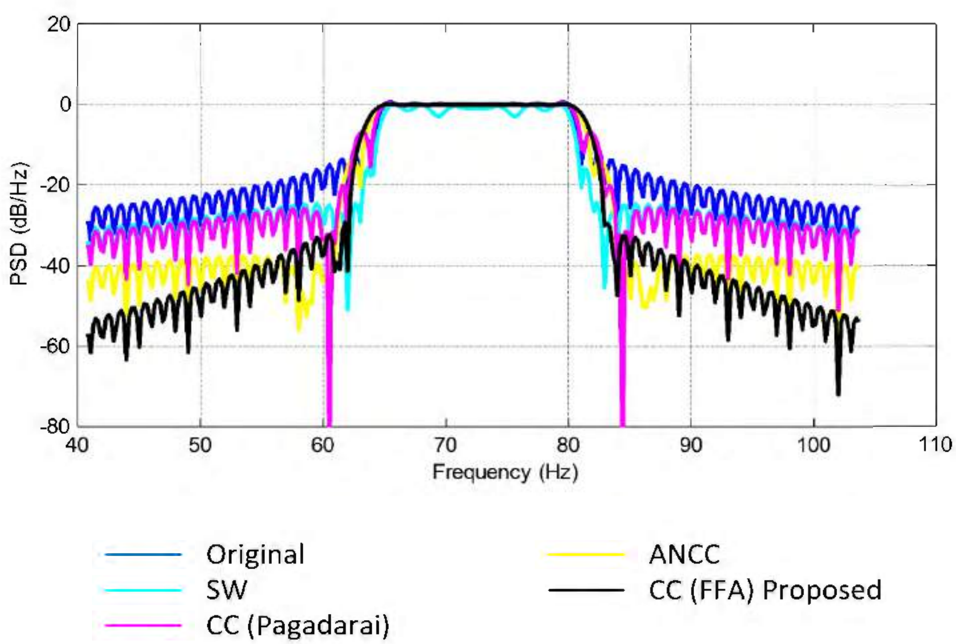

Figure 4. 6 Spectrum of OFDM signal of single SU; Comparison of FFA with existing techniques; N_s = 16 data carriers; Total K = 4 CCs are used on both sides; $q_{n,s}$ = 1, n = 0, , … , N_s – 1; Case I

4.5.1.3 Performance of DE

In this section, we will discuss the performance and effectiveness of DE in term of PSD and compare it with the existing techniques found in the literature and are shown in Figures. 4.7 – 4.8. The amplitudes of CCs calculated by using DE are given in Table 4.5, using our fitness function. Simulations results shows that with DE -65.5 dB and -62 dB suppression is achieved on the left and right sidd of the spectrum.

Table 4. 5 Amplitudes of CCs calculated using DE (Case I)

Amplitudes of left and right sided cancellation carriers (CC*s*)				
Technique used	**First left CC**	**Second left CC**	**First right CC**	**Second right CC**
DE	0.12727316	0.61115280	0.61115280	0.12727316

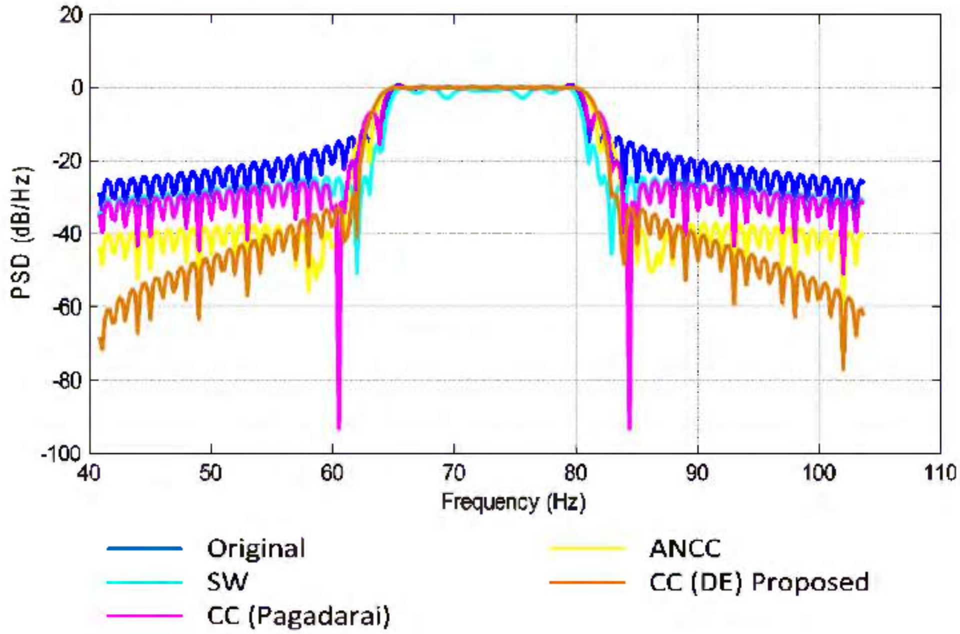

Figure 4. 7 Spectrum of OFDM signal of single SU; Comparison of DE with existing techniques; N_s = 16 data carriers; $K_l = K_r$ = 2 CCs; $q_{n,s}$ = 1, n = 0, 1, … , $N_s - 1$; Case I.

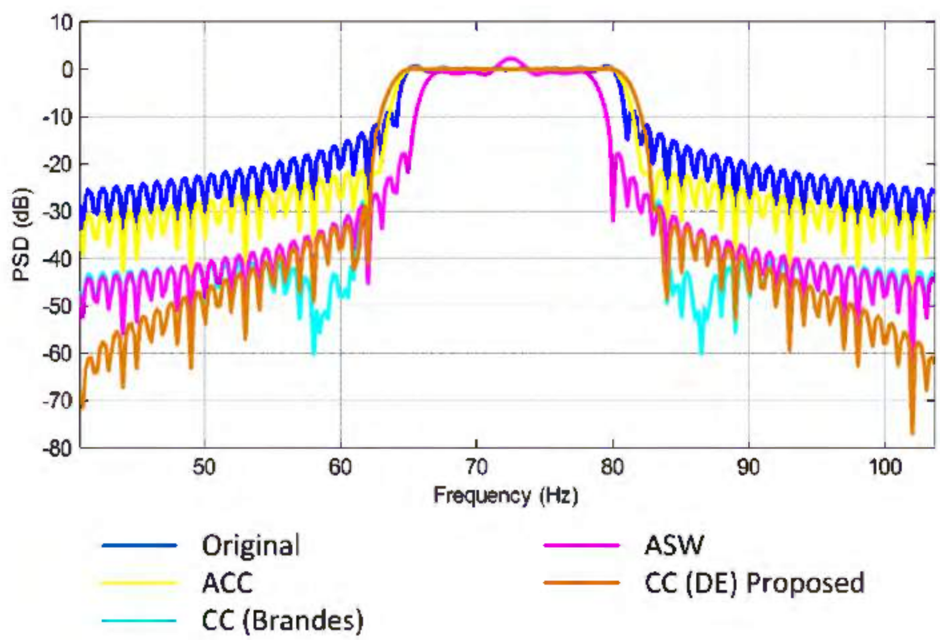

Figure 4. 8 Spectrum of OFDM signal of single SU; Comparison of DE with existing techniques; N_s = 16 data carriers; Total K = 4 CCs are used on both sides; $q_{n,s}$ = 1, n = 1, … , N_s ; Case I.

4.5.1.4 Performance of CSA

In this section, we will discuss the performance and effectiveness of CSA in term of PSD and compare it with the existing techniques found in the literature and are shown in Figures. 4.9 – 4.10. The amplitudes of CCs calculated by using CSA are given in Table 4.6, using our fitness function. With the help of CSA -68 dB on left and -66.5 dB on right side of spectrum is achieved.

Table 4. 6 Amplitudes of CCs calculated using CSA (Case I)

Amplitudes of left and right sided cancellation carriers (CCs)				
Technique used	**First left CC**	**Second left CC**	**First right CC**	**Second right CC**
CSA	0.12916316	0.61315280	0.61315280	0.12916316

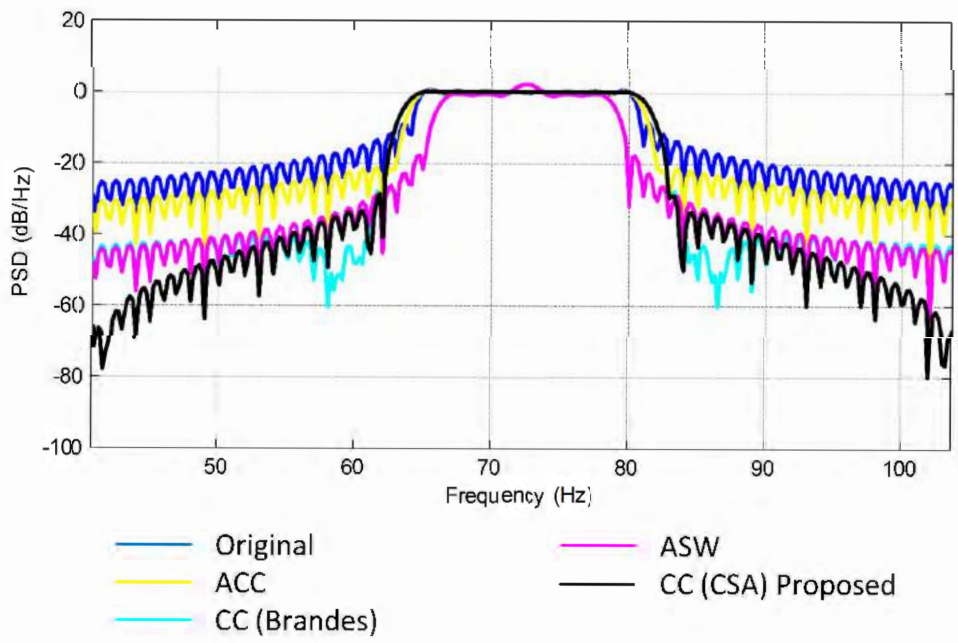

Figure 4. 9 Spectrum of OFDM signal of single SU; Comparison of CSA with existing techniques; N_s = 16 data carriers; $K_l = K_r$ = 2 CCs; $q_{n,s}$ = 1, n = 0, 1, … , N_s – 1; Case I.

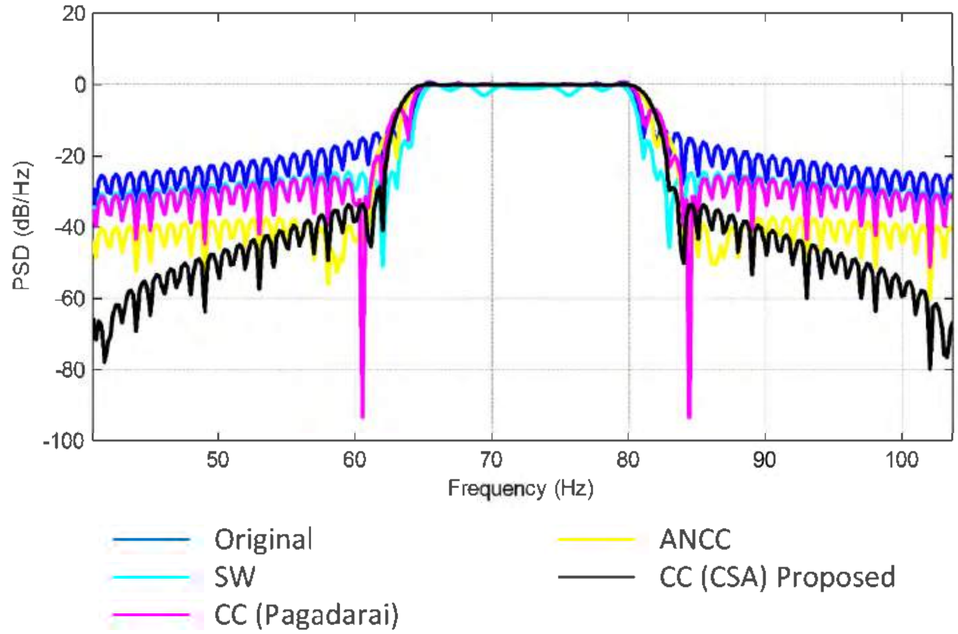

Figure 4. 10 Spectrum of OFDM signal of single SU; Comparison of CSA with existing techniques; N_s = 16 data carriers; total of K = 4 CCs; $q_{n,s}$ = 1, n = 0, 1, … , N_s – 1; Case I.

4.5.1.5 Performance comparison of proposed algorithms

In this section, the performance of all the proposed algorithms i.e. GA, FFA, DE and CSA with each other with the help of computer simulations in term of PSD as shown in Figure. 4.11 is discussed.

Table 4. 7 Sidelobe power levels at different locations occupied by LUs using our proposed algorithms in a spectrum sharing scenario, Case I

Algorithm used	Sidelobe power levels	
	Left side	**Right side**
Without CCs	- 29 dB	- 26 dB
GA	- 55.5 dB	- 52.5 dB
FFA	- 57 dB	- 54 dB
DE	- 65.5 dB	- 62 dB
CSA	- 68 dB	- 66.5 dB

These Figures clearly depicts that overall our proposed algorithm: CSA gets better suppression of sidelobes as compared to the GA, FFA and DE. Table 4.7 shows the suppression of sidelobes using GA, FFA, DE and CSA in dBs.

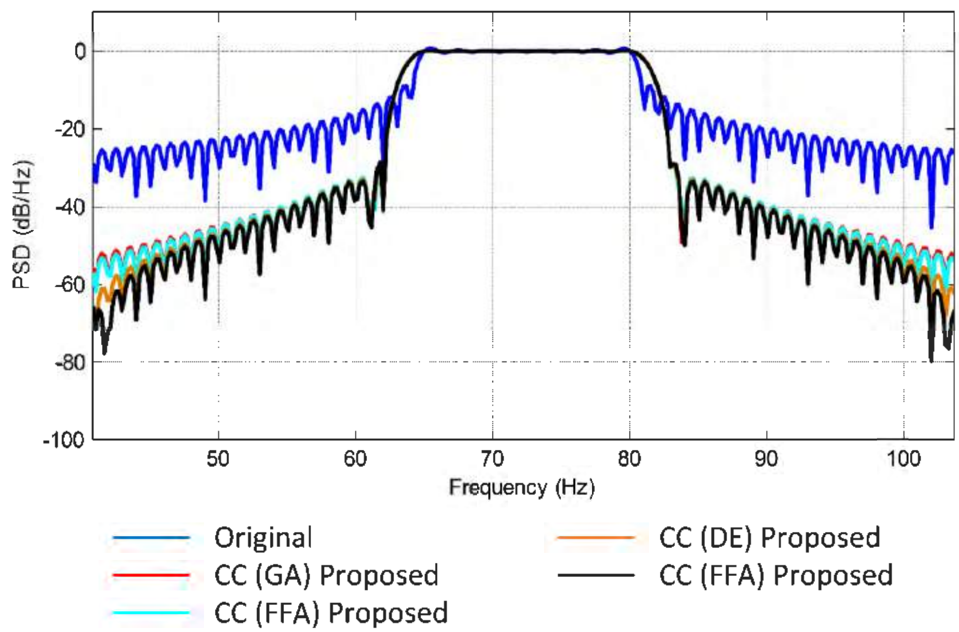

Figure 4. 11 Spectrum of OFDM signal of single SU; Comparison of GA, FFA, DE and CSA; N_s = 16 data carriers; K_l = Kr = 2 CCs; $q_{n,s}$ = 1; n = 0,1,…., N_s – 1; Case I

4.5.2 Case II

In this case, assuming that CR detects four vacant bands, denoted by II, IV, VI and VIII all having equal bandwidths. The spacing between these bands denoted by I, III, V, VII and IX is also considered as of equal bandwidths. Different SUs operating in band II, IV, VI and VIII are represented as SU 1, SU 2, SU 3 and SU 4 respectively. Each one of them utilizes 32 OFDM subcarriers, mapped with BPSK with power normalized to 1. In order to not to interfere with the PUs two CCs on the either side of the locations II, IV, VI and VIII are inserted. So N = 32 data subcarriers and K = 4 cancellation carriers are there in each location II, IV, VI and VIII.

The Optimization range for the calculation of amplitudes spans the sidelobes in the locations I, III, V, VII and IX, here we have taken 10 samples per sidelobes to keep the computational complexity low.

4.5.2.1 Performance of GA

In this section, the performance of GA is shown with the help of simulations in term of PSD and compared with the existing techniques found in literature. Figures. 4.12 – 4.13 shows the performance of GA that depict that better reduction of sidelobes are achieved by using GA as compared to the existing techniques found in the literature. The amplitudes of CCs calculated with the help of GA by using our proposed fitness function for all four SUs operating in white holes II, IV, VI and VIII are given in Table. 4.8.

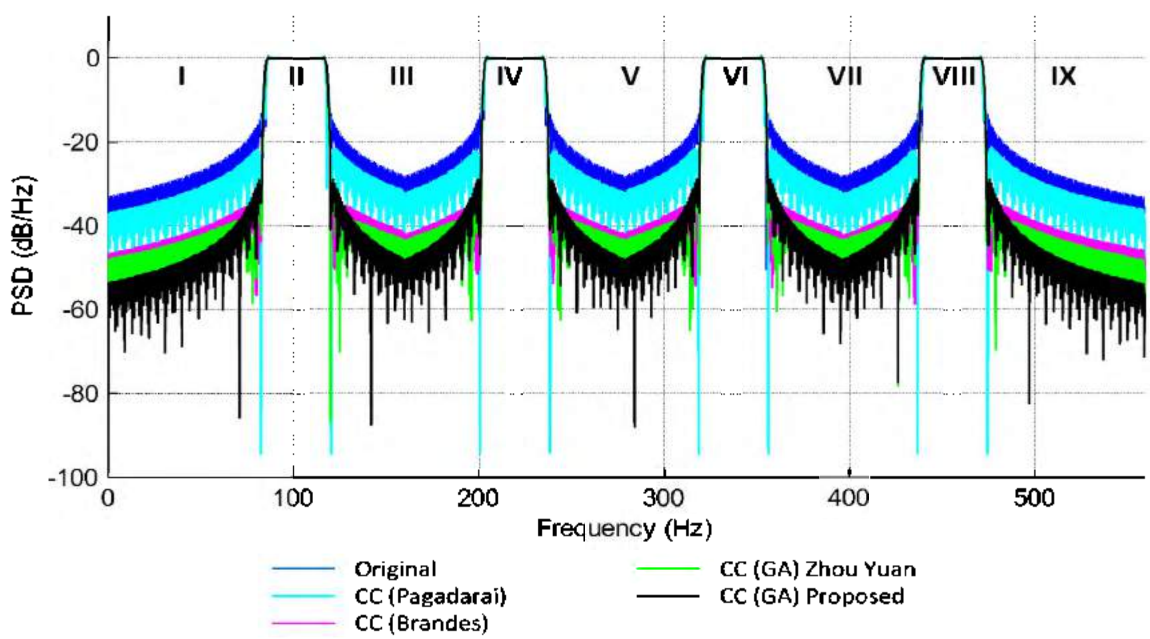

Figure 4. 12 Comparison of GA with existing techniques; N_s = 32 data subcarriers for each SU; $K_r = K_l$ = 2 CCs in each of the location II, IV, VI and VIII, $q_{n,s}$ = 1, n = 1, 2… N_s; Case II.

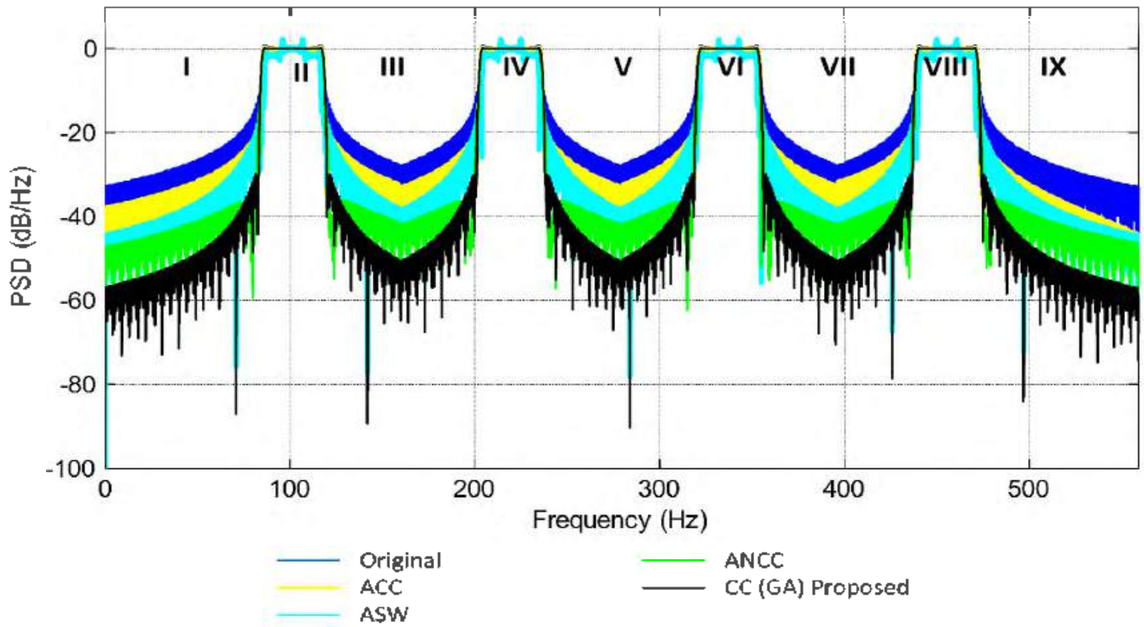

Figure 4. 13 Comparison of GA with existing techniques; N_s = 32 data subcarriers for each SU; total of K = 4 CCs inserted on both side of the location II, IV, VI and VIII, $q_{n,s}$ = 1, n = 1, 2… N_s; Case II.

Table 4. 8 Amplitudes of CCs calculated using GA (Case II)

Amplitudes of left and right sided CCs					
Algorithm used		**First left CC**	**Second left CC**	**First right CC**	**Second right CC**
GA	**SU 1**	0.13001062	0.62652007	0.62652007	0.13001062
	SU 2	0.13001062	0.62652007	0.62652007	0.13001062
	SU 3	0.13001062	0.62652007	0.62652007	0.13001062
	SU 4	0.13001062	0.62652007	0.62652007	0.13001062

4.5.2.2 Performance of FFA

In this section, the performance of FFA with the existing techniques with the help of simulations that are shown in Figures 4.14 – 4.15 is compared, while the amplitudes of CCs of all SUs utilizing the spectral white holes II, IV, VI and VIII are calculated using FFA based on our proposed fitness function given in Table 4.9 which shows that FFA shows better results as compared to the existing techniques found in the literature.

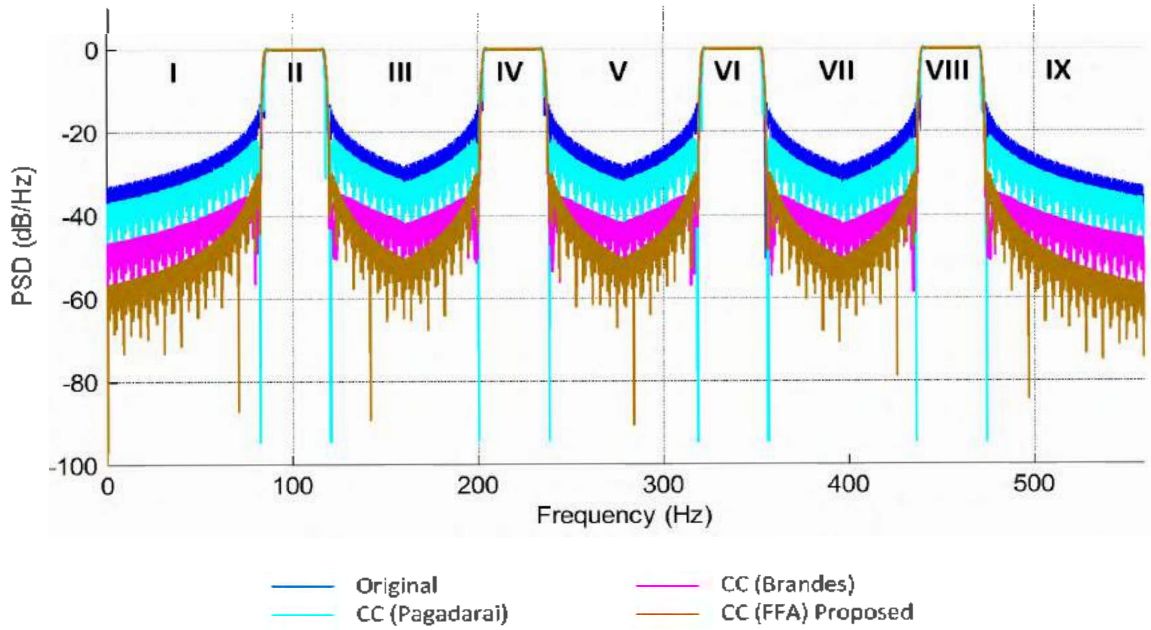

Figure 4. 14 Comparison of FFA with existing techniques; N_s = 32 data subcarriers for each SU; $K_r = K_l$ = 2 CCs in each of the location II, IV, VI and VIII, $q_{n,s} = 1$, $n = 1, 2\ldots N_s$; Case II.

Table 4. 9 Amplitudes of CCs calculated using FFA (Case II)

		Amplitudes of left and right sided CCs			
Algorithm used		**First left CC**	**Second left CC**	**First right CC**	**Second right CC**
FFA	**SU 1**	0.13201062	0.62652007	0.62652007	0.13201062
	SU 2	0.13201062	0.62652007	0.62652007	0.13201062
	SU 3	0.13201062	0.62652007	0.62652007	0.13201062
	SU 4	0.13201062	0.62652007	0.62652007	0.13201062

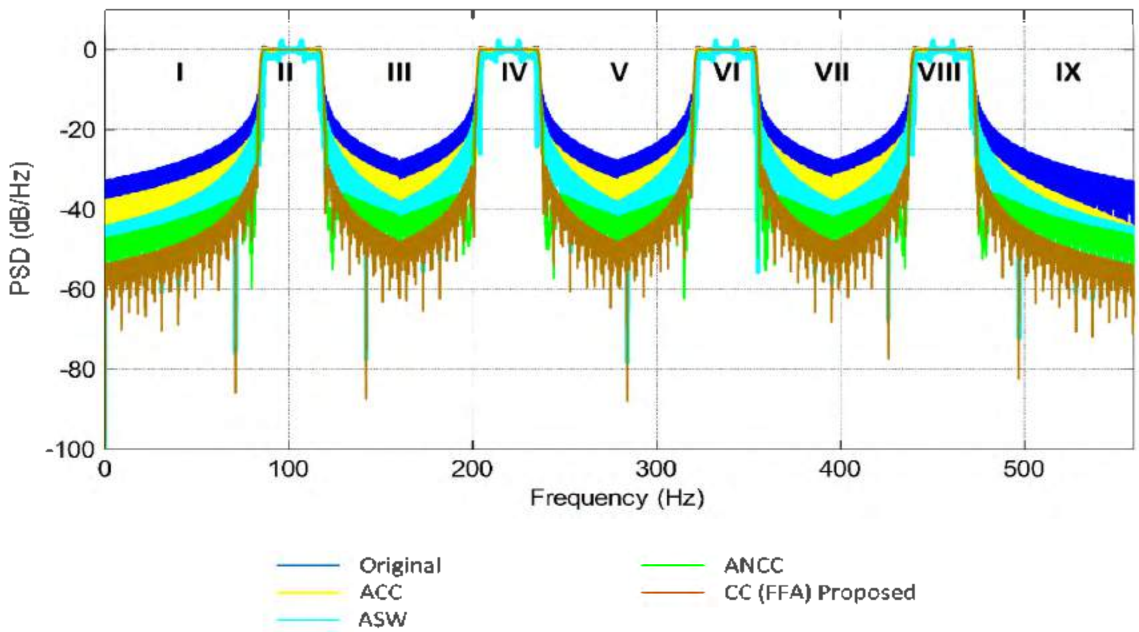

Figure 4. 15 Comparison of FFA with existing techniques; N_s = 32 data subcarriers for each SU; total of K = 4 CCs inserted on both sides of the location II, IV, VI and VIII, $q_{n,s}$ = 1, n = 1, 2… N_s; Case II.

4.5.2.3 Performance of DE

In this section, the effectiveness of DE using computer simulation in term of PSD is shown in Figures. 4.16 – 4.17 as compared to the techniques found in literature, which show that DE outclass

Table 4. 10 Amplitudes of CCs calculated using DE (Case II)

Amplitudes of left and right sided CCs					
Algorithm used		**First left CC**	**Second left CC**	**First right CC**	**Second right CC**
DE	**SU 1**	0.13686577	0.63049059	0.63049059	0.13686577
	SU 2	0.13686577	0.63049059	0.63049059	0.13686577
	SU 3	0.13686577	0.63049059	0.63049059	0.13686577
	SU 4	0.13686577	0.63049059	0.63049059	0.13686577

the existing techniques found in the literature. Amplitudes of CCs calculated using DE with the help of our proposed fitness function discussed above are given in Table 4.10.

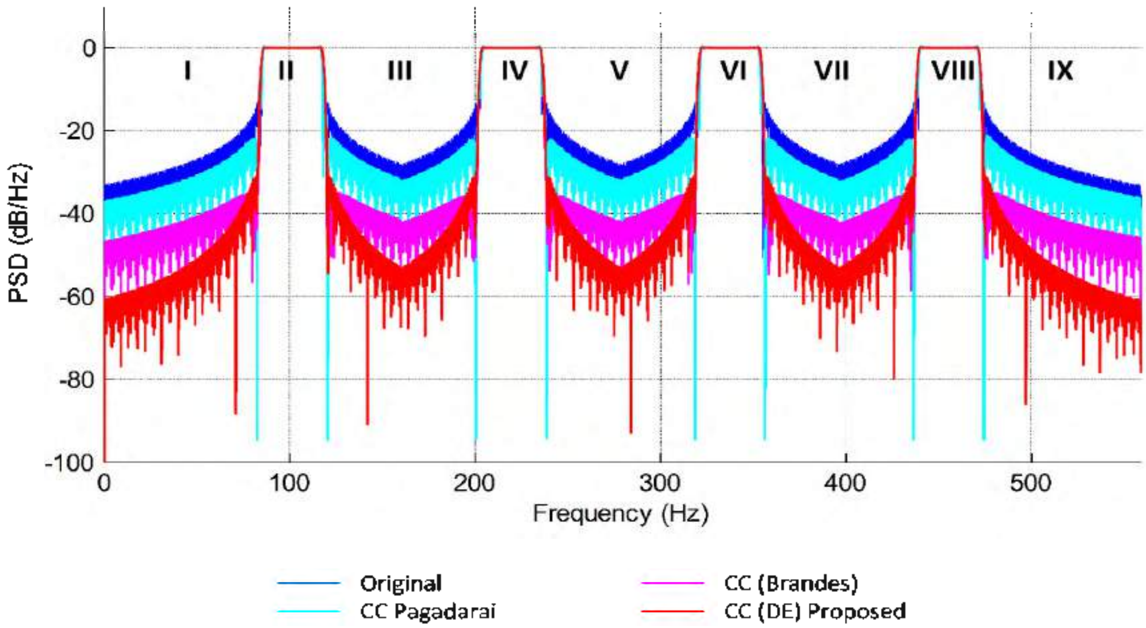

Figure 4. 16 Comparison of DE with existing techniques; N_s = 32 data subcarriers for each SU; K_l = K_r = 2 CCs in each of the location II, IV, VI and VIII, $q_{n,s}$ = 1, n = 1, 2… N_s; Case II.

4.5.2.4 Performance of CSA

In this section, the effectiveness and reliability of our proposed algorithm CSA with the existing techniques found in the literature is shown with the help of computer simulations in term of PSD that are depicted in Figures. 4.18 – 4.19, which shows that our proposed algorithm CSA shows better reduction of sidelobes. The amplitudes of CCs of all SUs operating in white holes II, IV, VI and VIII are calculated using CSA using our proposed fitness function are given in Table 4.11 respectively.

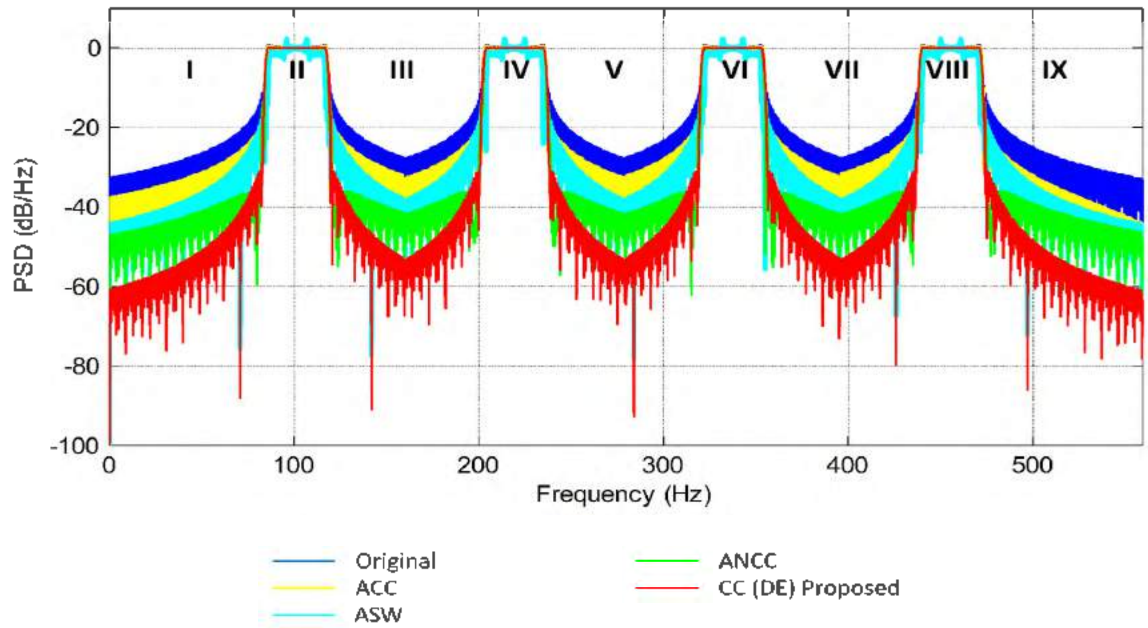

Figure 4. 17 Comparison of DE with existing techniques; N_s = 32 data subcarriers for each SU; tot al of K = 4 CCs inserted on both sides of the location II, IV, VI and VIII, $q_{n,s}$ = 1, n = 1, 2… N_S; Case II.

Table 4. 11 Amplitudes of CCs calculated using CSA (Case II)

Amplitudes of left and right sided CCs					
Algorithm used		**First left CC**	**Second left CC**	**First right CC**	**Second right CC**
CSA	**SU 1**	0.13886577	0.63049059	0.63049059	0.13886577
	SU 2	0.13886577	0.63049059	0.63049059	0.13886577
	SU 3	0.13886577	0.63049059	0.63049059	0.13886577
	SU 4	0.13886577	0.63049059	0.63049059	0.13886577

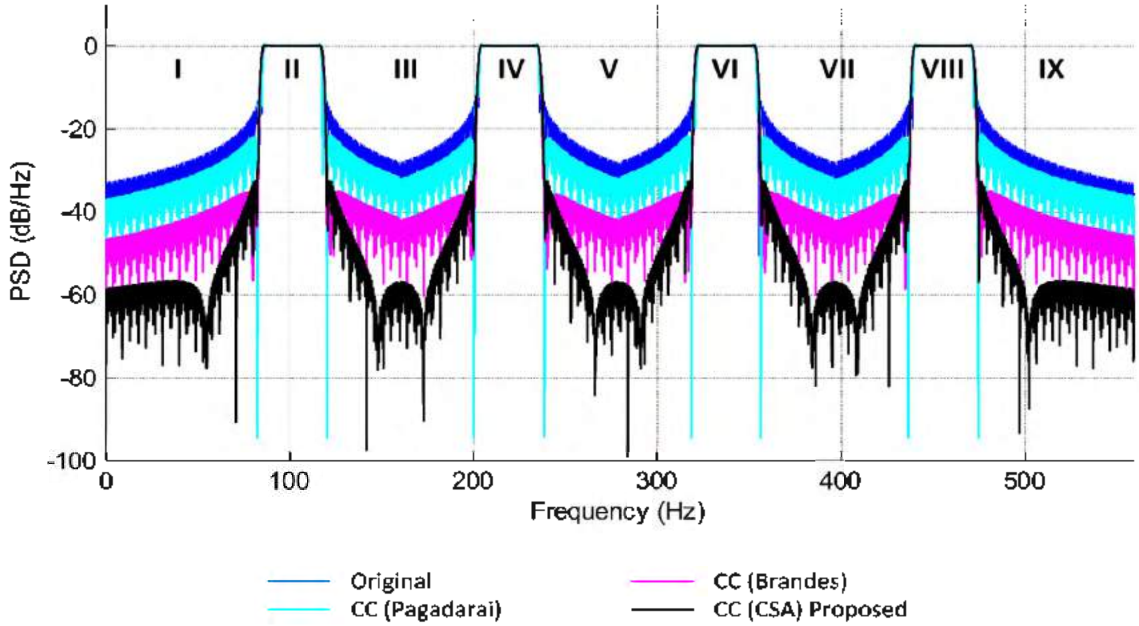

Figure 4. 18 Comparison of CSA with existing techniques; N_s = 32 data subcarriers for each SU; $K_r = K_l$ = 2 CCs in each of the location II, IV, VI and VIII, $q_{n,s}$ = 1, n = 1, 2… N_s; Case II.

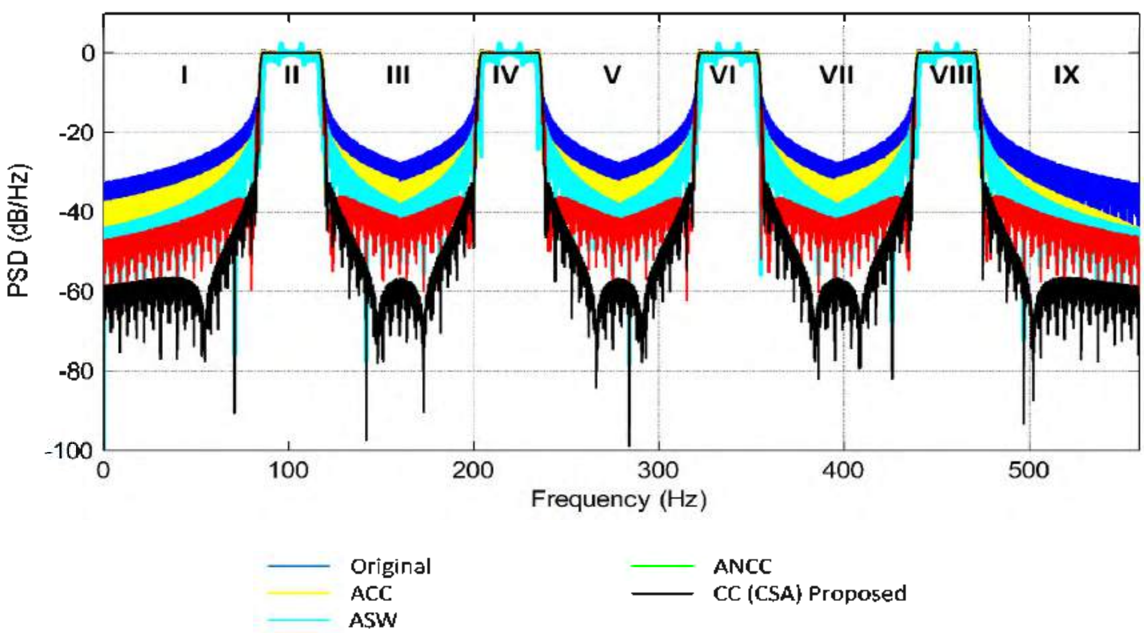

Figure 4. 19 Comparison of CSA with existing techniques; N_s = 32 data subcarriers for each SU; total of K = 4 CCs, $q_{n,s}$ = 1, n = 1, 2… N_s; Case II.

4.5.2.5 Performance comparison of the proposed technique

Here we will compare the performance of the proposed algorithms i.e. GA, FFA, DE and CSA for case II in term of PSD that are shown in Figure. 4.20 and overall the CSA shows better performance. Maximum sidelobe suppression achieved using these proposed algorithms are given in Table 4.12.

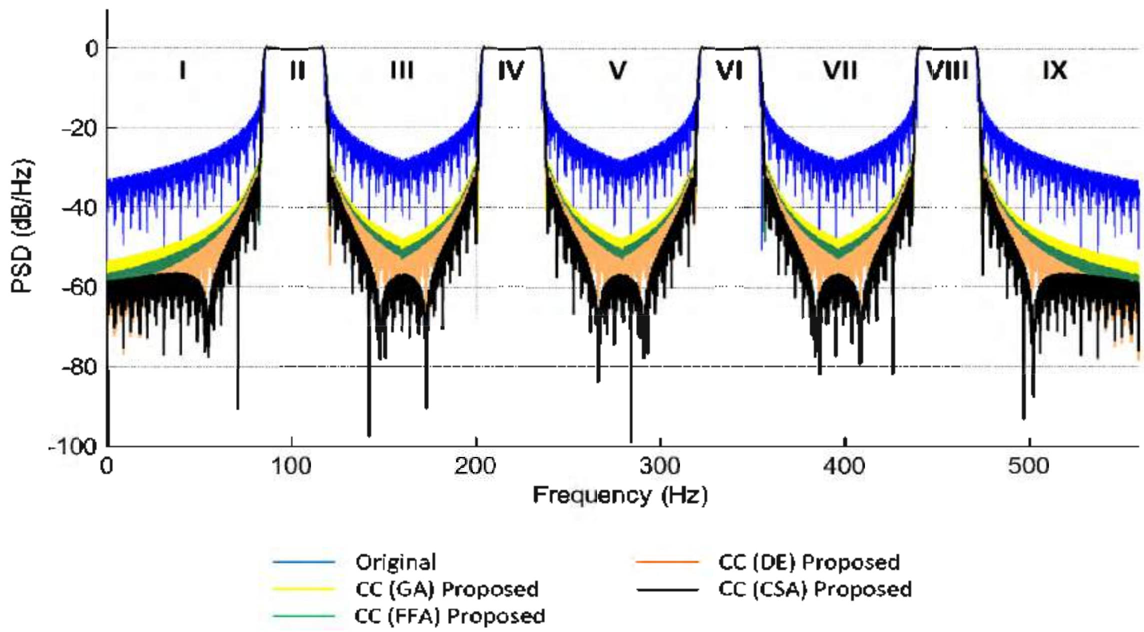

Figure 4. 20 Power spectrum of OFDM signals of 4 different SUs using our proposed algorithms i.e. GA, FFA, DE and CSA; Comparison of proposed algorithms with each other; N_s = 32 data subcarriers for each SU; $K_r = K_l = 2$ CCs in each of the location II, IV, VI and VIII, $q_{n,s} = 1$, $n = 1,2,\ldots, N_s$; Case II.

4.5.3 Case III

In this case, we consider interference suppression spectrum sharing scenario in OFDM having unequal bandwidth between the spectral white spaces II, IV, VI and VIII are unequal i.e. locations I, III, V, VII and IX have an unequal bandwidth, while locations II, IV, VI and VIII have equal bandwidth having 32 subcarriers each. In order, not to interfere with the PU's, two CC's on either side of the location II, IV, VI and VIII are inserted. N = 32 data subcarriers and K = 4 CC's are there in each location II, IV, VI and VIII. The Optimization range for the calculation of weights spans the sidelobes in the location I, III, V, VII and IX, 10 samples per sidelobes have been taken keeping the computational complexity low.

Table 4. 12 Sidelobe power levels at different locations occupied by LUs using our proposed algorithms in a spectrum sharing scenario, Case II

Algorithm used	**Sidelobe power in Locations of LUs**				
	I	**III**	**V**	**VII**	**IX**
Without CCs	-33dB	-28dB	-28dB	-28dB	-33dB
GA	-54dB	-48dB	-48dB	-48dB	-54dB
FFA	-57dB	-51dB	-51dB	-51dB	-57dB
DE	-61dB	-53dB	-53dB	-53dB	-61dB
CSA	-70dB	-64dB	-64dB	-64dB	-70dB

4.5.3.1 Performance of GA

Here, we consider the interference suppression scheme using GA and compare the results of GA using existing techniques. Figures 4.21 – 4.22 show the performance of GA in term of PSD. The amplitudes of CCs of four SUs in case III calculated using our proposed algorithm GA, with the

Table 4. 13 Amplitudes of CCs calculated using GA (Case III)

Amplitudes of left and right sided CCs					
Algorithm used		**First left CC**	**Second left CC**	**First right CC**	**Second right CC**
GA	**SU 1**	0.13001062	0.62652007	0.62652007	0.13001062
	SU 2	0.13001062	0.62652007	0.62652007	0.13001062
	SU 3	0.13001062	0.62652007	0.62652007	0.13001062
	SU 4	0.13001062	0.62652007	0.62652007	0.13001062

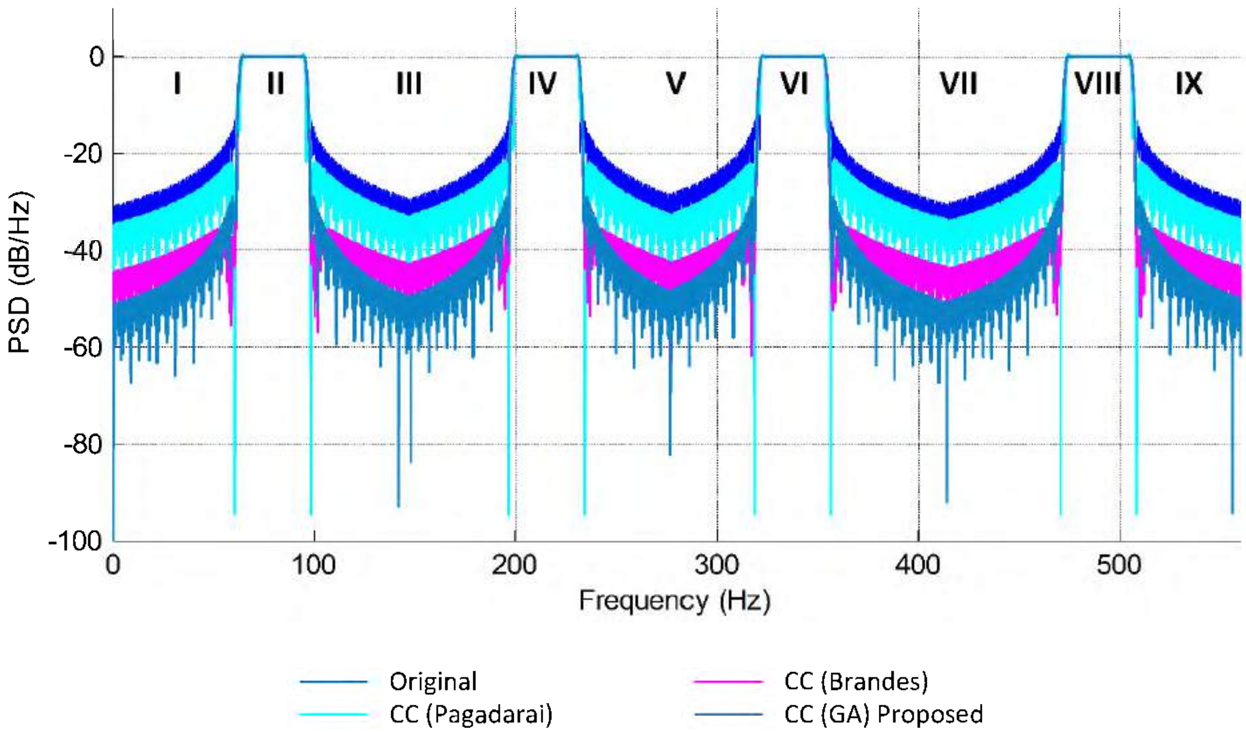

Figure 4. 21 Comparison of GA with other techniques; N_s = 32 data subcarriers for each SU; $K_l = K_r$ = 2 CCs, $q_{n,s}$ = 1, n =1, 2… N_s; Case III.

help of our proposed fitness function are given in Table. 4.13.

4.5.3.2 Performance of FFA

The performance and effectiveness of our proposed algorithm FFA using simulations in term of PSD and its comparison with different existing techniques are shown in Figures. 4.23 – 4.24. These Figures. 4.23 – 4.24 shows that better reduction of sidelobe suppression is achieved with the help of FFA. The amplitudes of CCs of all SUs utilizing the spectral white spaces II, IV, VI and VIII calculated with the help of our proposed algorithm FFA using our proposed fitness function are given in Table. 4.14.

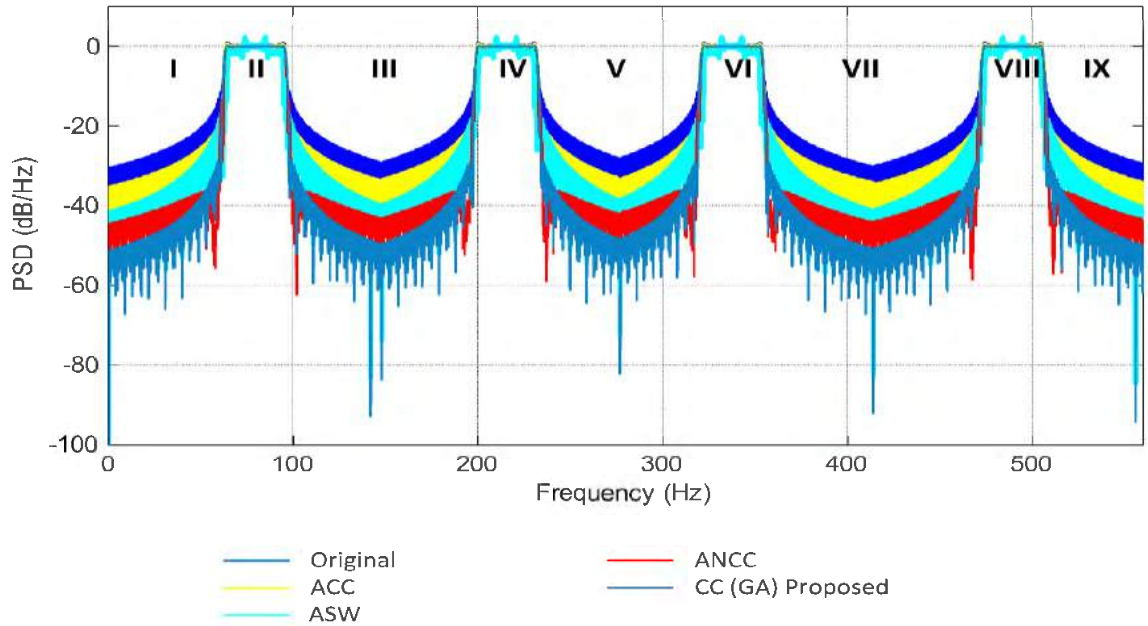

Figure 4. 22 Comparison of GA with other techniques: N_s = 32 data subcarriers for each SUs; total of K = 4 CCs, $q_{n,s}$ = 1, n = 1, 2… N_s; Case III.

Table 4. 14 Amplitudes of CCs calculated using FFA (Case III)

Amplitudes of left and right sided CCs					
Algorithm used		**First left CC**	**Second left CC**	**First right CC**	**Second right CC**
FFA	**SU 1**	0.13201062	0.62652007	0.62652007	0.13201062
	SU 2	0.13201062	0.62652007	0.62652007	0.13201062
	SU 3	0.13201062	0.62652007	0.62652007	0.13201062
	SU 4	0.13201062	0.62652007	0.62652007	0.13201062

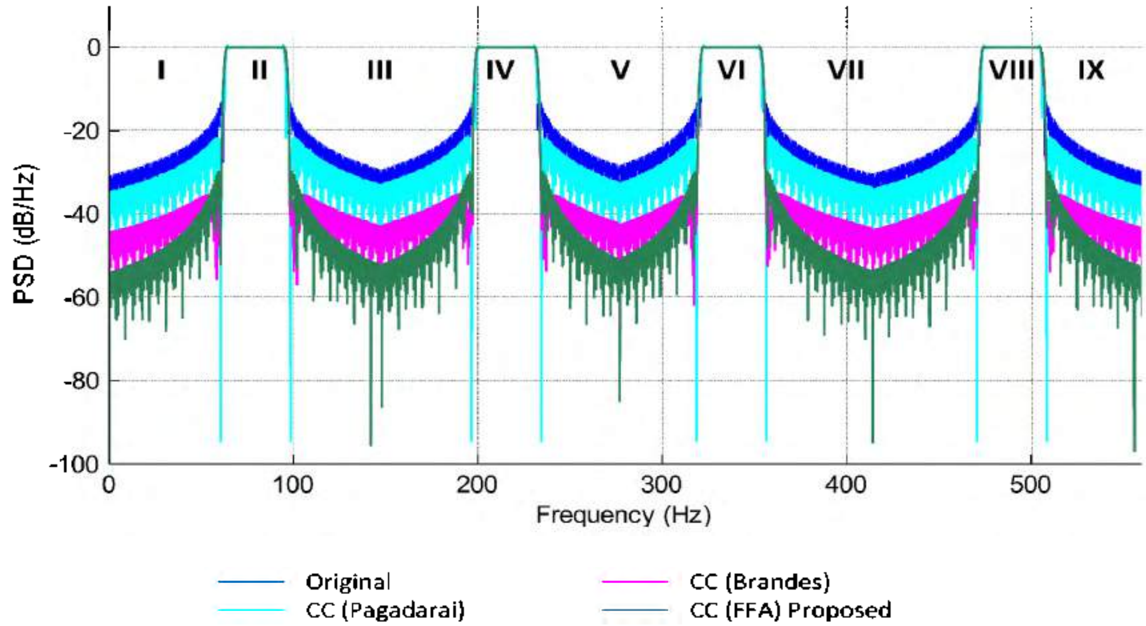

Figure 4. 23 Comparison of FFA with existing techniques; N_s = 32 data subcarriers for each SUs; $K_l = K_r$ = 2 CCs, $q_{n,s}$ = 1, n = 1, 2… N_s; Case III.

4.5.3.3 Performance of DE

In this section, the performance, efficiency and reliability of our proposed algorithm i.e. DE is shown with the help of computer simulation on the basis of PSD and its comparison with the results of the existing techniques found in the literature. Figures. 4.25 – 4.26 clearly depict that DE shows better reduction of sidelobes as compared to reduction of sidelobes using existing techniques.

The amplitudes of CCs of all SUs operating in spectral white holes II, IV, VI and VIII that is calculated by DE using our proposed fitness function for the case III are given in Table. 4.15.

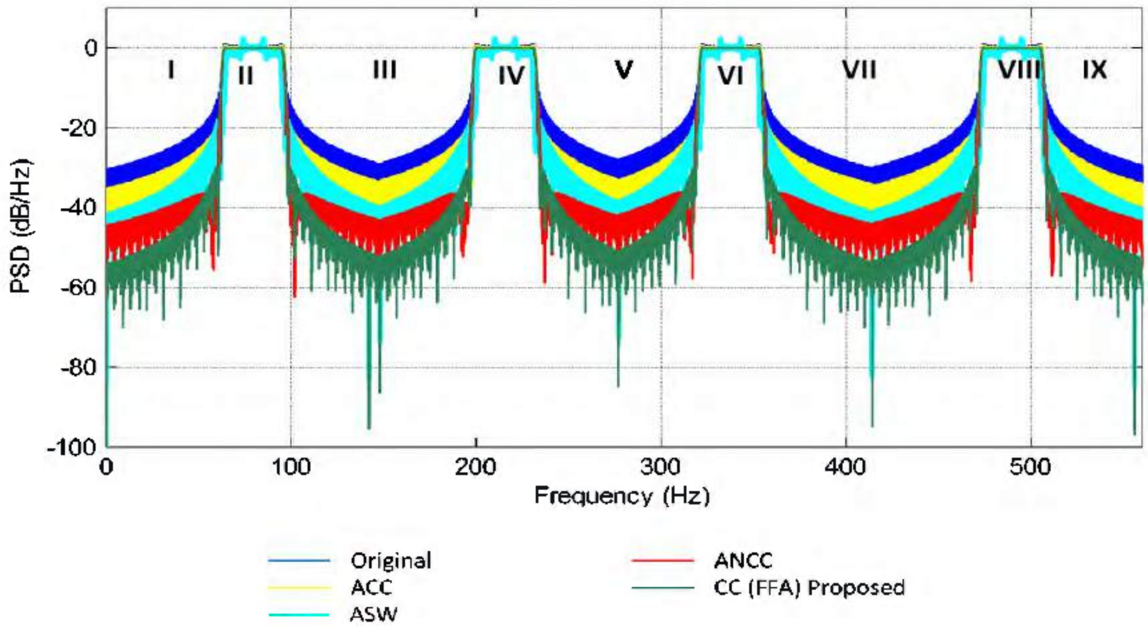

Figure 4. 24 Comparison of FFA with existing techniques; N_s = 32 data subcarriers for each SUs; total of K = 4 CCs $q_{n,s}$ = 1, n = 1, 2… N_s; Case III.

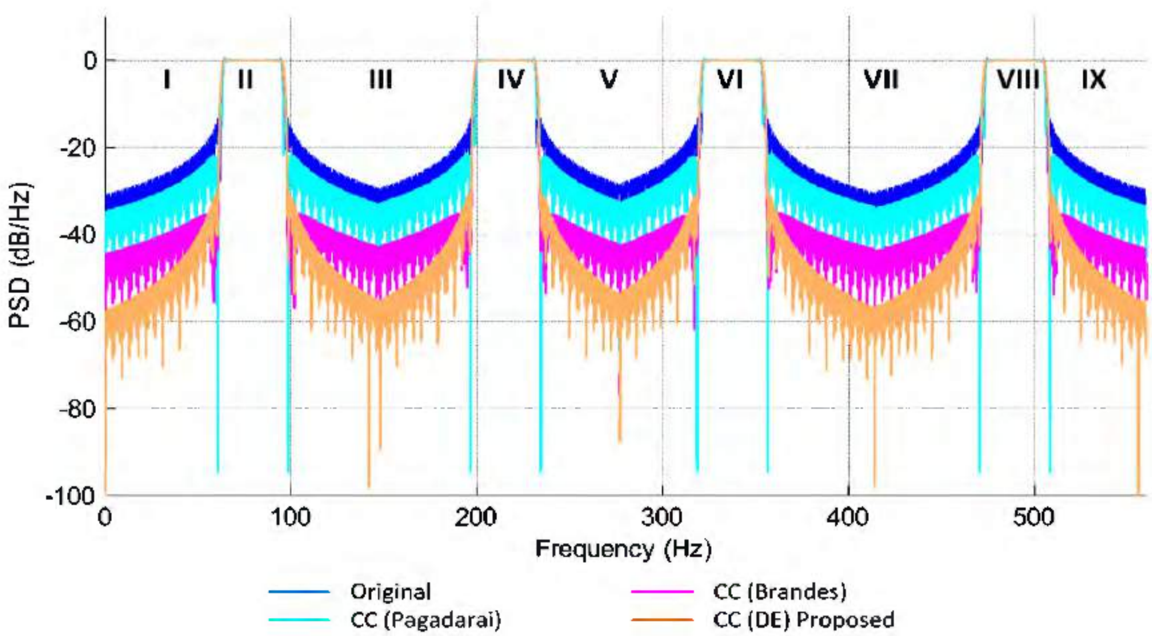

Figure 4. 25 Comparison of DE with existing techniques; N_s = 32 data subcarriers of each SUs; K_r = K_l = 2 CCs, $q_{n,s}$ = 1, n = 1, 2… N_s; Case III.

Table 4. 15 Amplitudes of CCs using DE (Case III)

Amplitudes of left and right sided CCs					
Algorithm used		**First left CC**	**Second left CC**	**First right CC**	**Second right CC**
DE	**SU 1**	0.13686577	0.63049059	0.63049059	0.13686577
	SU 2	0.13686577	0.63049059	0.63049059	0.13686577
	SU 3	0.13686577	0.63049059	0.63049059	0.13686577
	SU 4	0.13686577	0.63049059	0.63049059	0.13686577

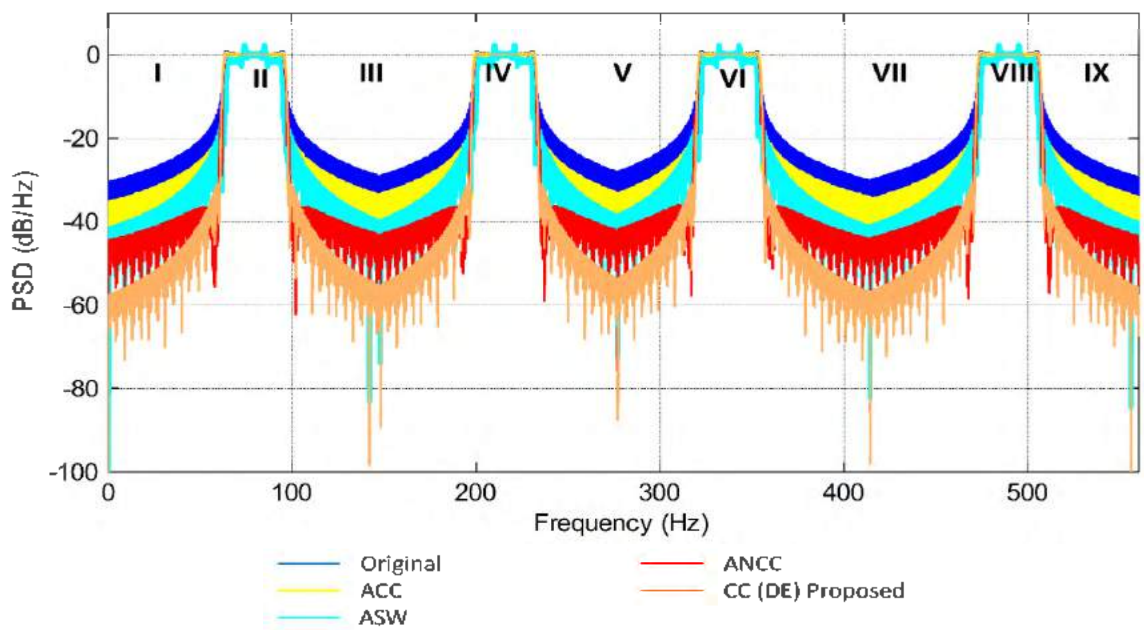

Figure 4. 26 Comparison of DE with existing techniques; N_s = 32 data subcarriers for each SUs; total of K = 4 cancellation carriers on both side of the location II, IV, VI and VIII, $q_{n,s}$ = 1, n = 1, 2… N_s; Case III

4.5.3.4 Performance of CSA

Here the performance and reliability of CSA are shown with the help of simulations in terms of PSD. The effectiveness of the proposed algorithm is shown in Figures. 4.27 – 4.28 which shows

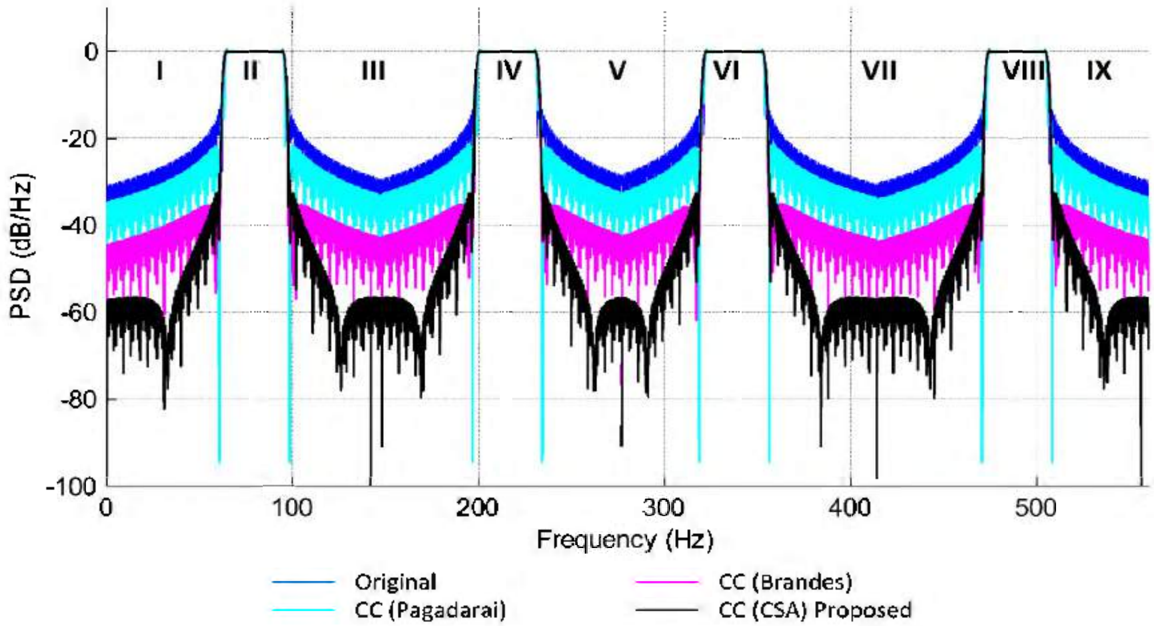

Figure 4. 27 Comparison of CSA with existing techniques; N_s = 32 data subcarriers for each; K_l = K_r = 2 CCs in each of the location II, IV, VI and VIII, $q_{n,s}$ = 1, n = 1, 2… N_s; Case III.

Table 4. 16 Amplitudes of CCs calculated using CSA (Case III)

Amplitudes of left and right sided CCs					
Algorithm used		**First left CC**	**Second left CC**	**First right CC**	**Second right CC**
CSA	**SU 1**	0.13886577	0.63049059	0.63049059	0.13886577
	SU 2	0.13886577	0.63049059	0.63049059	0.13886577
	SU 3	0.13886577	0.63049059	0.63049059	0.13886577
	SU 4	0.13886577	0.63049059	0.63049059	0.13886577

that with the help of CSA sidelobe are suppressed effectively as compared to the existing techniques found in the literature. The amplitudes of CCs of all SUs operating in white holes II, IV, VI and VIII calculated by using CSA in this case are given in Table. 4.16.

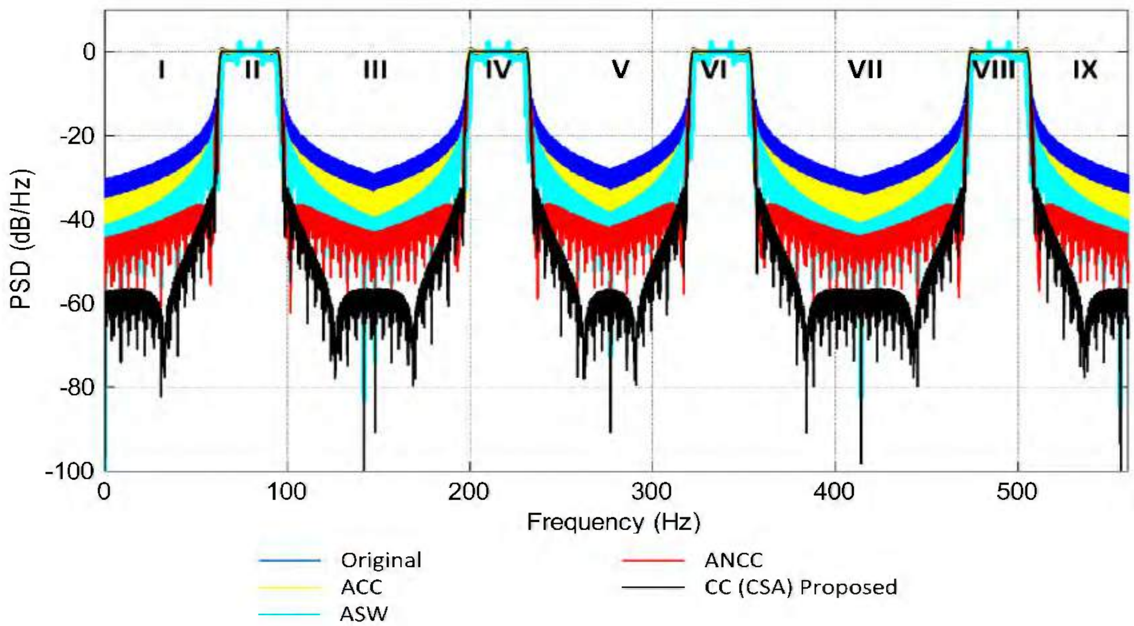

Figure 4. 28 Comparison of CSA with existing techniques; N_s = 32 data subcarriers for each SUs; total of K= 4 CCs, $q_{n,s}$ = 1, n = 1, 2… N_s; Case III.

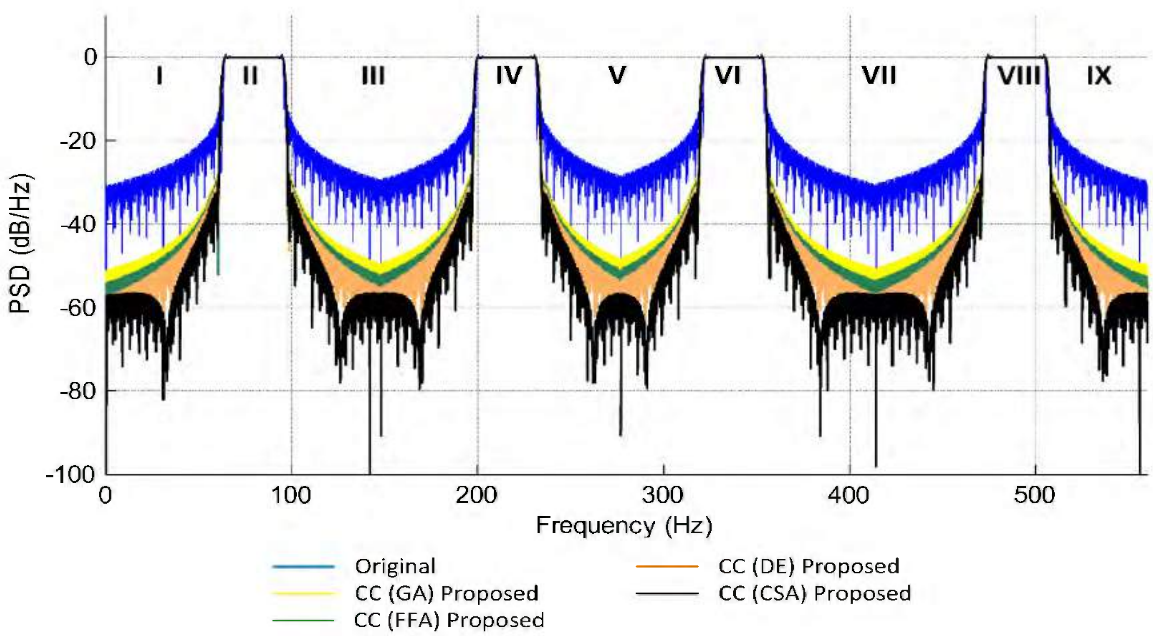

Figure 4. 29 Comparison of proposed algorithms with each other; N_s = 32 data subcarriers for each SUs; total of K = 4 CCs $q_{n,s}$ = 1, n = 1, 2… N_s; Case III.

4.5.3.5 Performance comparison of proposed algorithms

In this section the performance, effectiveness and reliability of the proposed algorithms are compared with the help of simulations. Figure. 4.29 shows that although all the proposed algorithm shows the significant reduction of sidelobes but overall the performance of CSA is better. Maximum sidelobe reduction achieved using our proposed algorithms is given in Table. 4.17.

Table 4. 17 Sidelobe power levels at different locations occupied by LUs using our proposed algorithms in a spectrum sharing scenario, Case III

Algorithms used	Sidelobe power in Locations of LUs				
	I	III	V	VII	IX
Without CCs	-31dB	-30dB	-28dB	-30dB	-30dB
GA	-51dB	-50dB	-48dB	-51dB	-50dB
FFA	-54dB	-51dB	-51dB	-54dB	-53dB
DE	-57dB	-55dB	-54dB	-55dB	-56dB
CSA	-64dB	-64dB	-64dB	-64dB	-64dB

4.5.4 Case IV

In this case, interference suppression spectrum sharing scenario in OFDM having equal bandwidth between the spectral white spaces II, IV, VI and VIII is discussed. The locations I, III, V, VII and IX have equal bandwidth, while the locations II, IV, VI and VIII have an un-equal bandwidth and are occupied by four SUs, SU1, SU2, SU3 and SU4 respectively, where SU 1 comprises of 16, SU2 comprises of 32, SU 3 comprises of 64 and SU 4 comprises of 128 subcarriers. In order, not to interfere with the PU's two CC's on either side of the location II, IV, VI and VIII are inserted. So N = 16 data subcarriers and K = 4 CC's are there in each location II, N = 32 data subcarriers and M = 4 CC's are there in location IV, N = 64 data carriers and M = 4 CC's are there in location VI and N = 128 data carriers and M = 4 CC's are there in location VIII. The Optimization range for the calculation of weights spans the sidelobes in the location I, III, V, VII and IX, here 10 samples per sidelobes have been taken to keep the computational complexity low.

4.5.4.1 Performance of GA

In this section, the performance of the GA in the spectrum sharing scenario, where the spectral white holes II, IV, VI and VIII are considered of having un-equal bandwidth, while the spacing between them are considered to be of equal bandwidth. The efficiency and reliability of GA and its comparison with other existing techniques using computer simulations in term of PSD are shown in Figures. 4.30 – 4.31 which shows that better suppression of sidelobes in a spectrum band I, III, V, VII, and IX are achieved using GA as compared to the existing techniques found in the literature.

Finally the amplitudes of CCs of all SUs utilizing in spectral white holes II, IV, VI and VIII are calculated using GA with the help of our proposed fitness function for case IV are given in Table. 4.18.

Table 4. 18 Amplitudes of CCs using GA (Case IV)

Amplitudes of left and right sided CCs					
Algorithm used		**First left CC**	**Second left CC**	**First right CC**	**Second right CC**
GA	**SU 1**	0.13910977	0.63090059	0.63090059	0.13910977
	SU 2	0.13001062	0.62652007	0.62652007	0.13001062
	SU 3	0.13247502	0.61821019	0.61821019	0.13247502
	SU 4	0.13765122	0.64327628	0.64327628	0.13765122

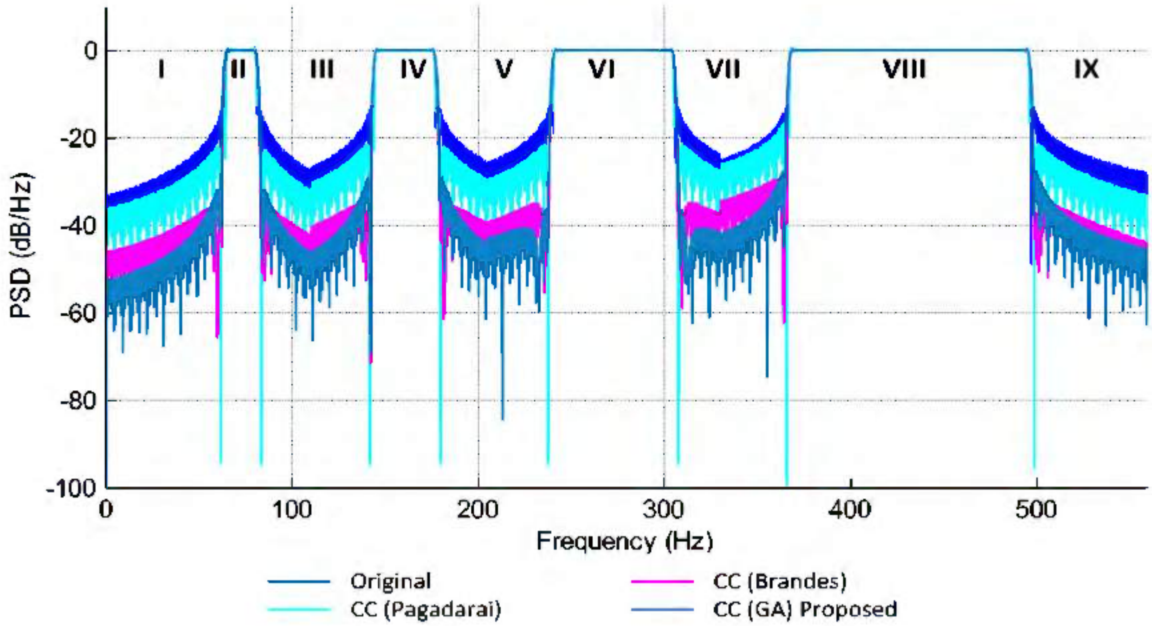

Figure 4. 30 Comparison of GA with existing techniques; 16 data subcarriers in location II, 32 in IV, 64 in VI and 128 in VIII; $K_l = K_r = 2$ CCs $q_{n,s} = 1$, $n = 1, 2\ldots N_s$; Case IV.

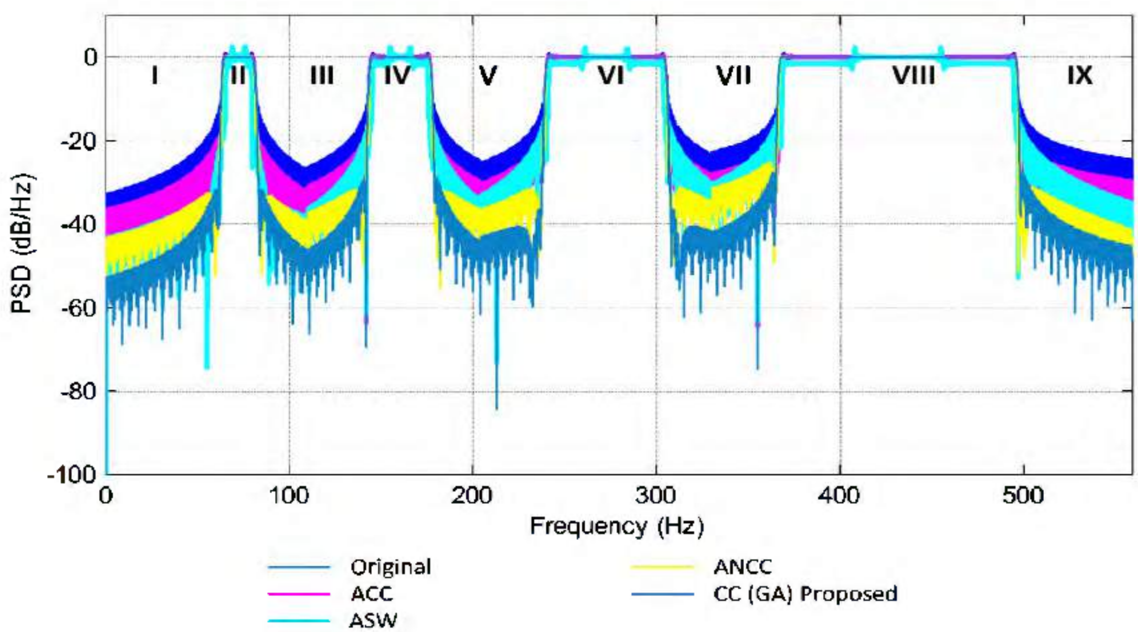

Figure 4. 31 Power spectrum of OFDM signals of 4 different SUs using GA; 16 data subcarriers in location II, 32 in IV, 64 in VI and 128 in VIII; total of $K = 4$ CCs $q_{n,s} = 1$, $n =1, 2\ldots N_s$; Case I

4.5.4.2 Performance of FFA

In this section, the performance of FFA in a spectrum sharing scenario, i.e. Case IV, where there are total of four SUs utilizing spectral holes II, IV, VI, and VIII that are un – equal in bandwidth and the gap between these spectral white holes are considered of equal bandwidth is discussed. The performance, efficiency and reliability of our proposed algorithm FFA is shown using simulations in term of PSD which is shown in Figures. 4.32 – 4.33. These Figures 4.2 – 4.33 shows that the suppression of sidelobes achieved in spaces I, III, V, VII, and IX are better as compared to the existing techniques found in the literature. The amplitudes of CCs of all four SUs operating in spectral white holes II, IV, VI and VIII using FFA with the help of our proposed fitness function are given in Table. 4.19.

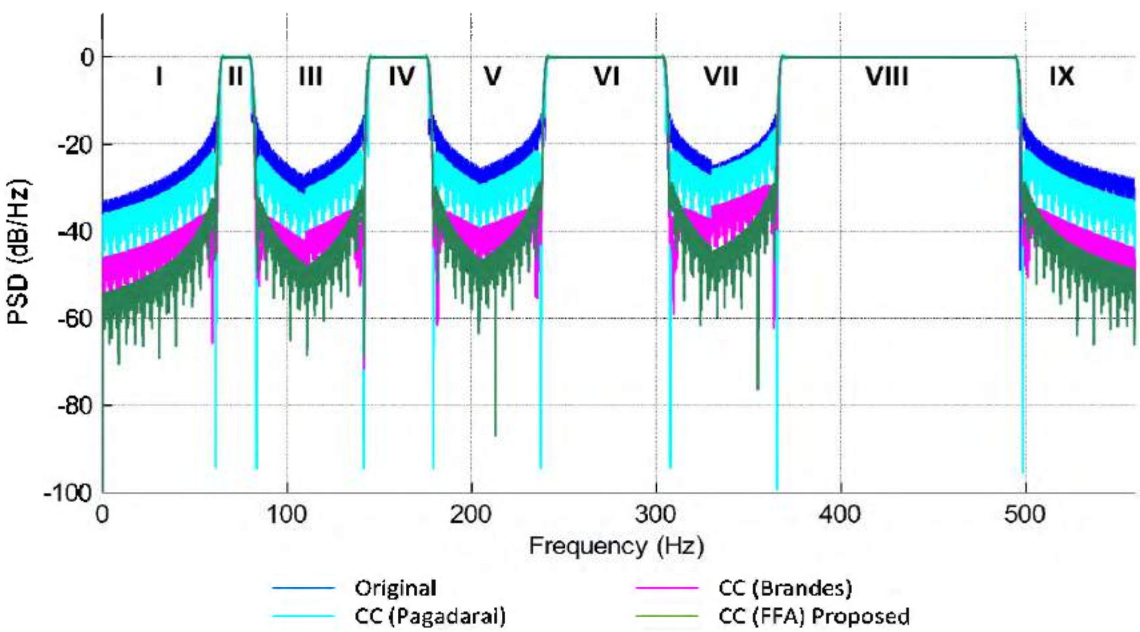

Figure 4. 32 Comparison of FFA with existing techniques; 16 data subcarriers in location II, 32 in IV, 64 in VI and 128 in VIII; $K_l = K_r = 2$ CCs, $q_{n,s} = 1$, $n = 1, 2\ldots N_s$; Case IV.

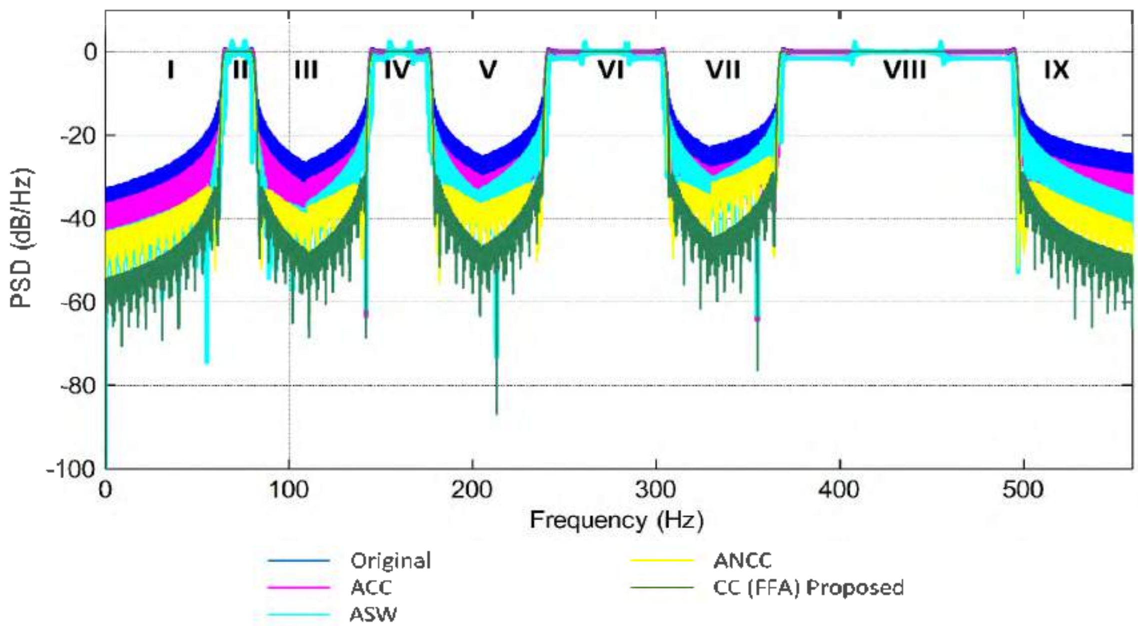

Figure 4. 33 Power spectrum of OFDM signals of 4 different SUs using FFA; 16 data subcarriers in location II, 32 in IV, 64 in VI and 128 in VIII; total of $K = 4$ CCs, $q_{n,s} = 1$, $n = 1, 2\ldots N_s$; Case IV

Table 4. 19 Amplitudes of CCs calculated using FFA (Case IV)

Amplitudes of left and right sided CCs					
Algorithm used		**First left CC**	**Second left CC**	**First right CC**	**Second right CC**
FFA	**SU 1**	0.13896577	0.62909059	0.62909059	0.13896577
	SU 2	0.13201062	0.62652007	0.62652007	0.13201062
	SU 3	0.13197502	0.62990019	0.62990019	0.13197502
	SU 4	0.13895122	0.63999098	0.63999098	0.13895122

4.5.4.3 Performance of DE

In this section, the reliability and effectiveness of DE are discussed in spectrum sharing scenario, where we have considered four spectral holes II, IV, VI and VIII having un-equal bandwidth occupied by four different SUs and the spectrums used by PUs i.e. the spectrum I, III, V, VII and

IX are considered to be of equal bandwidth. The performance comparison of DE in term of PSD are shown in Figures. 4.34 – 4.35 with the techniques already present in the literature. The amplitudes of CCs of each SU operating in spectral spaces II, IV, VI and VIII are calculated by DE using our proposed fitness function given in Table. 4.20.

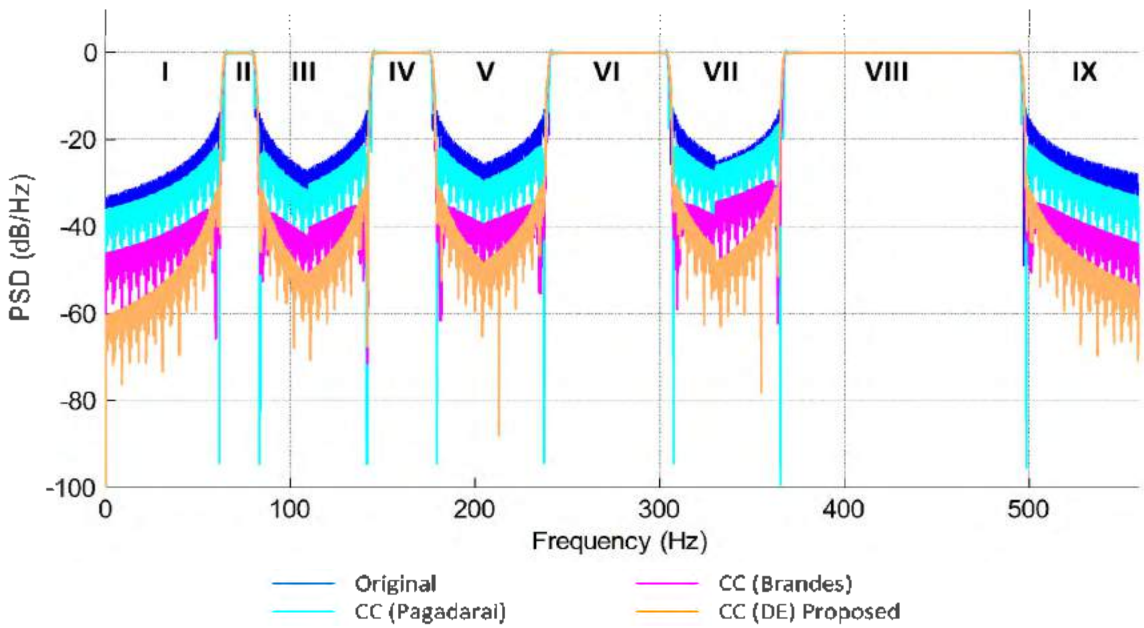

Figure 4. 34 Power spectrum of OFDM signals of 4 different SUs using DE; 16 data subcarriers in location II, 32 in IV, 64 in VI and 128 in VIII; $K_l = K_r = 2$ CCs $q_{n,s} = 1$, $n = 1, 2\ldots N_s$; Case IV.

Table 4. 20 Amplitudes of CCs calculated using DE (Case IV)

Algorithm used		First left CC	Second left CC	First right CC	Second right CC
		Amplitudes of left and right sided CCs			
DE	**SU 1**	0.12610316	0.61205280	0.61205280	0.12610316
	SU 2	0.13686577	0.63049059	0.63049059	0.13686577
	SU 3	0.13969887	0.63702942	0.63702942	0.13969887
	SU 4	0.14901664	0.64771389	0.64771389	0.14901664

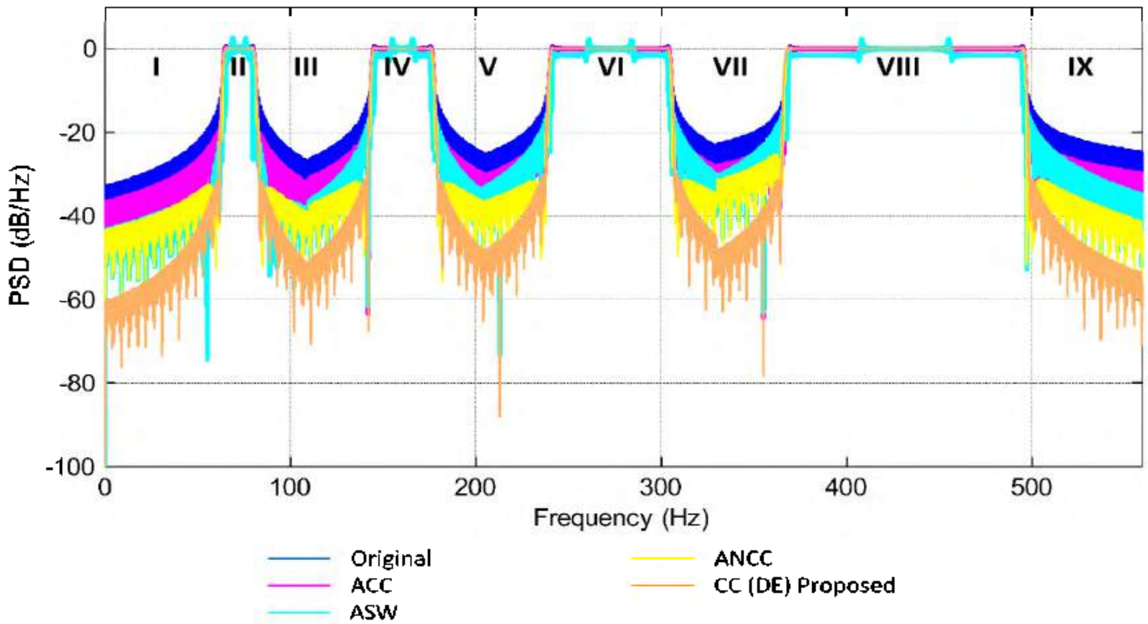

Figure 4. 35 Comparison of DE with existing techniques; 16 data subcarriers in location II, 32 in IV, 64 in VI and 128 in VIII; total of K = 4 CCs $q_{n,s}$ = 1, n = 1, 2… N_s; Case IV

4.5.4.4 Performance of CSA

In this section, the performance, reliability and effectiveness of CSA in spectrum sharing scenario, where four different SUs are utilizing the spectral holes II, IV, VI and VIII having un-equal bandwidth and the spacing between these spectral holes I, III, V, VII and IX that are in possession of PUs are considered to be of same bandwidth are shown with the help of computer simulations. Figures 4.36 – 4.37 show the comparison of our proposed algorithm, CSA with other existing techniques found in literature that shows that CSA outperforms all the existing techniques. Amplitudes of CCs for each SUs operating in different spectral holes are calculated by CSA with the help of our proposed fitness function is given in Table. 4.21.

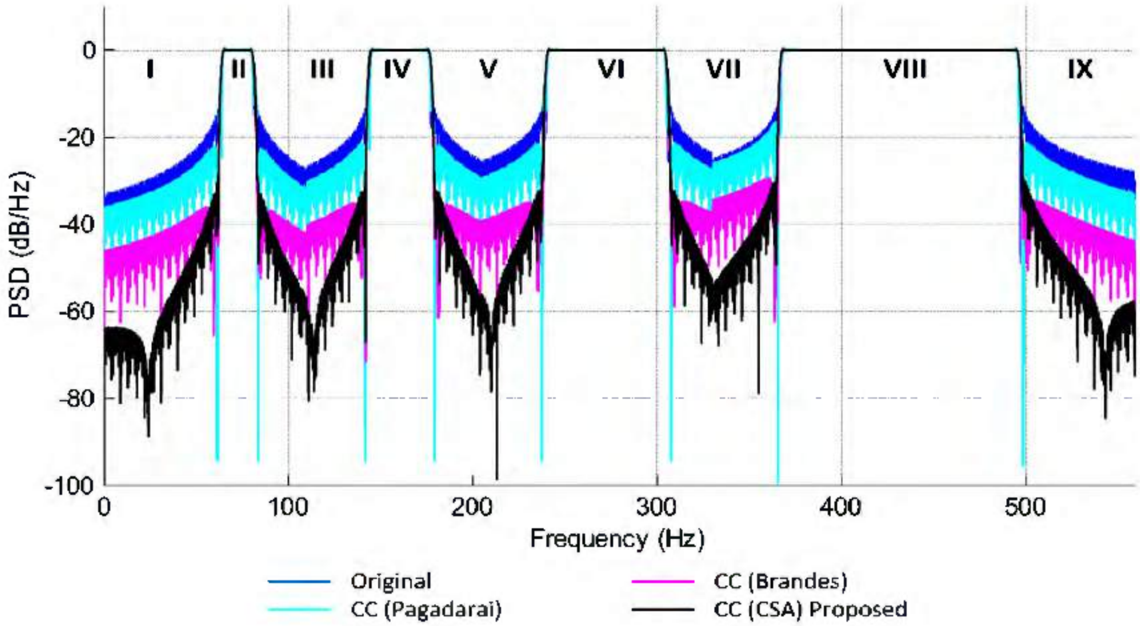

Figure 4. 36 Power spectrum of OFDM signals of 4 different SUs using CSA; 16 data subcarriers in location II, 32 in IV, 64 in VI and 128 in VIII; $K_l = K_r = 2$ CCs $q_{n,s} = 1$, n =1, 2… N_s; Case IV.

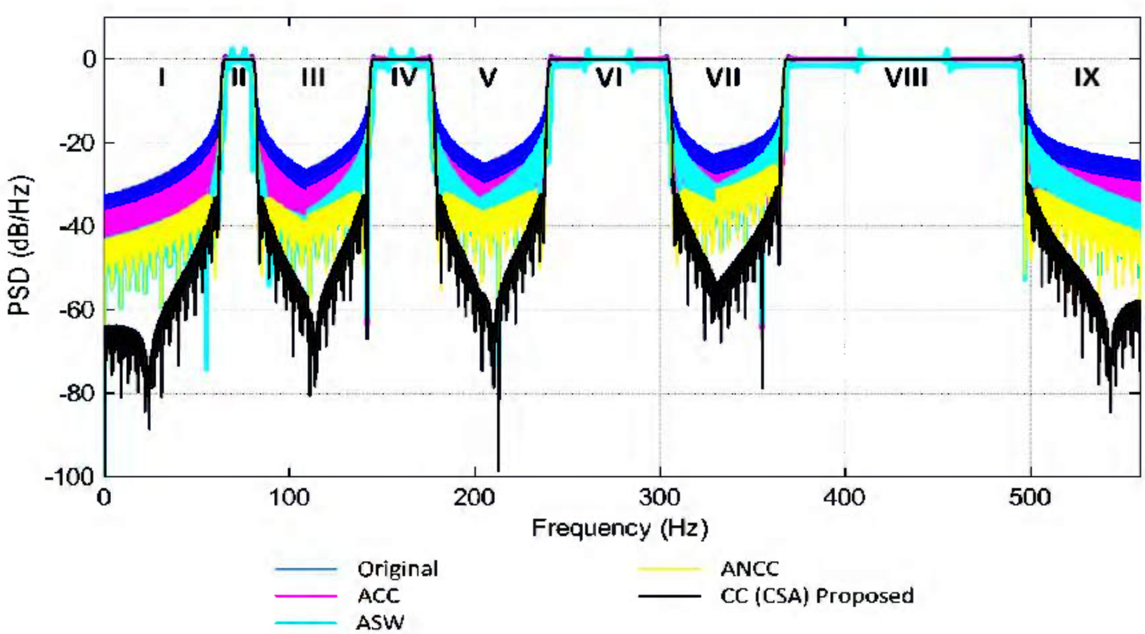

Figure 4. 37 Comparison of CSA with existing techniques; 16 data subcarriers in location II, 32 in IV, 64 in VI and 128 in VIII; total $K = 4$ CCs, $q_{n,s} = 1$, n = 1, 2… N_s; Case IV

Table 4. 21 Amplitudes of CCs calculated using CSA (Case IV)

Algorithm used		Amplitudes of left and right sided CCs			
		First left CC	**Second left CC**	**First right CC**	**Second right CC**
CSA	**SU 1**	0.13009249	0.61528217	0.61528217	0.13009249
	SU 2	0.13886577	0.63049059	0.63049059	0.13886577
	SU 3	0.14369887	0.63822942	0.63822942	0.14369887
	SU 4	0.13865122	0.63527628	0.63527628	0.13865122

4.5.4.5 Performance comparison of proposed algorithms

Here the performance of the proposed algorithms are compared with each other. Figure. 4.38 shows the simulated comparison of these proposed algorithms, which concludes that better suppression of sidelobes are achieved by CSA. Maximum suppression of sidelobes achieved by the proposed algorithms is given in Table. 4.22.

Table 4. 22 Sidelobe power levels at different locations occupied by LUs using our proposed algorithms in a spectrum sharing scenario, Case IV

Algorithm used	Sidelobe power in Locations of LUs				
	I	**III**	**V**	**VII**	**IX**
Without CCs	-33dB	-27dB	-26dB	-25dB	-28dB
GA	-52dB	-46dB	-44dB	-42dB	-46dB
FFA	-54dB	-48dB	-47dB	-45dB	-49dB
DE	-60dB	-51dB	-48dB	-48dB	-54dB
CSA	-75dB	-64dB	-60dB	-54dB	-70dB

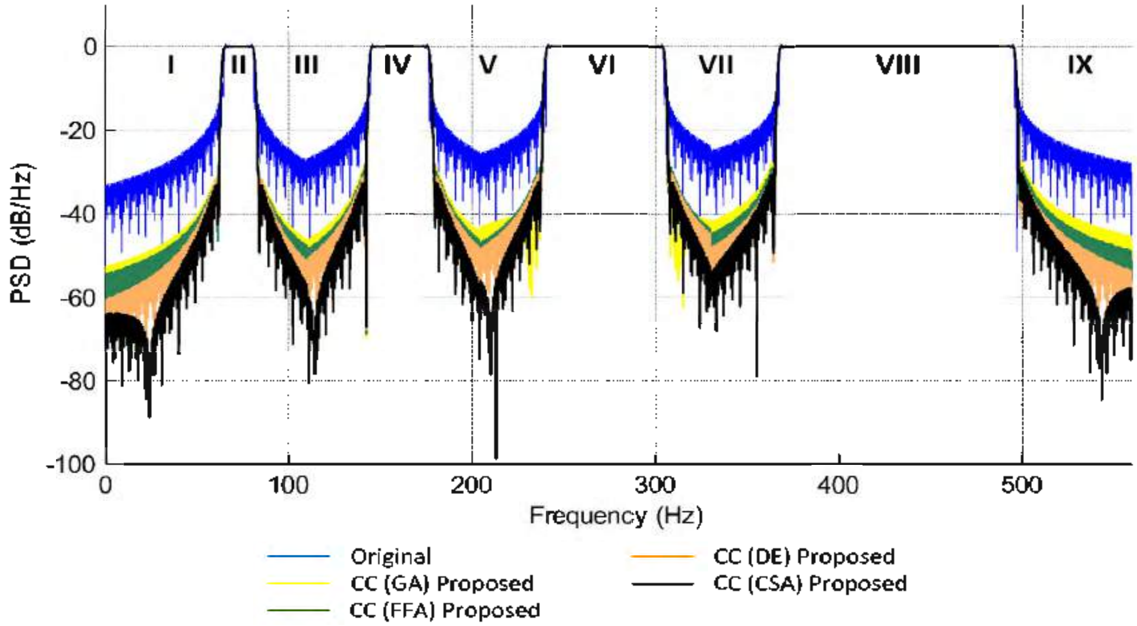

Figure 4. 38 Power spectrum of OFDM signals of 4 different SUs using proposed algorithms i.e. GA, FFA, DE and CSA; 16 data subcarriers in location II, 32 in IV, 64 in VI and 128 in VIII; $K_l = K_r = 2$ CCs, $q_{n,s} = 1$, $n = 0, 1, \ldots, N_s - 1$; Case IV

4.5.5 Case V

In this case interference suppression spectrum sharing scenario in OFDM having unequal bandwidth between the spectral white spaces II, IV, VI and VIII i.e. location I, III, V, VII and IX have un-equal bandwidth, while location II, IV, VI and VIII is also have an un-equal bandwidth comprising 16, 32, 64 and 128 subcarriers utilized by SUs, SU 1, SU2, SU3 and SU4 respectively is discussed. In order to not to interfere with the PU's two CC's on either side of the location II, IV, VI and VIII are inserted. So $N = 16$ data subcarriers and $M = 4$ CC's are there in location II, $N = 32$ data subcarriers and $M = 4$ CC's are there in location IV, $N = 64$ data carriers and $M = 4$ CC's are there in location VI and $N = 128$ data carriers and $M = 4$ CC's are there in location VIII. The Optimization range for the calculation of weights spans the sidelobes in the location I, III, V, VII and IX, here we have taken 10 samples per sidelobes to keep the computational complexity low.

Table 4. 23 Amplitudes of CCs calculated using GA (Case V)

Algorithm used		First left CC	Second left CC	First right CC	Second right CC
		Amplitudes of left and right sided CCs			
GA	**SU 1**	0.13910977	0.63090059	0.63090059	0.13910977
	SU 2	0.13101062	0.62952007	0.62952007	0.13101062
	SU 3	0.13547502	0.61891019	0.61891019	0.13547502
	SU 4	0.13565122	0.64327628	0.64327628	0.13565122

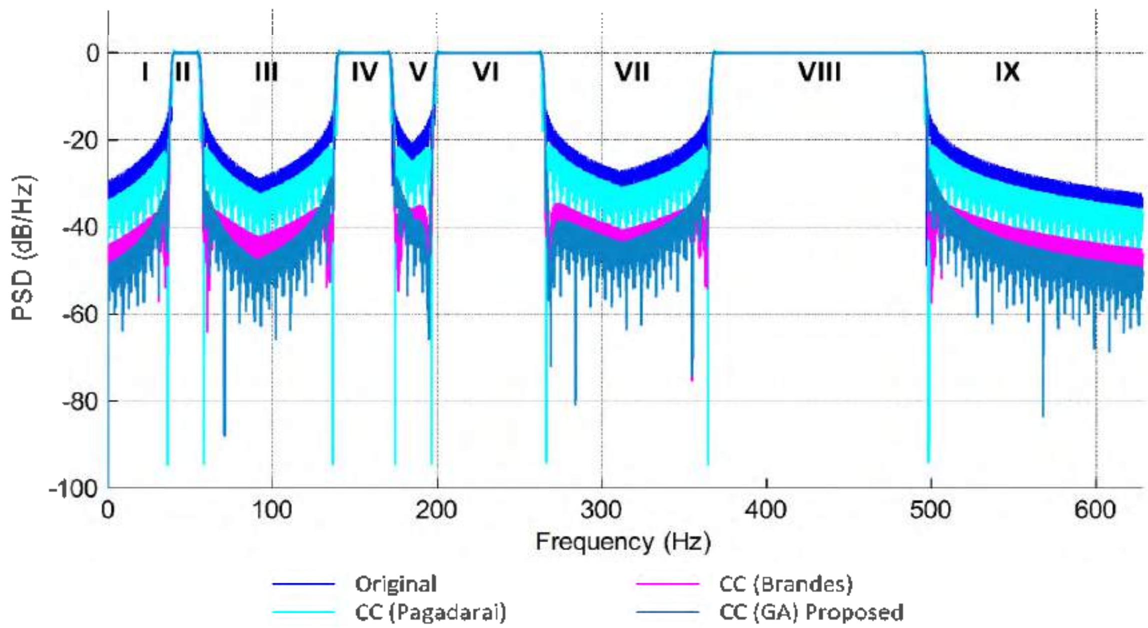

Figure 4. 39 Power spectrum of OFDM signals of 4 different SUs using GA; 16 data subcarriers in location II, 32 in IV, 64 in VI and 128 in VIII; $K_l = K_r = 2$ CCs , $q_{n,s} = 1$, $n = 1, 2\ldots N_s$; Case V.

4.5.5.1 Performance of GA

In this section, we consider the spectrum sharing scenario, where the spectral holes occupied by SUs and the spectrums utilized by PUs are of un-equal bandwidth. GA is used in this section for the calculation of CCs that are given in Table 4.23. The effectiveness and reliability of GA and its comparison with other techniques are shown in Figures. 4.39 – 4.40.

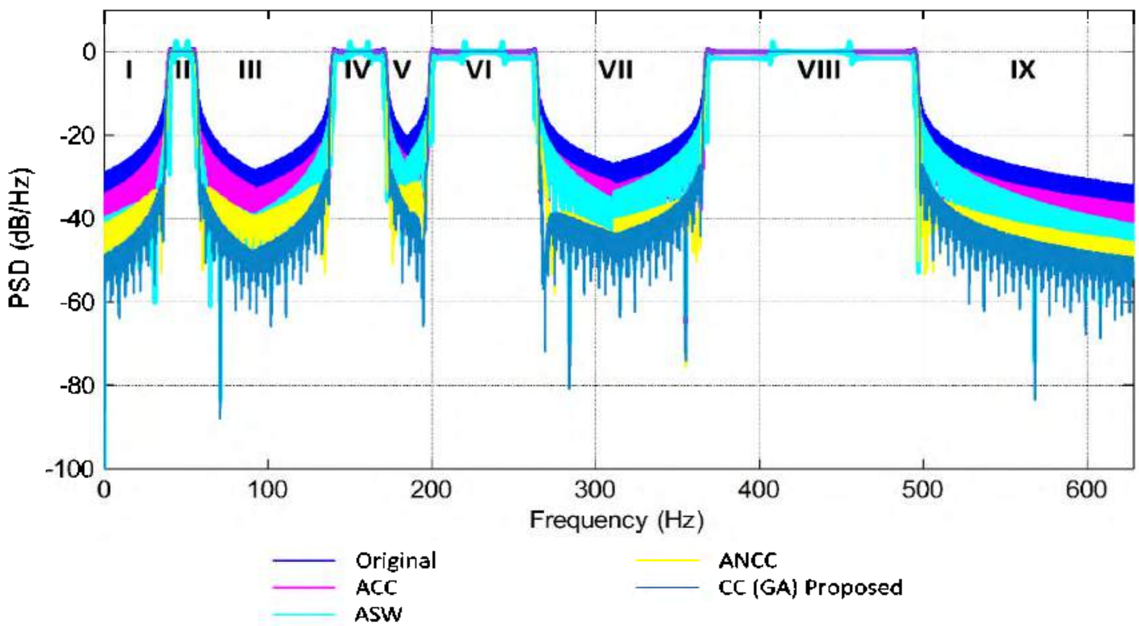

Figure 4. 40 Comparison of GA with existing techniques; 16 data subcarriers in location II, 32 in IV, 64 in VI and 128 in VIII; total of $K = 4$ CCs, $q_{n,s} = 1$, $n = 1, 2\ldots N_s$; Case V.

4.5.5.2 Performance of FFA

In this section, performance of FFA in spectrum sharing scenario, consisting of four SUs utilizing the spectral holes II, IV, VI and VIII having un-equal bandwidth and with PUs operating in the neighboring spectrums I, III, V, VII and IX also of un-equal bandwidth is discussed. The effectiveness, performance and reliability of FFA using simulations in terms of PSD in comparison with existing techniques found in the literature is shown in Figures. 4.41 – 4.42.

The amplitudes of CCs of all four SUs utilizing in spectrum white holes II, IV, VI and VIIII calculated by FFA using our proposed fitness function are given in Table. 4.24.

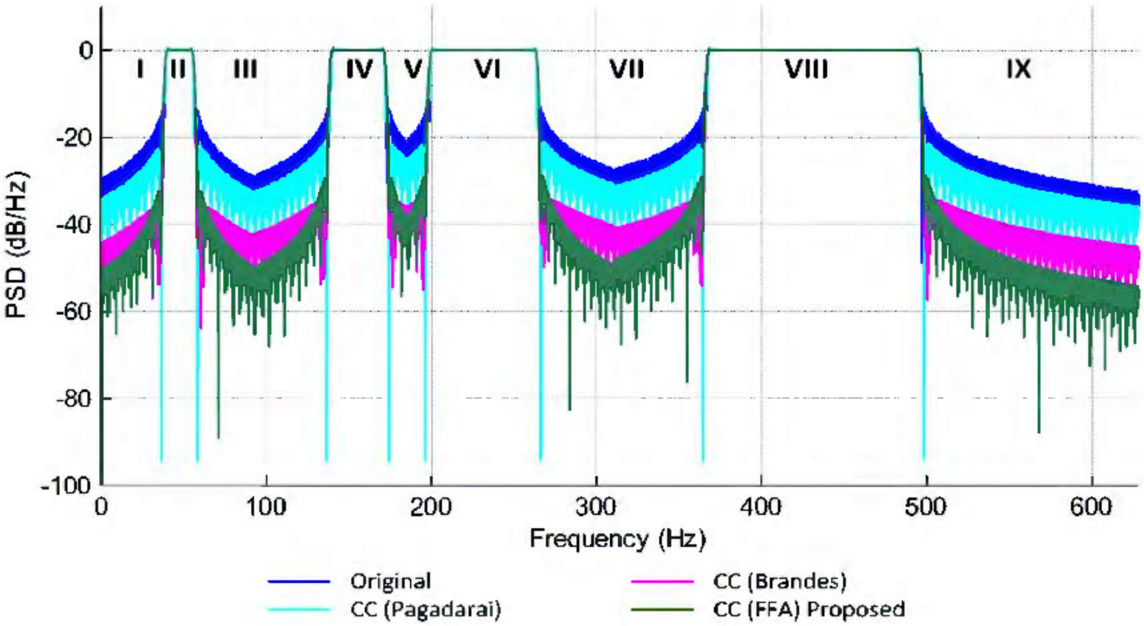

Figure 4. 41 Power spectrum of OFDM signals of 4 different SUs using FFA; 16 data subcarriers in location II, 32 in IV, 64 in VI and 128 in VIII; $K_l = K_r = 2$ CCs, $q_{n,s} = 1$, $n = 1, 2\ldots N_s$; Case V.

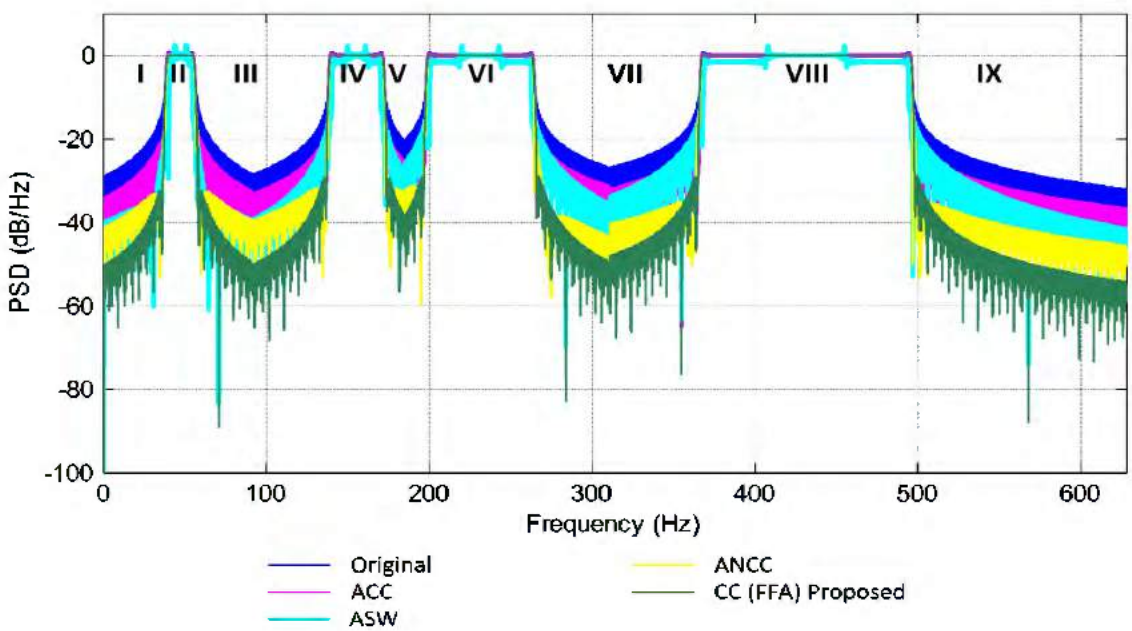

Figure 4. 42 Comparison of FFA with existing techniques; 16 data subcarriers in location II, 32 in IV, 64 in VI and 128 in VIII; total of $K = 4$ CCs , $q_{n,s} = 1$, $n = 1, 2\ldots N_s$; Case V

Table 4. 24 Amplitudes of CCs calculated using FFA (Case V)

Algorithm used		First left CC	Second left CC	First right CC	Second right CC
		Amplitudes of left and right sided CCs			
FFA	**SU 1**	0.13896577	0.62909059	0.62909059	0.13896577
	SU 2	0.13101062	0.62652007	0.62652007	0.13101062
	SU 3	0.13197502	0.62990019	0.62990019	0.13197502
	SU 4	0.13895122	0.63999098	0.63999098	0.13895122

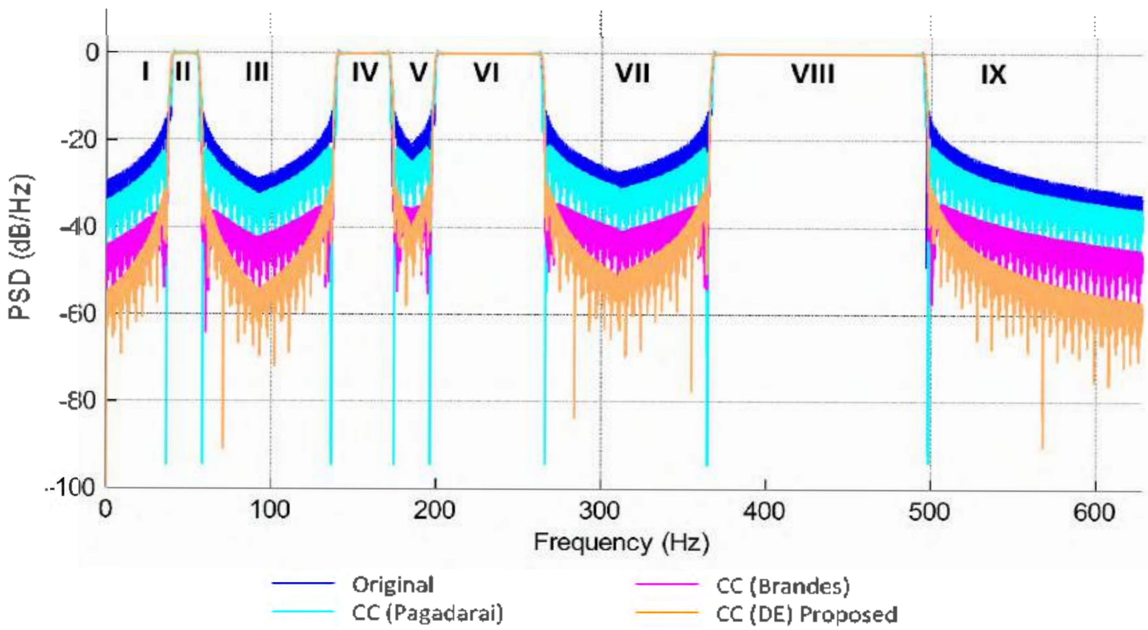

Figure 4. 43 Power spectrum of OFDM signals of 4 different SUs using DE; 16 data subcarriers in location II, 32 in IV, 64 in VI and 128 in VIII; $K_l = K_r = 2$ CCs, $q_{n,s} = 1$, $n = 1, 2 \ldots N_s$; Case V

4.5.5.3 Performance of DE

In this section we consider spectrum sharing scenario in which four SUs utilizing the spectral holes of un-equal bandwidth and the PUs operating in neighboring holes are also of un-equal bandwidth. Here DE is used for the calculation of amplitudes of CCs that are used for the suppression of sidelobes. The amplitudes of CCs are given in Table. 4.25, while the performance of DE is shown in Figures. 4.43 – 4.44 respectively.

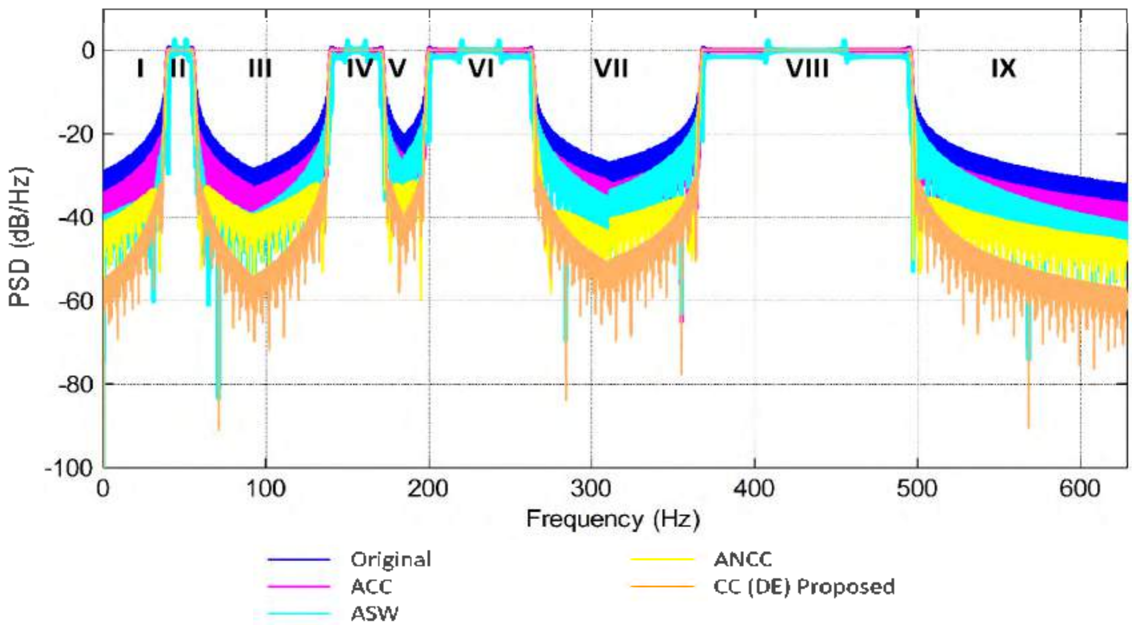

Figure 4. 44 Comparison of DE with existing techniques; 16 data subcarriers in location II, 32 in location IV, 64 in VI and 128 in VIII; total of $K = 4$ CCs, $q_{n,s} = 1$, $n = 1, 2\ldots N_s$; Case V

Table 4. 25 Amplitudes of CCs calculated using DE (Case V)

Amplitudes of left and right sided CCs					
Algorithm used		**First left CC**	**Second left CC**	**First right CC**	**Second right CC**
DE	**SU 1**	0.12610316	0.61205280	0.61205280	0.12610316
	SU 2	0.13686577	0.63049059	0.63049059	0.13686577
	SU 3	0.13969887	0.63702942	0.63702942	0.13969887
	SU 4	0.14901664	0.64871389	0.64871389	0.14901664

4.5.5.4 Performance of CSA

In this section the performance of CSA in spectrum sharing scenario, where four different SUs occupying four spectral holes II, IV, VI and VIII and of un-equal bandwidth and the spacing between them are also of un-equal bandwidth is discussed. The effectiveness and reliability of CSA in term of PSD are shown in Figures. 4.45 – 4.46, while the amplitudes of CCs are calculated using CSA, given in Table. 4.26.

Table 4. 26 Amplitudes of CCs calculated using CSA (Case V)

Amplitudes of left and right sided CCs					
Algorithm used		**First left CC**	**Second left CC**	**First right CC**	**Second right CC**
CSA	**SU 1**	0.13009249	0.61528217	0.61528217	0.13009249
	SU 2	0.13886577	0.63149059	0.63149059	0.13886577
	SU 3	0.14369887	0.63822942	0.63822942	0.14369887
	SU 4	0.13895122	0.63627628	0.63627628	0.13895122

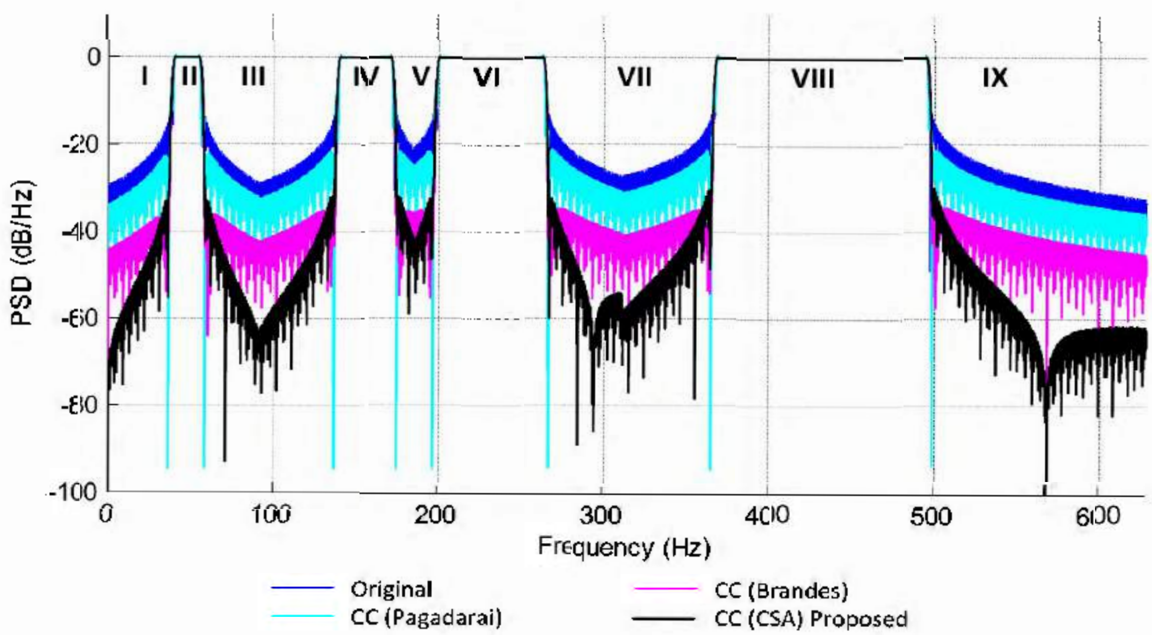

Figure 4. 45 Power spectrum of OFDM signals of 4 different SUs using CSA; 16 data subcarriers in location II, 32 in, 64 in VI and 128 in; $K_l = K_r = 2$ CCs, $q_{n,s} = 1$, $n = 1, 2\ldots N_s$; Case V

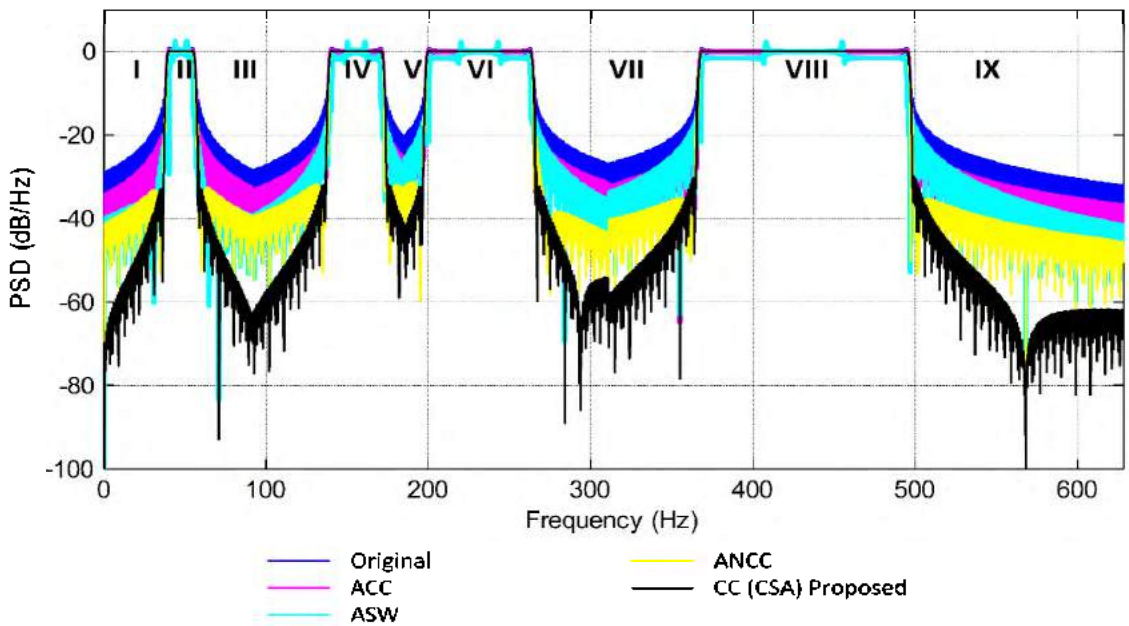

Figure 4. 46 Comparison of CSA with existing techniques; 16 data subcarriers in location II, 32 in IV, 64 in VI and 128 in VIII; total of K = 4 CCs, $q_{n,s}$ = 1, n =1, 2… N_s; Case V

4.5.5.5 Performance comparison of proposed algorithms

Here the performance comparison of proposed algorithms in a spectrum sharing scenario, where four spectral holes II, IV, VI and VIII of un-equal sizes are detected that are utilized by four different SUs and the spectral spacing between these holes also of un-equal bandwidth are utilized by different PUs is considered. Figure. 4.47 shows the performance comparison of all four proposed algorithms i.e. GA, FFA, DE and CSA in terms of PSD with each other and with the existing techniques found in the literature, which shows that CSA got better suppression of sidelobes as compared to the GA, FFA, DE and with the existing techniques. Maximum suppression of sidelobes achieved in terms of dBs by the proposed algorithms are given in Table. 4.27.

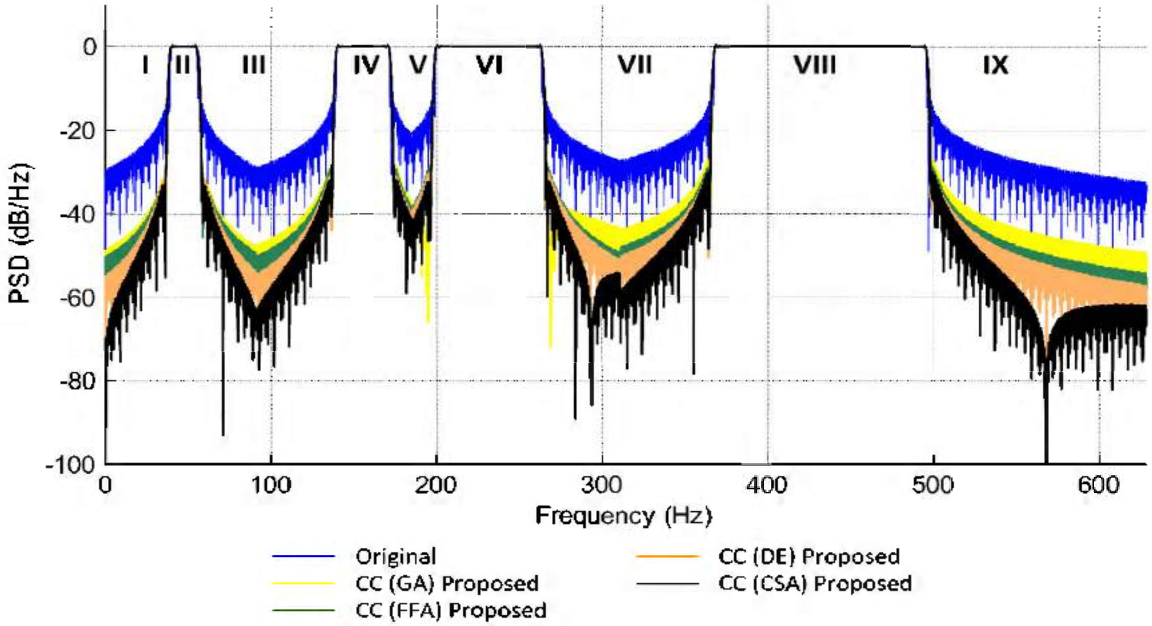

Figure 4. 47 Power spectrum of OFDM signals of 4 different SUs using proposed algorithms i.e. GA, FFA, DE and CSA; 16 data subcarriers in location II, 32 in location IV, 64 in location VI and 128 in location VIII; $K_l = K_r = 2$ CCs in each of the location II, IV, VI and VIII, $q_{n,s} = 1$, $n = 1, 2\ldots N_s$; Case V

Table 4. 27 Sidelobe power levels at different locations occupied by LUs using our proposed algorithms in a spectrum sharing scenario, Case V

Algorithm used	**Sidelobe power in Locations of LUs**				
	I	**III**	**V**	**VII**	**IX**
Without CCs	-30dB	-29dB	-21dB	-27dB	-32dB
GA	-48dB	-48dB	-38dB	-44dB	-50dB
FFA	-50dB	-50dB	-40dB	-48dB	-54dB
DE	-55dB	-54dB	-42dB	-53dB	-57dB
CSA	-70dB	-62dB	-44dB	-58dB	-74dB

4.6 Conclusion

In this chapter, we have discussed the CCs based sidelobe reduction scheme. Here some subcarriers are reserved or inserted mainly on the edges of the OFDM spectrum of SUs, that are basically not used to carry information but to cancel the sidelobes of the OFDM spectrum of SUs. To calculate the amplitudes of the main lobe of CCs, we have proposed four different HA: GA, FFA, DE and CSA by using our proposed Fitness function. Five different spectrum sharing scenario are considered to check the performance, efficiency and reliability of the proposed algorithms.

Chapter 5

Reduction of out of Band Radiation using Generalized Sidelobe Canceller

5.1 Introduction

In this chapter, we present a novel technique for the reduction of OOB radiation in OFDM-based CR by using a generalized sidelobe canceller (GSC) at the transmitter of OFDM. It has been observed that so far in OFDM-based CR system, a GSC has not been used to tackle the OOB radiation problem. In the proposed technique, the signal is passed through two branches of a GSC. The upper branch consists of the weight vector designed by multiple constraints to preserve the desired portion of the signal, while the lower branch consists of a blocking matrix followed by a weight vector. The blocking matrix blocks the desired portion and preserves the undesired portions (sidelobes). The weight vector adjusts the undesired portion (sidelobes) in such a way that when subtracted from the signal of the upper branch, it results in significant cancellation of the sidelobes of the OFDM signal. We have compared the performance of the proposed technique with already existing techniques via simulations. The proposed technique achieves better suppression of the sidelobes as compared to the existing methods.

The data model used for our proposed technique that we will discuss in this chapter will be same as we have developed in chapter 4.

5.2 Proposed Methodology

In this section, we propose a novel technique by using GSC at the transmitter of OFDM. GSC is the simplest version of linearly constrained minimum variance (LCMV), where the constrained optimization problem is converted into an unconstrained problem. The block diagram of GSC is shown in Figure 5.1, having two branches, the upper branch and the lower branch. The upper branch is the main channel of the GSC, usually called a Fixed Beamformer (FBF). It consists of quiescent weight vector $\mathbf{w}_q$, which preserves the signal coming from SU, *i.e.*, the OFDM signal, and provides the necessary gain to the desired portion, *i.e.*, the region from f_1 to f_N satisfying the constraint, as shown in Figure 5.2. The lower branch consists of the blocking matrix **B** followed by an adaptive weight vector $\mathbf{w}_a$. The blocking matrix **B** blocks the desired portion of the signal and preserves the sidelobes of OFDM signal, as shown by region $f < f_1$ and $f > f_N$ in Figure 5.2. The adaptive weight vector $\mathbf{w}_a$ adjusts the amplitudes of the sidelobes. The sidelobes that are preserved and adjusted in the lower branch are then subtracted from the signal of the upper branch, resulting in the signal of OFDM having suppressed or zero sidelobes.

To find the expressions for $\mathbf{w}_q$, **B** and $\mathbf{w}_a$, consider the OFDM signal given in equation (4.3), represented by M samples, which are collected in the vector $\mathbf{u} = [\mathrm{u}_1, \mathrm{u}_2, ...\mathrm{u}_M]^T$ with uncorrelated elements. After passing through GSC it is given as:

$$Y = \mathbf{w}^H \mathbf{u} \tag{5.1}$$

where the superscript H represents Hermitian and $\mathbf{w} = [\mathrm{w}_0, \mathrm{w}_1, ..., \mathrm{w}_{M-1}]^T$ is a weight vector with dimension $M \times 1$.

LCMV determines the optimal weight vector $\mathbf{w}^H$ that minimizes the output power having multiple linear constraints. The optimization problem for LCMV is given by:

$$\min_{\mathbf{w}} \mathbf{w}^H \mathbf{R}_{\mathbf{u}} \mathbf{w} \;\; s.t \;\; \mathbf{w}^H \mathbf{C} = \mathbf{g}^H \tag{5.2}$$

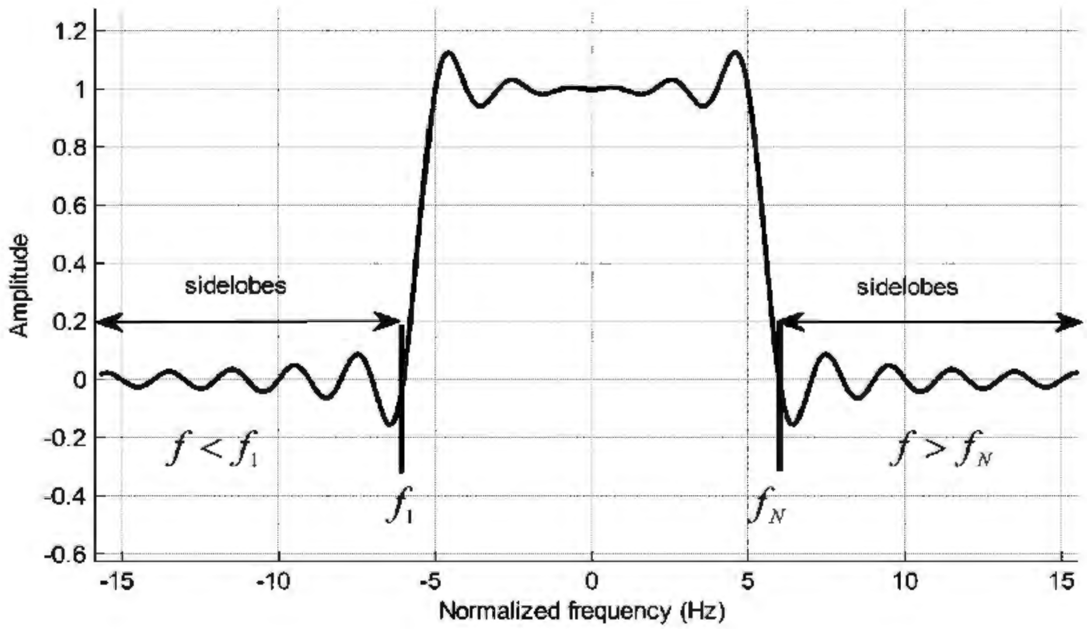

Figure 5. 2 OFDM signal in Frequency domain

On solving Equation (5.2), we obtain:

$$\mathbf{w}_o^H = \mathbf{g}^H (\mathbf{C}^H \mathbf{R}_{\mathbf{u}}^{-1} \mathbf{C})^{-1} \mathbf{C}^H \mathbf{R}_{\mathbf{u}}^{-1} \tag{5.3}$$

where $\mathbf{R}_{\mathbf{u}} = E[\mathbf{u}\mathbf{u}^H] = \sigma^2 \mathbf{I}$ is the correlation matrix, with dimension $M \times M$, **I** is the identity matrix with dimension $M \times M$, σ^2 is the variance, while **C** is the constraint matrix with dimension $M \times N$, having N steering vectors given by equation (5.4):

$$\mathbf{C} = [\mathbf{s}_1, \mathbf{s}_2, ..., \mathbf{s}_N] \tag{5.4}$$

where N represents the total number of frequencies in the desired portion of the signal, as shown in Figure 5.1; $\mathbf{s}_i = [s_1, s_2, \ldots s_M]^T$ is an i^{th} steering vector with dimension $M \times 1$ containing M samples of the i^{th} spectrum; and $\mathbf{g} = [1, 1, \ldots, 1]^T$ is called the gain vector with dimension $N \times 1$, which contains the desired gain related to each steering vector.

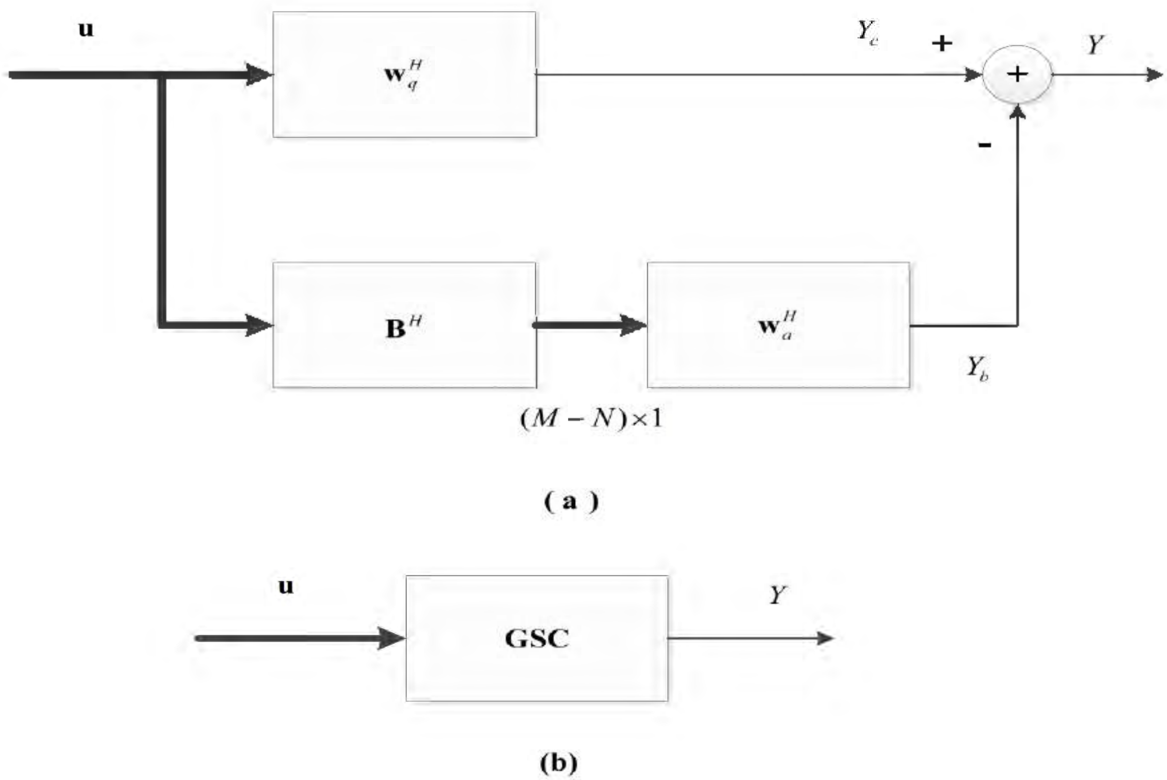

Figure 5. 1 Generalized sidelobe canceller (GSC) (a) Block Diagram of GSC (b) Equivalent Diagram of GSC

The effective implementation of LCMV is the division of a field with dimension $M \times M$ into the constraint subfield defined by columns of **C**, an $M \times N$ matrix, and an orthogonal subfield defined by columns of **B** an $M \times (M - N)$ matrix such that

$$\mathbf{C}^H\mathbf{B} = \mathbf{O} \tag{5.5}$$

where **O** is a null matrix with dimension $N \times (M - N)$ and **B** is a blocking matrix that blocks the desired portion of the OFDM signal.

Now consider the decomposition of $\mathbf{w}_o^H$ given in equation (5.3) as:

$$\mathbf{w}_o^H = \mathbf{w}_o^H\mathbf{P}_c - \mathbf{w}_o^H\mathbf{P}_o \tag{5.6}$$

where $\mathbf{w}_o^H\mathbf{P}_c$ represents the projection of $\mathbf{w}_o^H$ onto the constraint subfield and $\mathbf{w}_o^H\mathbf{P}_o$ represents the projection of $\mathbf{w}_o^H$ onto the orthogonal subfield. $\mathbf{P}_c$ and $\mathbf{P}_o$ are the projection matrices onto the constraint and orthogonal subfields with dimension $M \times M$ given by:

$$\mathbf{P}_c = \mathbf{C}[\mathbf{C}^H\mathbf{C}]^{-1}\mathbf{C}^H \tag{5.7}$$

$$\mathbf{P}_o = \mathbf{B}[\mathbf{B}^H\mathbf{B}]^{-1}\mathbf{B}^H \tag{5.8}$$

where $\mathbf{P}_o$ can also be written as

$$\mathbf{P}_o = \mathbf{I} - \mathbf{P}_c \tag{5.9}$$

where **I** is an identity matrix with dimension $M \times M$.

The first component of equation (5.6) represents the upper portion of GSC, which on solving becomes:

$$\mathbf{w}_o^H\mathbf{P}_c = \mathbf{g}^H[\mathbf{C}^H\mathbf{R}_{\mathbf{u}}^{-1}\mathbf{C}]^{-1}\mathbf{C}^H\mathbf{R}_{\mathbf{u}}^{-1}\mathbf{C}[\mathbf{C}^H\mathbf{C}]^{-1}\mathbf{C}^H \tag{5.10}$$

$$\mathbf{w}_o^H \mathbf{P}_c = \mathbf{g}^H [\mathbf{C}^H \mathbf{C}]^{-1} \mathbf{C}^H \triangleq \mathbf{w}_q^H \tag{5.11}$$

where $\mathbf{w}_q^H$ is the quiescent weight vector having dimension $1 \times M$.

The second component of equation (5.6) represents the lower portion of the GSC. On substituting the values for $\mathbf{w}_o^H$ and $\mathbf{P}_o$, equation (5.6) becomes

$$\mathbf{w}_o^H \mathbf{P}_o = \mathbf{g}^H [\mathbf{C}^H \mathbf{R}_\mathbf{u}^{-1} \mathbf{C}]^{-1} \mathbf{C}^H \mathbf{R}_\mathbf{u}^{-1} \mathbf{B} [\mathbf{B}^H \mathbf{B}]^{-1} \mathbf{B}^H \tag{5.12}$$

As equation (5.12) is not particularly useful for implementation, it is divided into two parts. The first part consists of blocking matrix B, and the second part consists of an adaptive weight vector $\mathbf{w}_a^H$ with dimension $1 \times (M - N)$.

The blocking matrix **B** can be constructed by first finding the $\mathbf{P}_o$ as given in Equation (5.9), then orthonormalizing $\mathbf{P}_o$ and choosing the first $(M - N)$ columns of the orthonormalized matrix that will be the resulting blocking matrix **B**, having the property given by

$$\mathbf{B}^H \mathbf{B} = \mathbf{I} \tag{5.13}$$

The output of the GSC as shown in Figure 5.2 after replacing $\mathbf{w}_o^H$ with $(\mathbf{w}_q - \mathbf{B}\mathbf{w}_a)^H$ will become:

$$Y = (\mathbf{w}_q - \mathbf{B}\mathbf{w}_a)^H \mathbf{u} \tag{5.14}$$

the output power of which is given by:

$$P = (\mathbf{w}_q - \mathbf{B}\mathbf{w}_a)^H \mathbf{R}_\mathbf{u} (\mathbf{w}_q - \mathbf{B}\mathbf{w}_a) \tag{5.15}$$

Solving equation (5.15), we get the optimum adaptive weight vector $\mathbf{w}_{a(opt)}$, given by the following equation:

$$\mathbf{w}_{a(opt)}^{H} = \mathbf{w}_{q}^{H}\mathbf{R_u B}(\mathbf{B}^{H}\mathbf{R_u B})^{-1} \tag{5.16}$$

5.3 Results and Discussions

In this section both the accuracy and the reliability of the proposed technique are discussed for the reduction of sidelobe suppression of the OFDM signal. The performance comparison of the proposed technique has been done in terms of normalized PSD with already existing techniques in this area. Several cases have been discussed on the basis of spectral white spaces and its bandwidth between spectral white spaces. Throughout the simulations, the number of samples M is taken as 501, while the number of frequencies N in Case I is taken as 16, in Cases II and IV as 32, while in Case III and Case V, it is taken as 16, 32, 64, and 128, respectively.

5.3.1 Case I

In this case, we are considering a spectral white space that is not used by the PU and is available for the SU. The total number of OFDM subcarriers used by SU is 16 modulated with BPSK, whose power is normalized to $|d_n|^2 = 1$. The performance of the proposed technique is compared with different existing techniques. In CC techniques, two CC*s* have been used either side of the data subcarriers, whereas in advanced subcarriers weighting techniques all subcarriers are used for weighting. Figures 5.3 and 5.4 show the comparison of the proposed technique with the existing techniques in terms of PSD. It can be observed from Figures 5.3 and 5.4 that the existing techniques give a maximum of 36 dB improvement, while the proposed technique gives 92 dB improvement

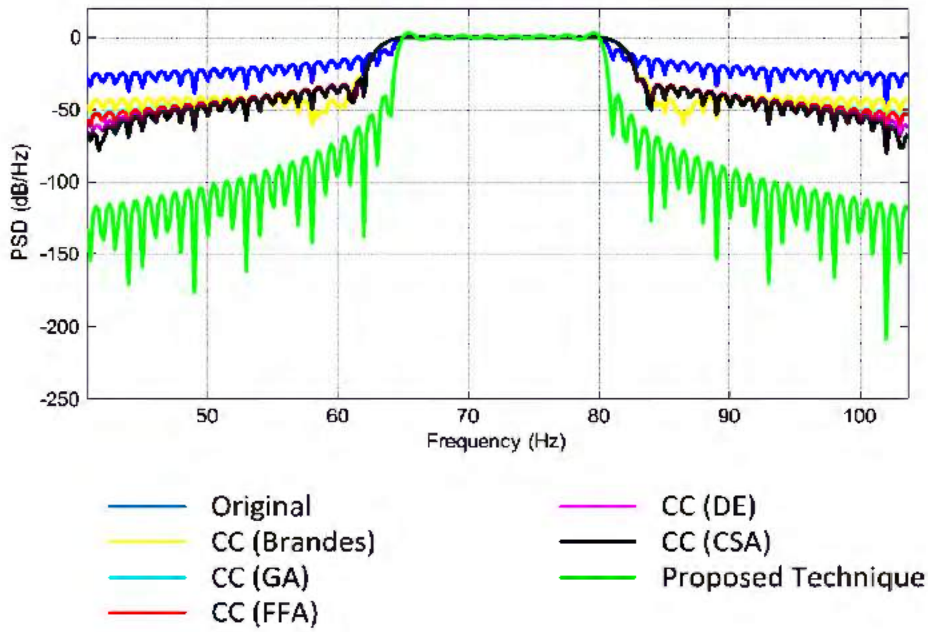

Figure 5. 3 The PSD comparison between the proposed technique and existing techniques, Case I

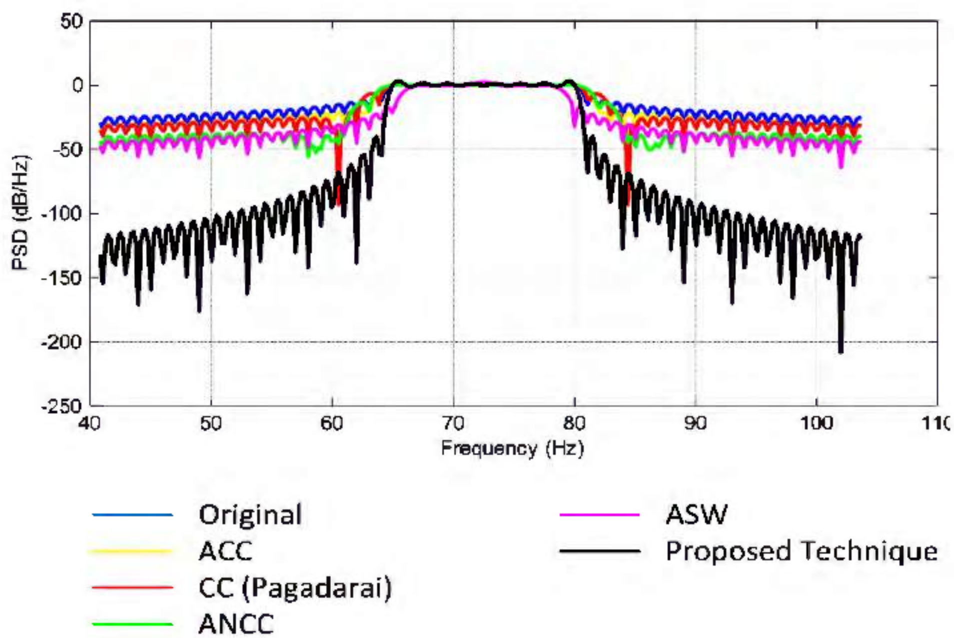

Figure 5. 4 The PSD performance comparison between the proposed technique and existing techniques, Case I

compared with the original OFDM spectrum and 58 dB improvement as compared with the existing techniques.

5.3.2 Case II

In this case, we are considering nine sub-bands mentioned as regions in Figures 5.5 and 5.6. We assume that regions I, III, V, VII, and IX are occupied by PU*s*, while regions II, IV, VI, and VIII are occupied by SU*s*. Each SU has an equal number of subcarriers, *i.e.*, 32 OFDM subcarriers modulated with BPSK, whose power is normalized to $|d_n|^2 = 1$. The bandwidth allocated to each PU is considered equal in all regions. The comparison of the proposed technique is done with already existing techniques. In CC techniques, two CC*s* have been used on either side of data subcarriers, while in the advanced subcarrier weightings technique all subcarriers are taken into consideration. Figures 5.5 and 5.6 show the superiority of the proposed technique in terms of PSD, even in a spectrum-sharing scenario. The proposed technique performs well and outclasses all these techniques and gets significant suppression in all regions.

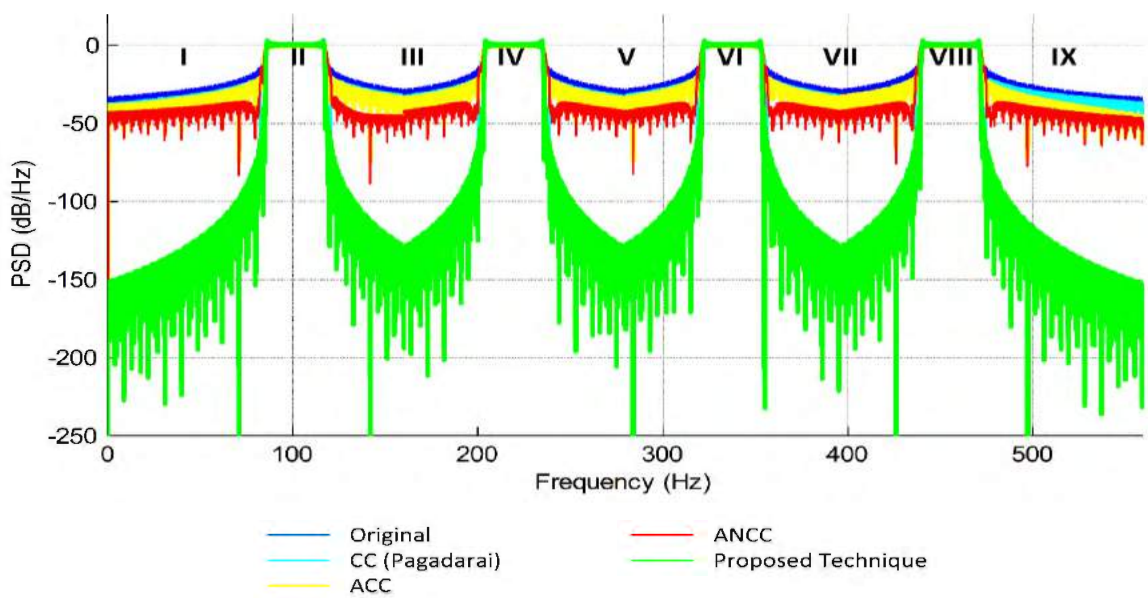

Figure 5. 5 The PSD comparison between the proposed and existing techniques, Case II

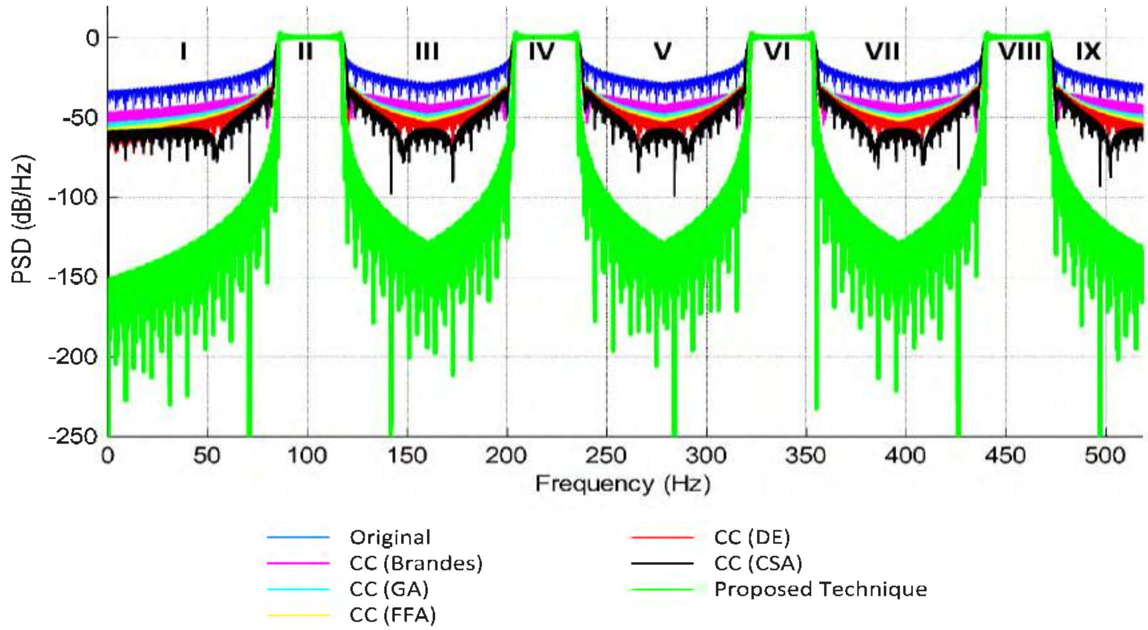

Figure 5. 6 The PSD performance comparison between the proposed technique and existing techniques, Case II

5.3.3 Case III

In this case, we are considering the spectrum-sharing scenario shown in Figures 5.7 and 5.8, consisting of nine sub-bands in total. Out of these nine, four are given to different SU*s* designated by regions II, IV, VI, and VIII, while the remaining regions I, III, V, VII, and IX are given to PU*s*. Consider that the bandwidth II, IV, VI and VIII allocated to these four SU*s* is equal, while the bandwidths I, III, V, VII and IX allocated to different PU*s* are unequal. Each SU divide the available bandwidth into 32 OFDM subcarriers modulated with BPSK with normalized power equal to 1. Figures 5.7 and 5.8 shows the performance, reliability and effectiveness of our proposed technique with already existing sidelobe suppression techniques in terms of PSD which shows that our proposed technique has got effective reduction of sidelobes.

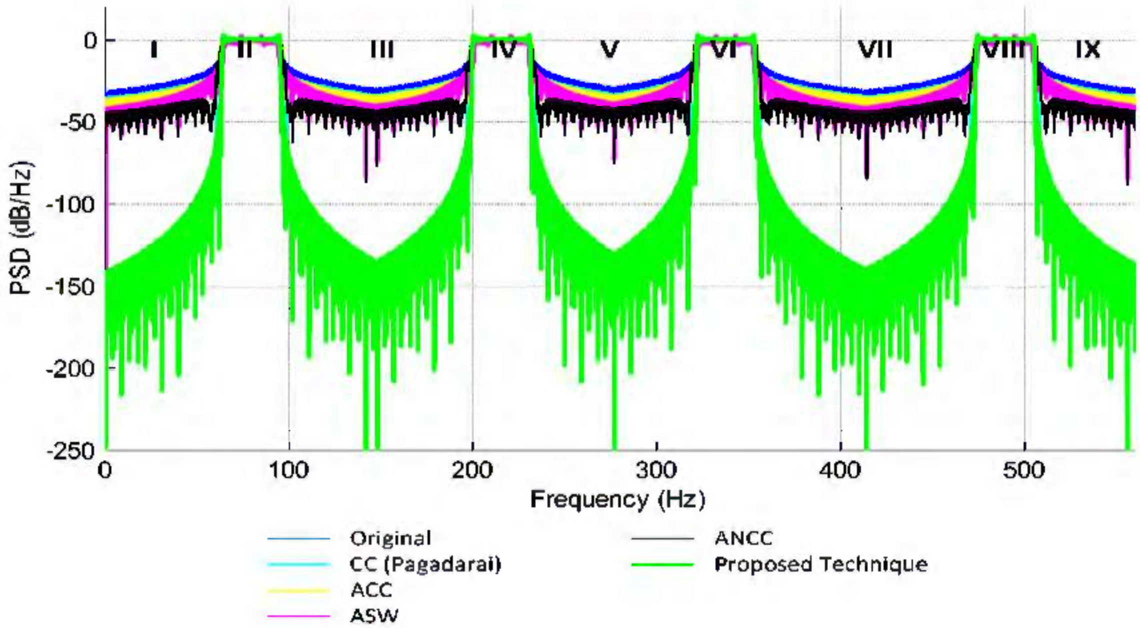

Figure 5. 7 The PSD comparison between the proposed and existing techniques, Case III

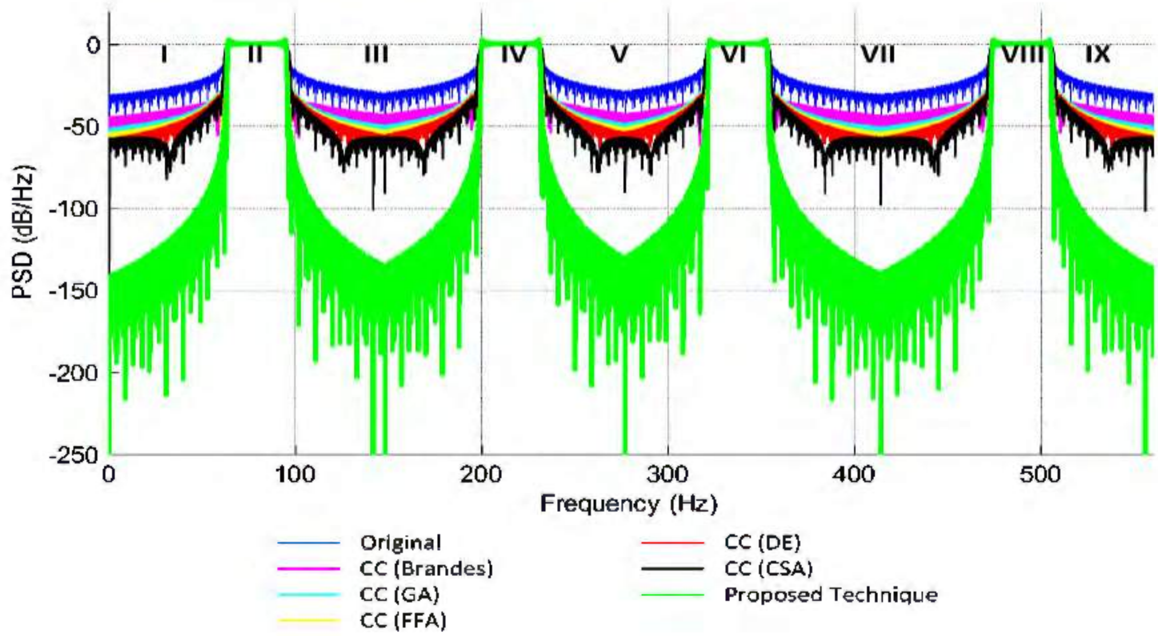

Figure 5. 8 The PSD performance comparison between the proposed technique and existing techniques, Case III

In all CC techniques, two CC*s* have been taken on both sides of the data subcarriers. In terms of normalized PSD, Figures 5.7 and 5.8 show that clear reduction of OOB radiation is achieved in all regions of PU by the proposed technique.

5.3.4 Case IV

In this case, we are considering the spectrum-sharing scenario consisting of a total of nine sub-bands mentioned as regions in Figures 5.9 and 5.10. We assume that regions I, III, V, VII, and IX are used by PU*s*, while regions II, IV, VI, and VIII are used by SU*s*. An equal bandwidth is allocated to each PU, whereas it is unequal in the case of SU. The SU operating in region II has 16 subcarriers, region IV has 32, region VI has 64, and SU, operating in region VIII, has 128 subcarriers, modulated with BPSK, whose power is normalized to $|d_n|^2 = 1$. The performance of the proposed technique is compared with different existing techniques.

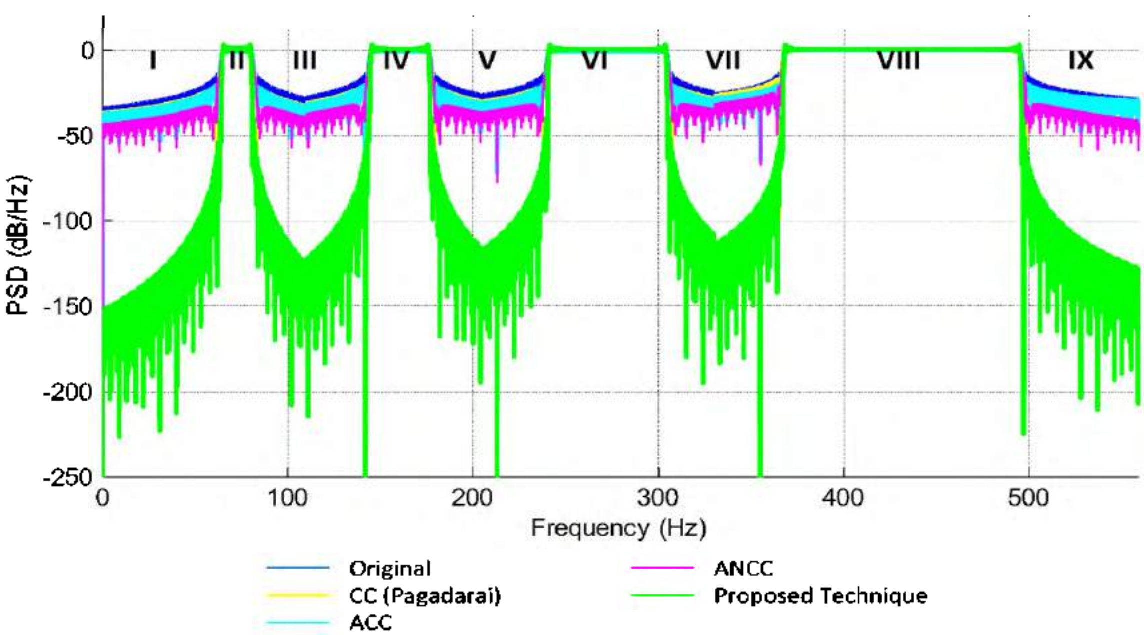

Figure 5. 9 The PSD comparison between the proposed and existing techniques, Case IV

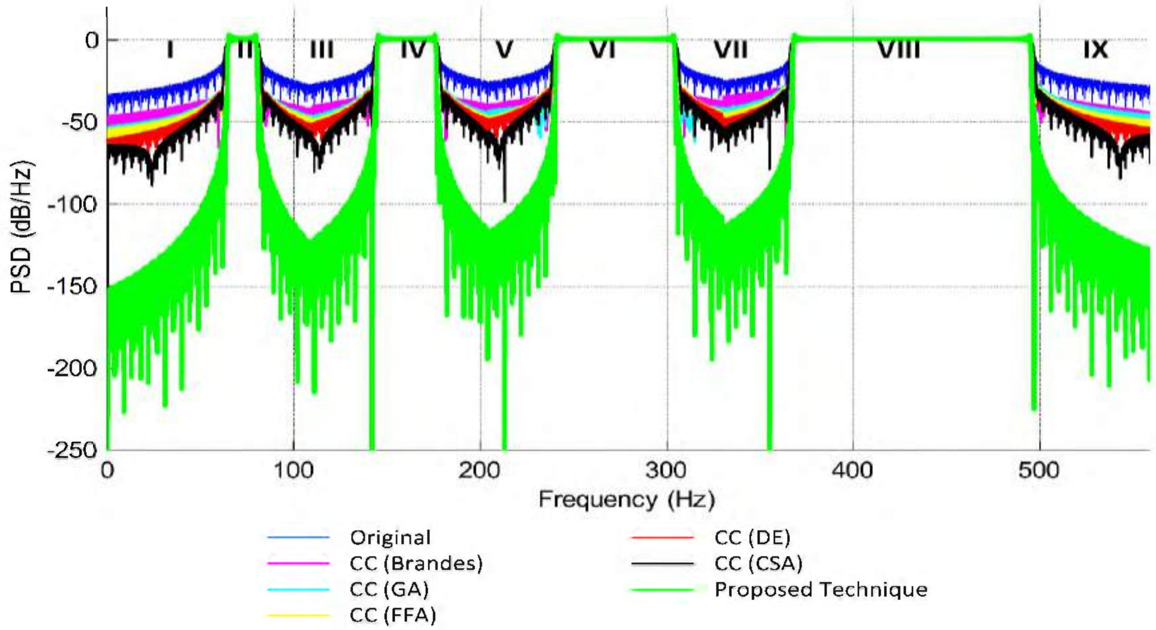

Figure 5. 10 The PSD performance comparison between the proposed technique and existing techniques, Case IV

In CC techniques, two CC*s* have been taken on either side of the data subcarriers, and in SW techniques all subcarriers are used for suppression. Figure 5.9 and 5.10 show that the proposed technique outclasses all these techniques and gives a significant suppression in all regions of the spectrum-sharing scenario.

5.3.5 Case V

In this case, five out of nine sub-bands of unequal bandwidth are allocated to the PU*s*, designated as regions I, III, V, VII, and IX. Four sub-bands of unequal bandwidths allocated to SU*s*, designated as regions II, IV, VI, and VIII, are shown in Figures 5.11 and 5.12.

We consider that the SU operating in regions II, IV, VI, and VIII has 16, 32, 64, and 128 OFDM subcarriers, respectively. The comparison of the proposed technique is done with the existing

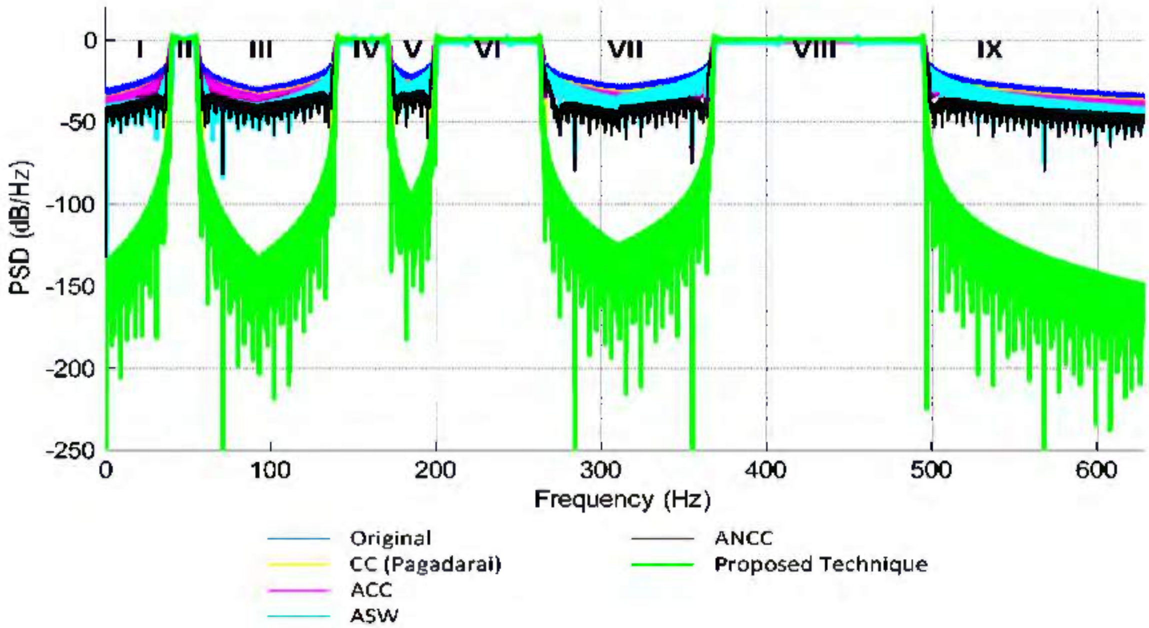

Figure 5. 11 The PSD comparison between the proposed and existing techniques, Case V

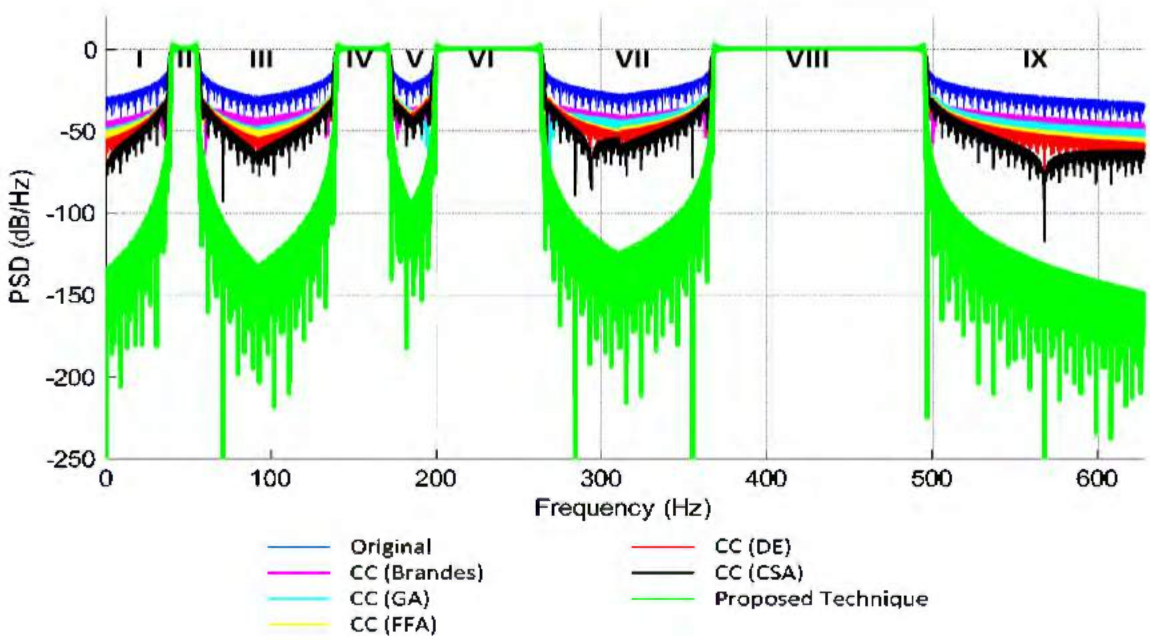

Figure 5. 12 The PSD performance comparison between the proposed technique and existing techniques, Case V

techniques. Two CC*s* have been taken on both sides of the data subcarriers in all cancellation carrier techniques. In terms of normalized power spectral density, Figures 5.11 to 5.12 show that the proposed technique achieved significant suppression when compared to the existing techniques in all regions of PU*s*.

5.4 Conclusion

We have proposed a novel wave-shaping technique, GSC, for the reduction of sidelobes of OFDM signal. The proposed technique allows the desired portion of the signal to pass and blocks the undesired portion, *i.e.*, the sidelobes. The performance comparison of the proposed technique in different spectrum-sharing scenarios with already existing sidelobe suppression techniques is done through simulations, which show that the proposed technique achieves more than 90 dB reduction in sidelobes as compared to the existing techniques.

Chapter 6

Reduction of out of Band Radiation using Combination of Different Techniques

6.1 Introduction

In this chapter, an OFDM framework is presented as shown in figure 6.1, which has an ability of representing any OOB radiation reduction technique, regardless of individual or multiple schemes are applied. Then, according to the place where different schemes are applied are categorized into three groups, namely symbol mapping, precoding and times domain techniques. Based on that framework, different techniques are introduced that can be viewed as the two level suppression techniques. In the first level the OOB radiation is reduced by using CCs with existing and our proposed CCs techniques, while in the second level, further reduction of OOB radiation are achieved using GSC. The data model for this chapter is same as it is developed in chapter 4. This chapter is divided into two parts. Part I discusses the combination of our proposed technique GSC with the existing OOB radiation reduction techniques, while Part II discussed the combination of our proposed techniques discussed in chapter 4 and 5 i.e. combination of GSC with GA based CC, FFA based, FFA based CC and CSA based CC.

6.2 Combination of our propsed technique i.e. GSC with the existing techniques

In this section, we present four techniques, each having two levels to minimize the OOB radiation. In the first level OOB radiation is reduced using existing techniques including CC proposed by

Brandes, CC proposed by Pagadarai, ACC and ANCC, while in the second level further reduction is achieved using GSC. The performance of this proposed combined technique is checked by considering three different spectrum sharing scenario discussed below.

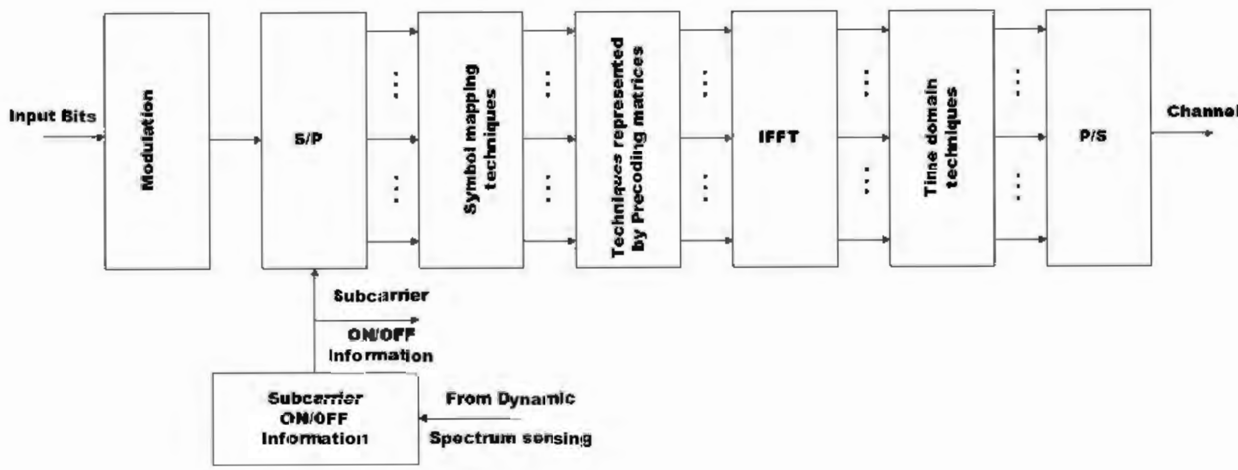

Figure 6. 1: Framework of OFDM transmitter

6.2.1 Results and Simulations

In this section, we consider three different spectrum sharing scenarios to check the effectiveness and reliability of the proposed techniques. The performance of the proposed techniques in term of PSD has been compared with already existing techniques via simulations. In all the simulation results discussed in all three cases, the Proposed scheme I represents the combination of GSC with CC proposed by Brandes, Proposed scheme II represents the combination of GSC with ACC, Proposed scheme III represents the combination of GSC with ANCC and Proposed scheme IV represents the combination of GSC with CC proposed by Pagadarai.

6.2.1.1 Case I

In this case, assume that CR detects a single vacant band available for the SU, it is considered that the total number of OFDM subcarriers used by the SU in this band is 16, modulated with BPSK.

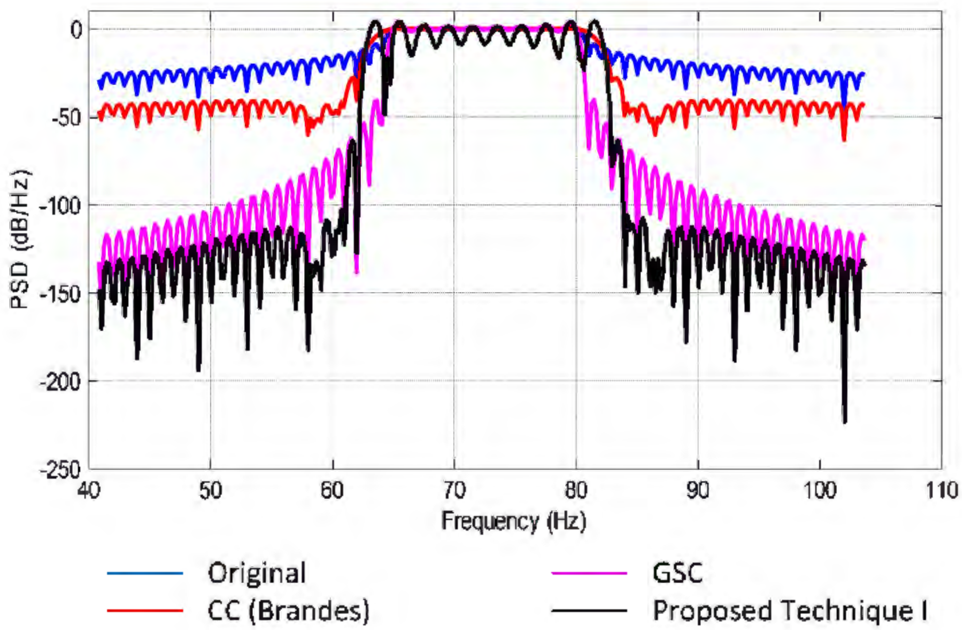

Figure 6. 2 PSD curve of single SU with Proposed technique I; Case I

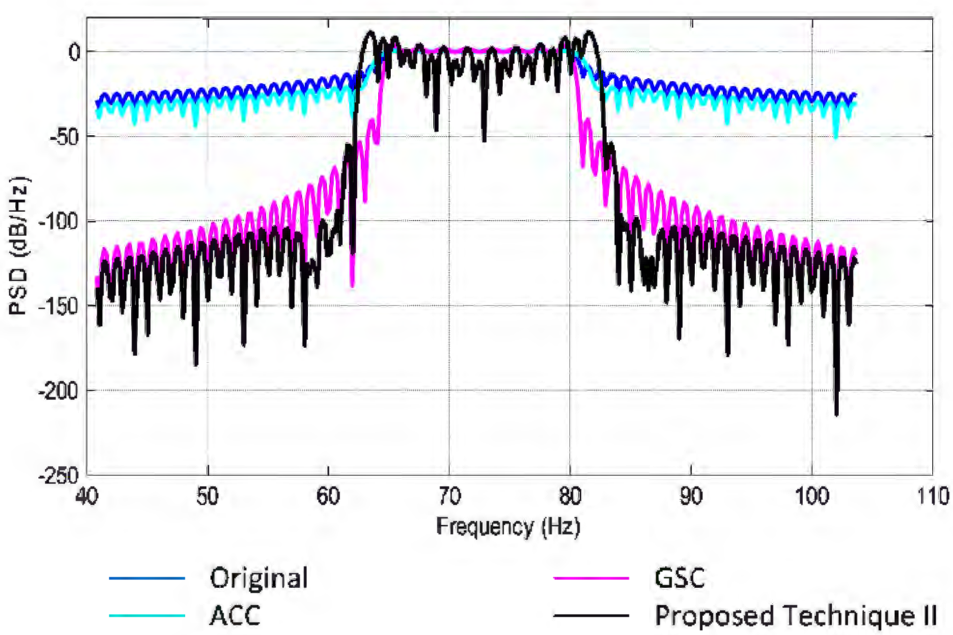

Figure 6. 3 PSD curve of single SU with Proposed technique II; Case I

In first step suppression two CC*s* are taken on the left and right sides of the OFDM spectrum. Ten sidelobes are taken on both sides of the spectrum with one frequency sample taken in the middle

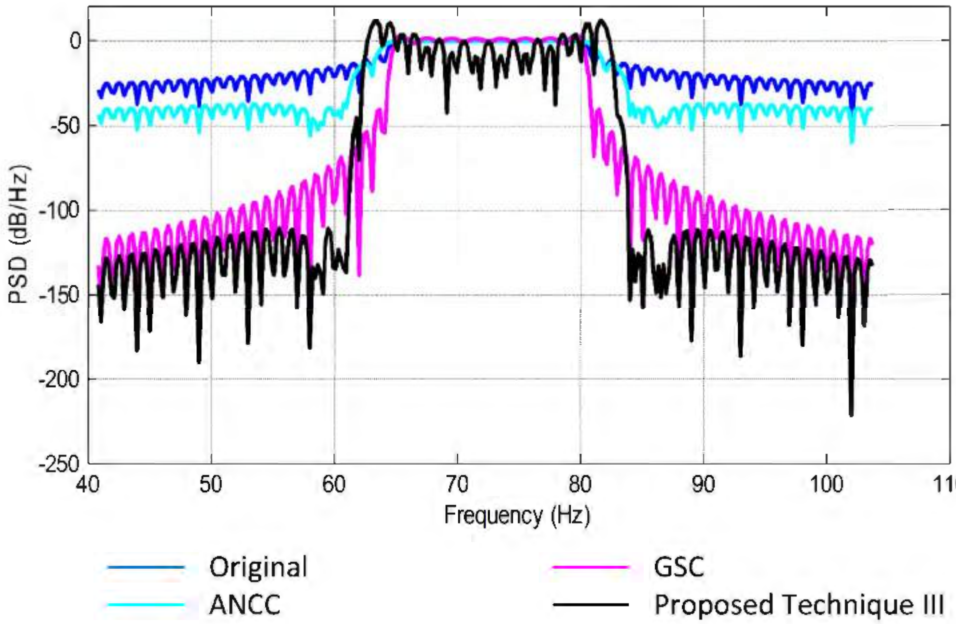

Figure 6. 4 PSD curve of single SU with Proposed technique III; Case I

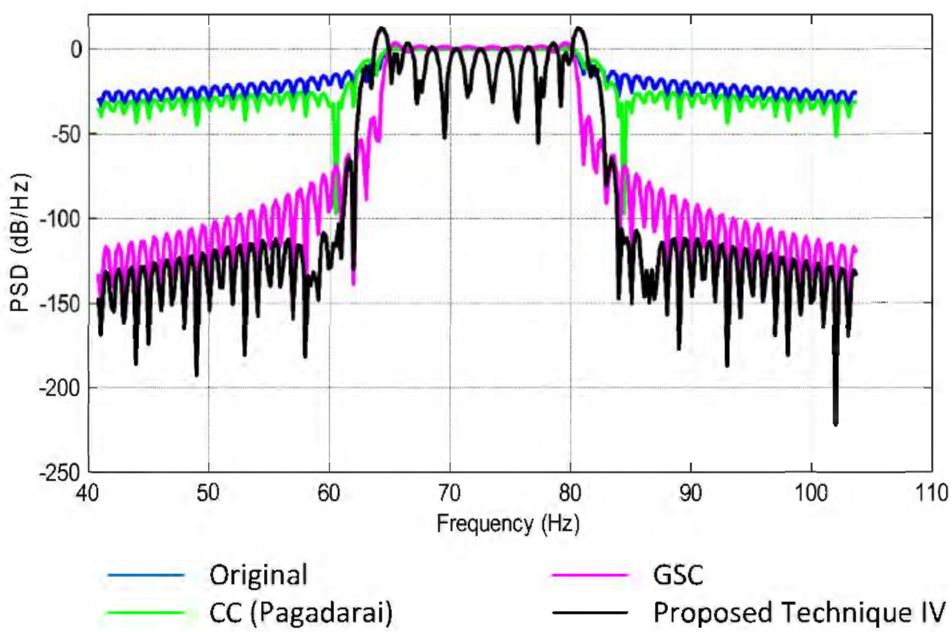

Figure 6. 5 PSD curve of single SU with Proposed technique IV; Case I

of every sidelobe in the optimization range, resulting in $M_l = M_r = 10$. For the second step 301 samples are taken. From Figures 6.2 – 6.5, it is observed that the proposed techniques give better suppression of sidelobes as compared to other techniques.

6.2.1.2 Case II

In this scenario, assuming that CR detects four vacant bands, denoted by II, IV, VI and VIII all having equal bandwidths. The spacing between these bands are also considered as of equal bandwidths. SU*s* operating in band II, IV, VI and VIII use 32 OFDM subcarriers, modulated with BPSK. In first step of suppression two CC*s* on either side of the original spectrum are inserted in all the CC based suppression techniques. Ten sidelobes on either side of the used spectrum in the optimization range are considered. In the second step of suppression 766 samples are considered. Figures 6.6 – 6.9, show clearly that the proposed technique get a significant reduction in all regions compared with other existing techniques.

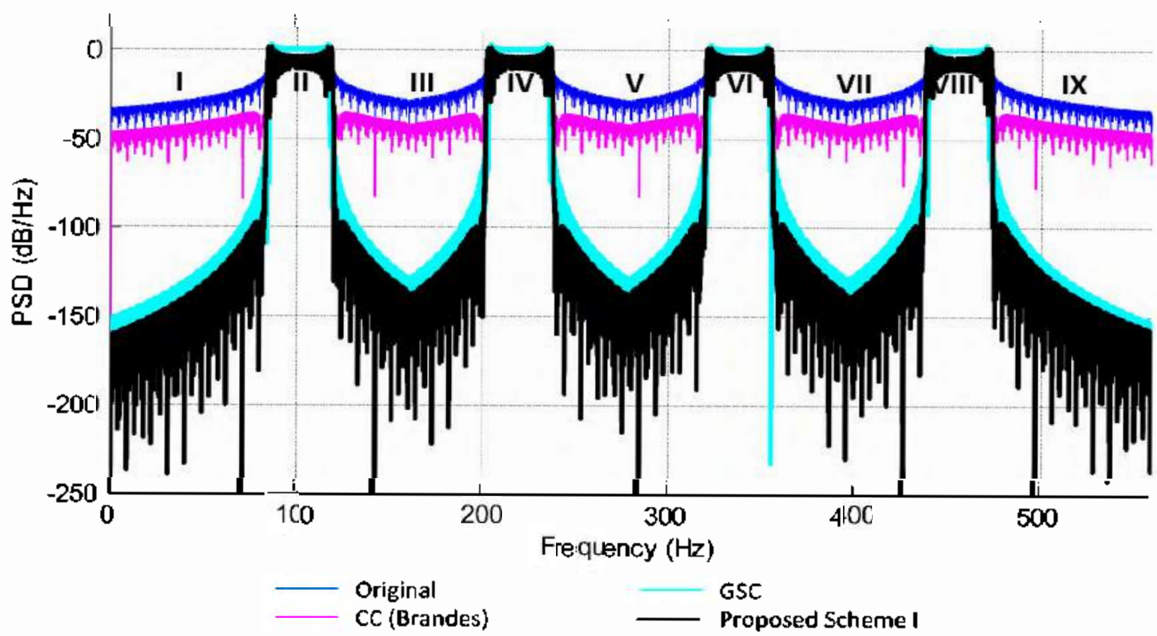

Figure 6. 6 PSD curve of four SUs having equal spacing with Proposed technique I; Case II

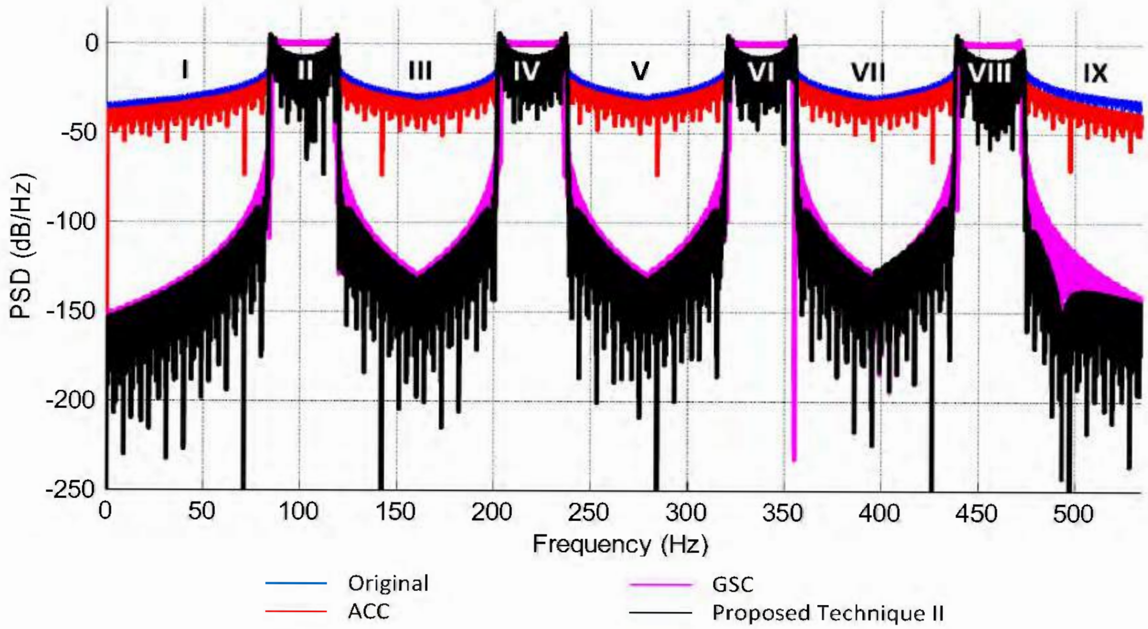

Figure 6. 7 PSD curve of four SUs having equal spacing with Proposed technique II; Case II

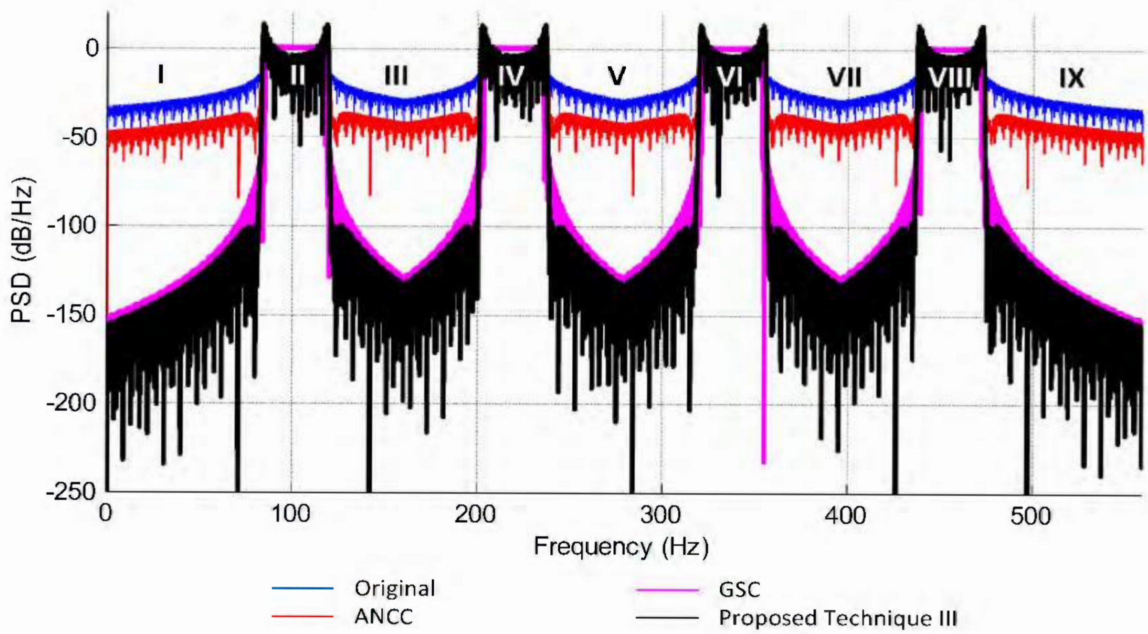

Figure 6. 8 PSD curve of four SUs having equal spacing with proposed technique III; Case II

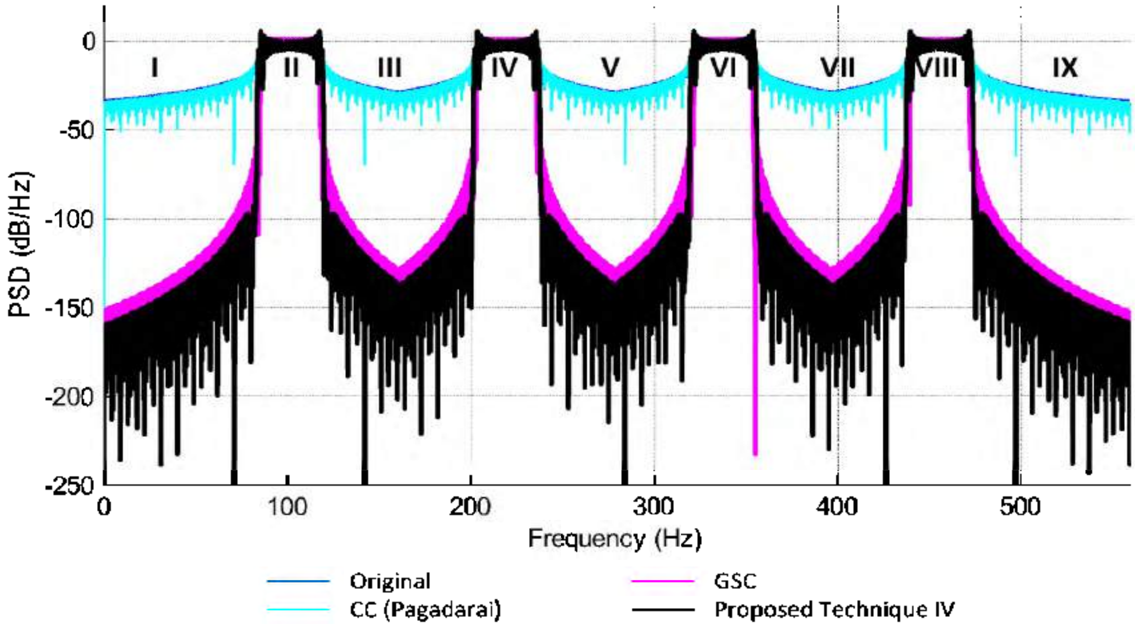

Figure 6. 9 PSD curve of four SUs having equal spacing with Proposed technique IV; Case II

6.2.1.3 Case III

In this scenario, considering that white holes detected by CR are given by II, IV, VI and VIII, have same bandwidth. The spacing between white holes I, III, V, VII and IX having un-equal bandwidths. Equal number of OFDM subcarriers i.e. 32 subcarriers is used by each SU operating in holes II, IV, VI and VIII, modulated with BPSK with normalized power equal to 1. The performance, reliability and effectiveness of the proposed techniques as compared with the existing techniques in terms of PSD are shown using computer simulations. Figures. 6.10 – 6.13 that show the performance comparison of our proposed techniques with the existing techniques which clearly depict that better reduction of sidelobes are achieved using our different techniques proposed in this subsection of the chapter.

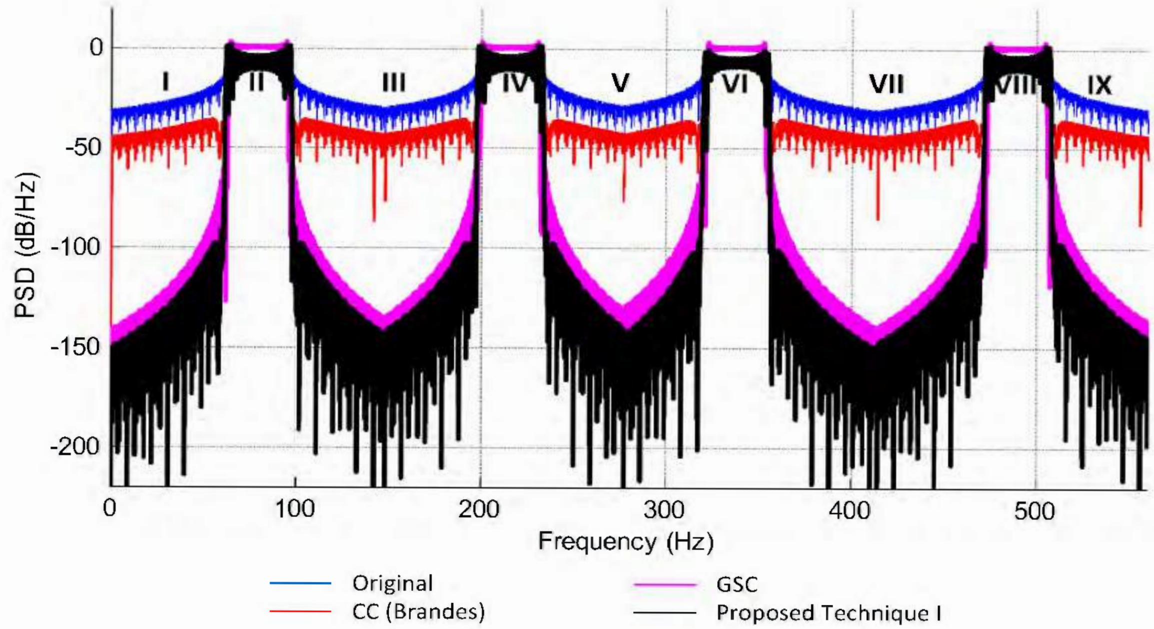

Figure 6. 10 PSD curves of four SUs signals having un-equal spacing with Proposed technique I; Case III

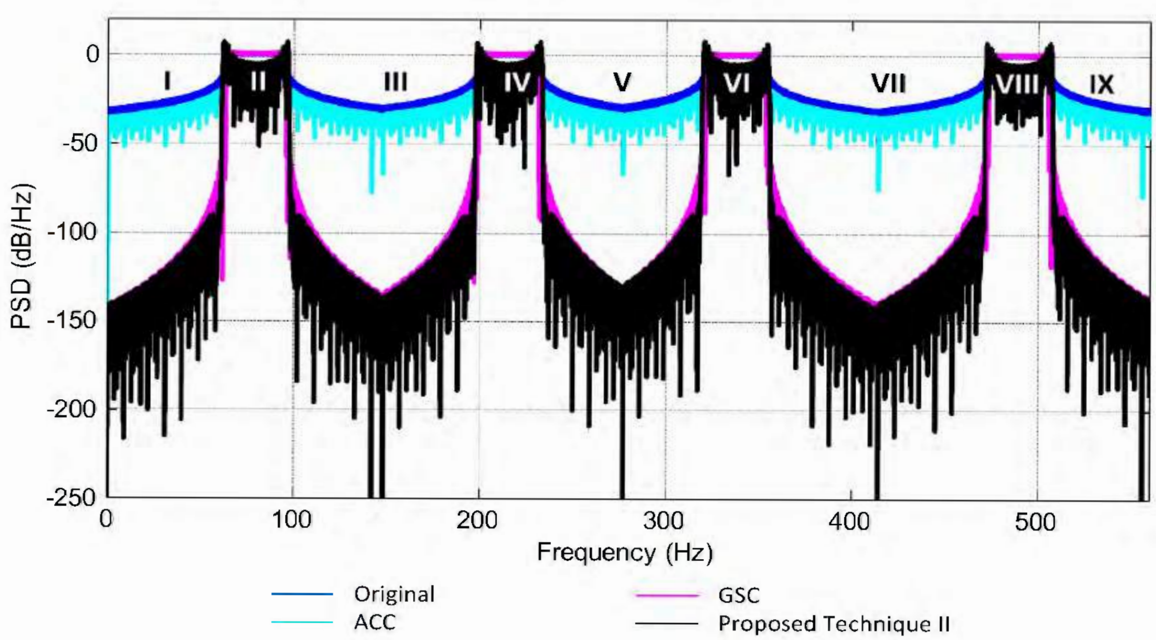

Figure 6. 11 PSD curves of four SUs signals having un-equal spacing with Proposed technique II; Case III

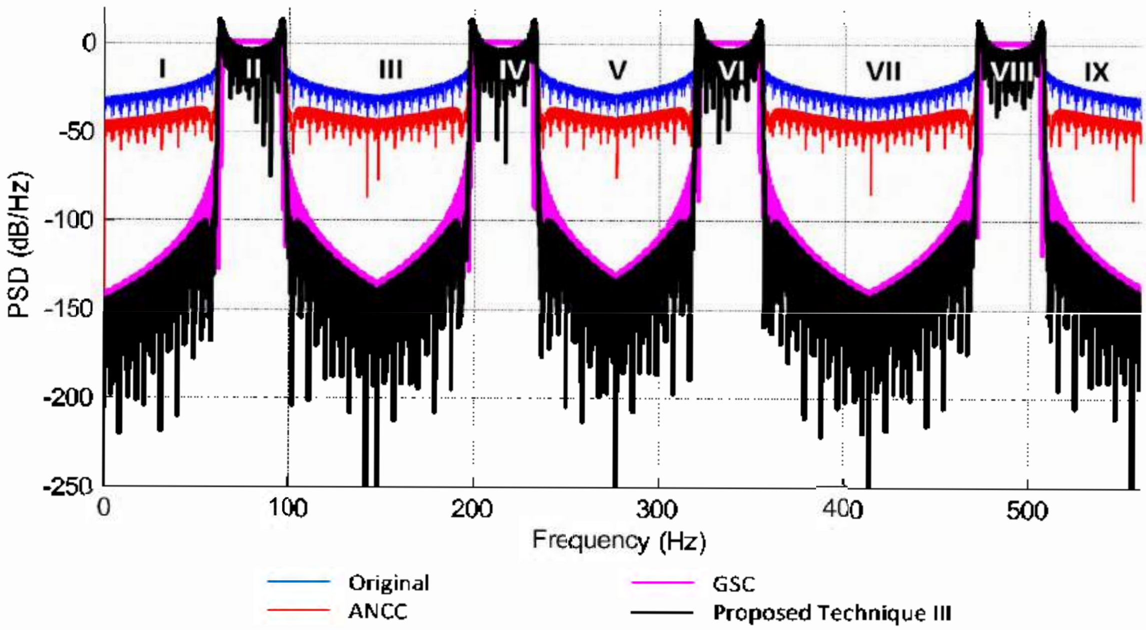

Figure 6. 12 PSD curves of four SUs signals having un-equal spacing with Proposed technique III; Case III

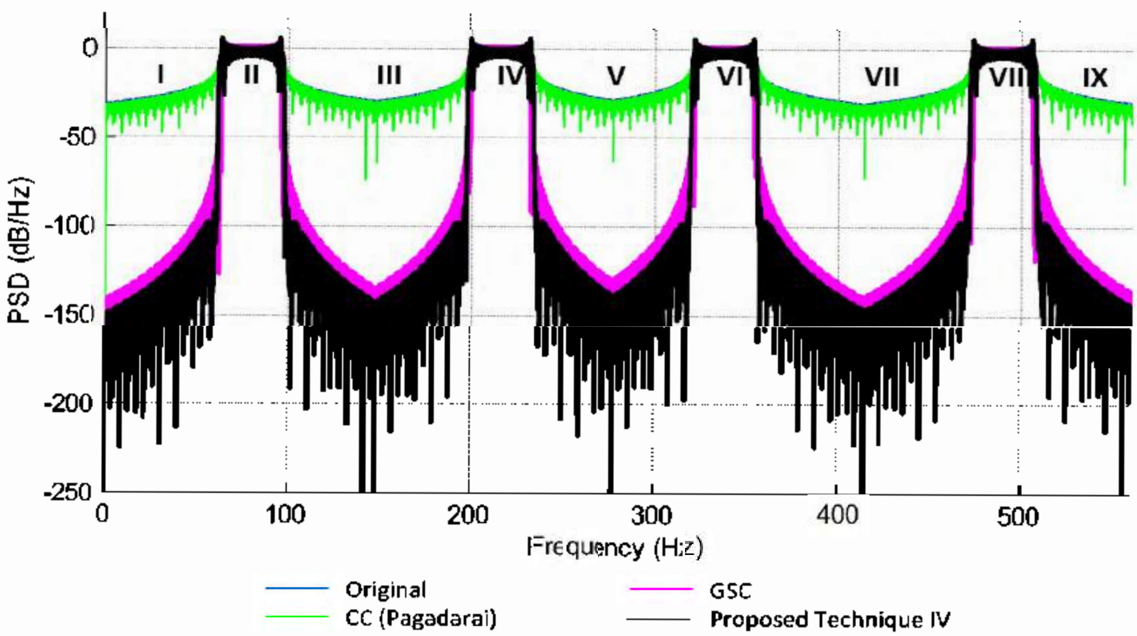

Figure 6. 13 PSD curves of four SUs signals having un-equal spacing with Proposed technique IV; Case III

6.3 Combination of our proposed techniques

In this section, we will also present four techniques, each having two levels to minimize the OOB radiation. In the first level OOB radiation is reduced using our proposed technique discussed in chapter 4, including GA based CC, FFA based CC, DE based CC and CSA based CC, while in the second level further reduction is achieved using GSC discussed in chapter 5. The proposed techniques are constructed to maintain the advantages of the individual techniques. Simulation results show the PSD performance of the proposed techniques in comparison with already existing techniques, demonstrating that the proposed techniques minimize the OOB radiation significantly thus qualifying for more effective spectrum sharing.

6.3.1 Results and Simulations

In this section, we consider five different spectrum sharing scenarios to check the effectiveness and reliability of the proposed techniques. In all the simulation results discussed in all five cases, the Proposed technique I represents the combination of GSC with GA based CC, Proposed technique II represents the combination of GSC with DE based CC, Proposed technique III represents the combination of GSC with FFA based CC and Proposed technique IV represents the combination of GSC with CSA based CC. The performance of the proposed techniques in term of PSD has been compared with already existing techniques via simulations.

6.3.1.1 Case I

In this scenario, assume that CR detects a single vacant band available for the SU, it is considered that the total number of OFDM subcarriers used by the SU in this band is 16, modulated with BPSK. The performance comparison of the proposed techniques in this scenario with already

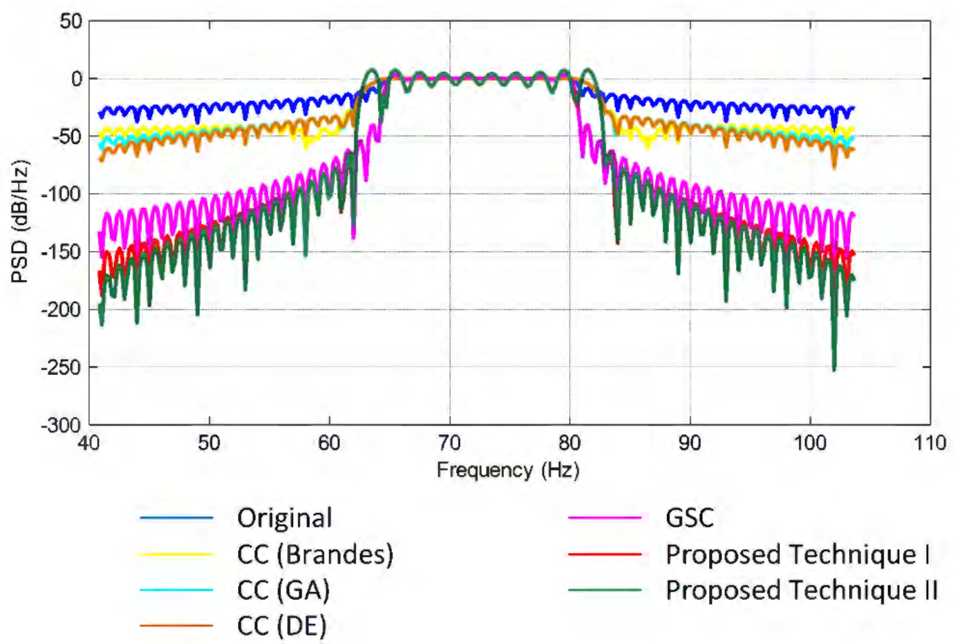

Figure 6. 14 PSD comparison between proposed technique I and II with others; Case I

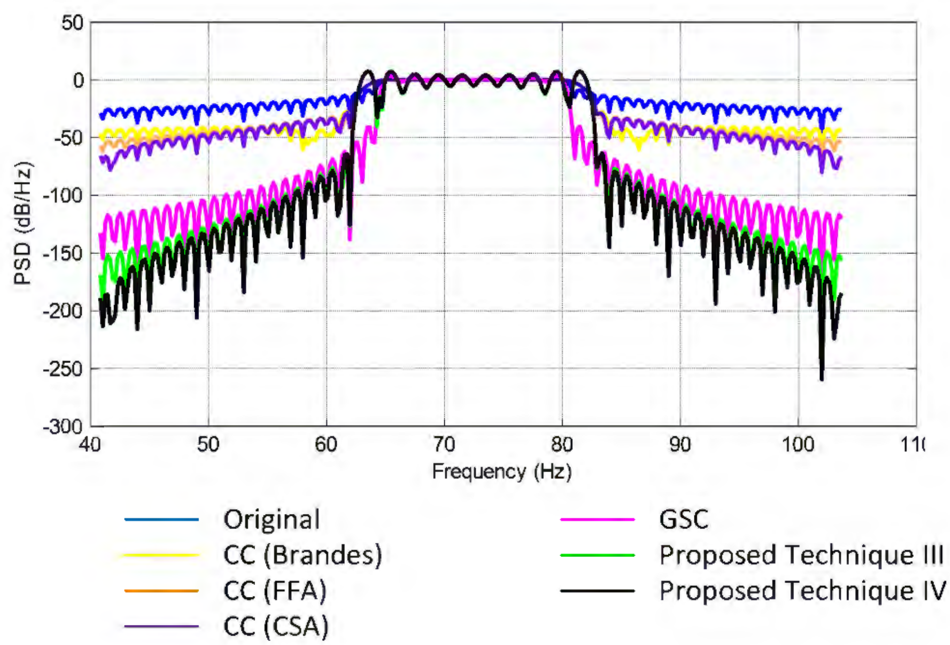

Figure 6. 15 The PSD performance comparison between proposed technique III and IV with other techniques; Case I

existing techniques is shown in Figures 6.14 – 6.16. In all CC techniques two CC*s* are taken on the left and right sides of the OFDM spectrum.

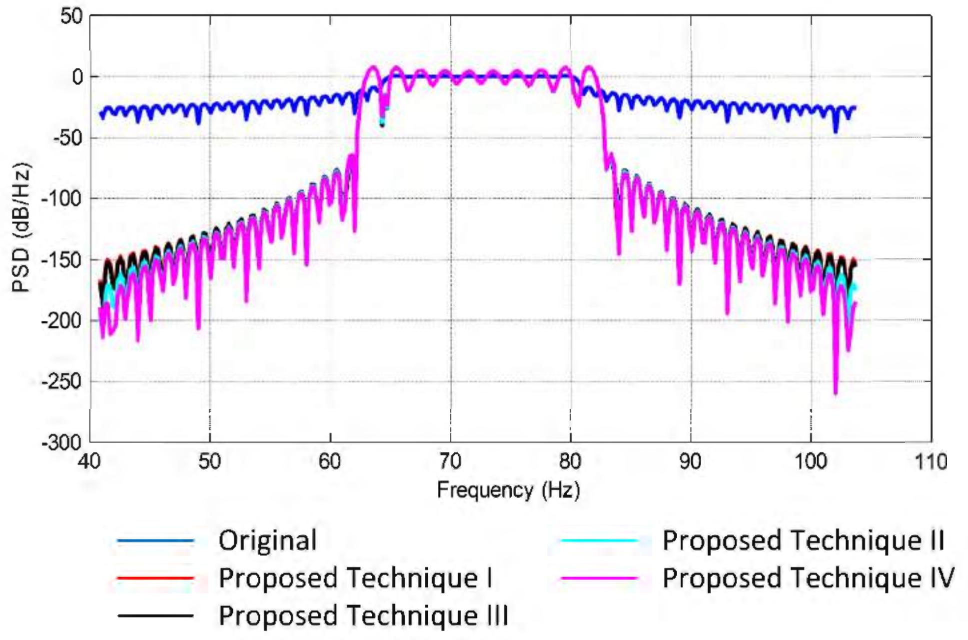

Figure 6. 16 The PSD performance comparison between proposed techniques; Case I

6.3.1.2 Case II

In this case, assuming that CR detects four vacant bands, denoted by II, IV, VI and VIII all having equal bandwidths. The spacing between these bands denoted by I, III, V, VII and IX are also considered as of equal bandwidths. SU*s* functioning in band II, IV, VI and VIII use 32 OFDM subcarriers, mapped with BPSK. The performance of the proposed techniques in term of PSD with others techniques and GSC is shown in Figures 6.17 – 6.19. Two CC*s* on either side of the original spectrum are inserted in all the CC based suppression techniques. Figures 6.17 – 6.19 show that the proposed technique get a reduction considerably, as compared with other existing techniques, while Figure 6.19 shows the performance of our proposed techniques with each other, which shows that proposed technique IV overall gets better suppression.

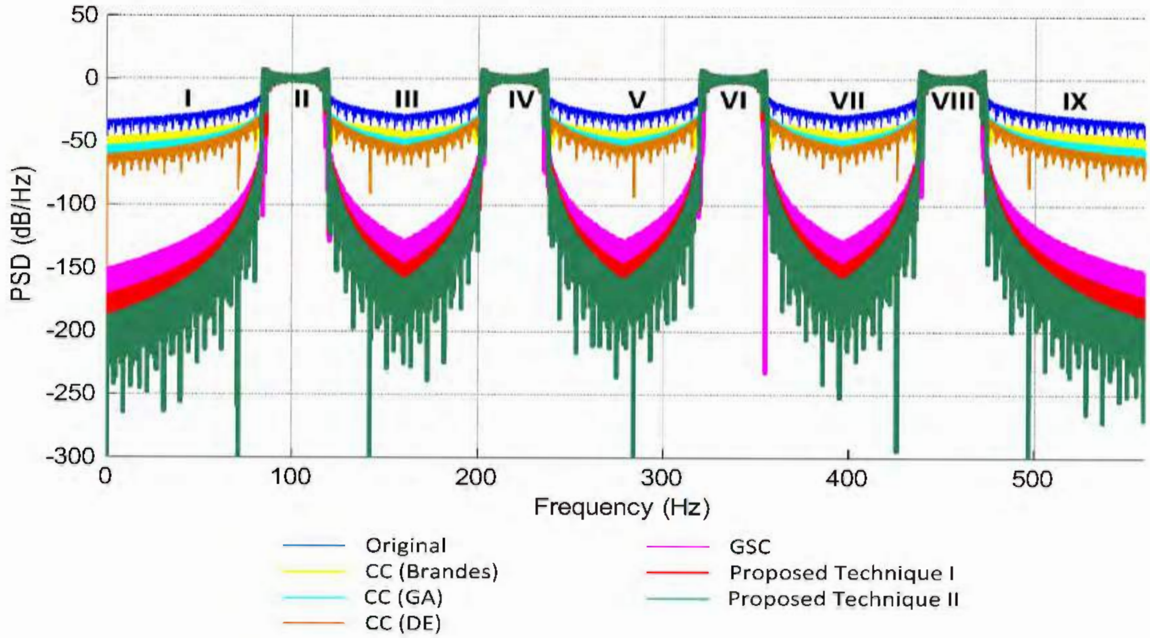

Figure 6. 17 The PSD performance comparison between proposed technique I and II with the other techniques; Case II

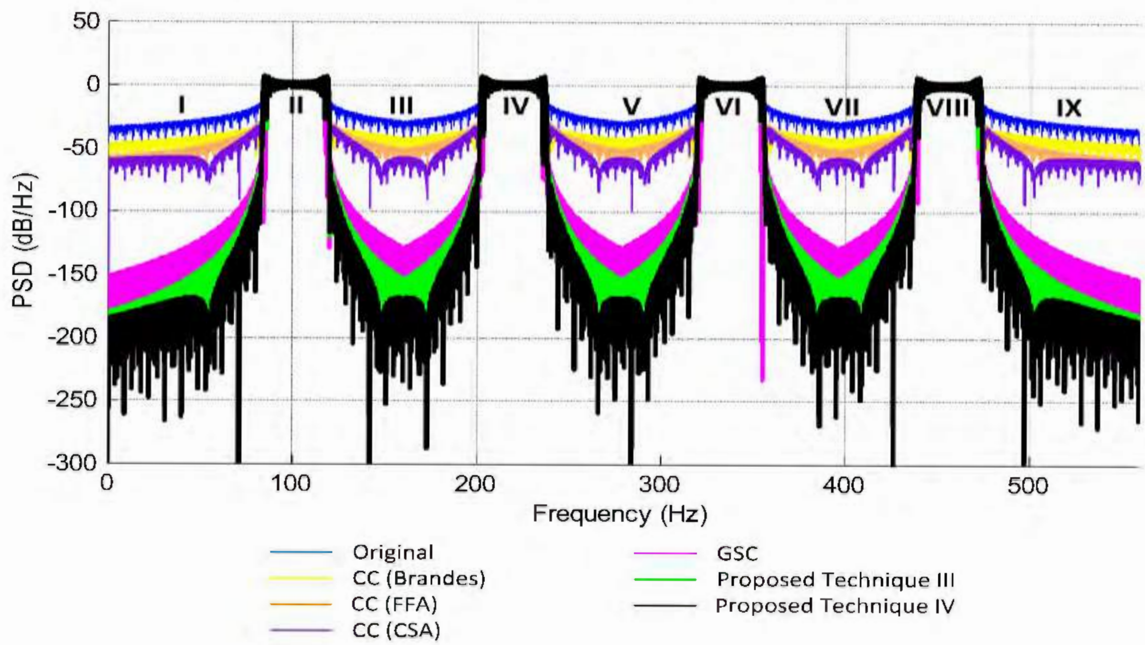

Figure 6. 18 The PSD performance comparison between proposed techniques III and IV with the other techniques; Case II

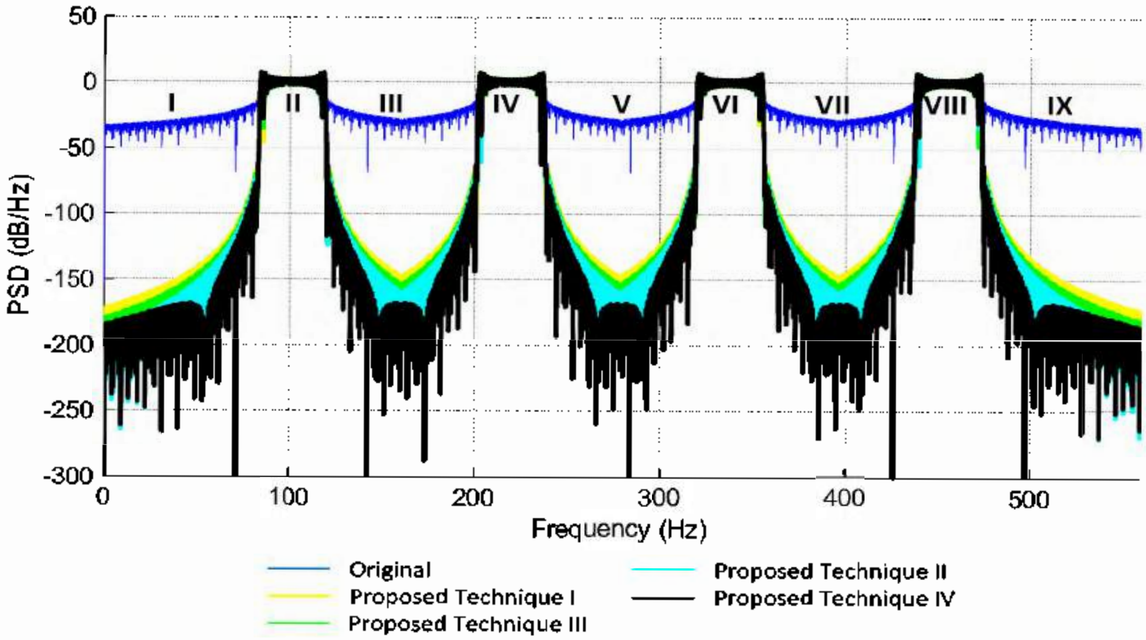

Figure 6. 19 The PSD performance comparison the proposed techniques; Case II

6.3.1.3 Case III

In this scenario, considering that white holes detected by CR are given by II, IV, VI and VIII, having the same bandwidth are utilized by four different SUs. The spacing between white holes are given by I, III, V, VII and IX respectively, having different bandwidths are utilized by five different PUs. Equal number of OFDM subcarriers (i.e. 32) are used by these four different SUs operating in these white holes, mapped with BPSK and with normalized power equal to 1. The performance, reliability and effectiveness of the proposed techniques are shown in Figures. 6.20 – 6.22 that show the comparison with current techniques in term of PSD. These Figures 6.20 – 6.22 shows that our proposed techniques, get better suppression of sidelobes in that spectrum sharing scenario, and outclasses all the existing techniques.

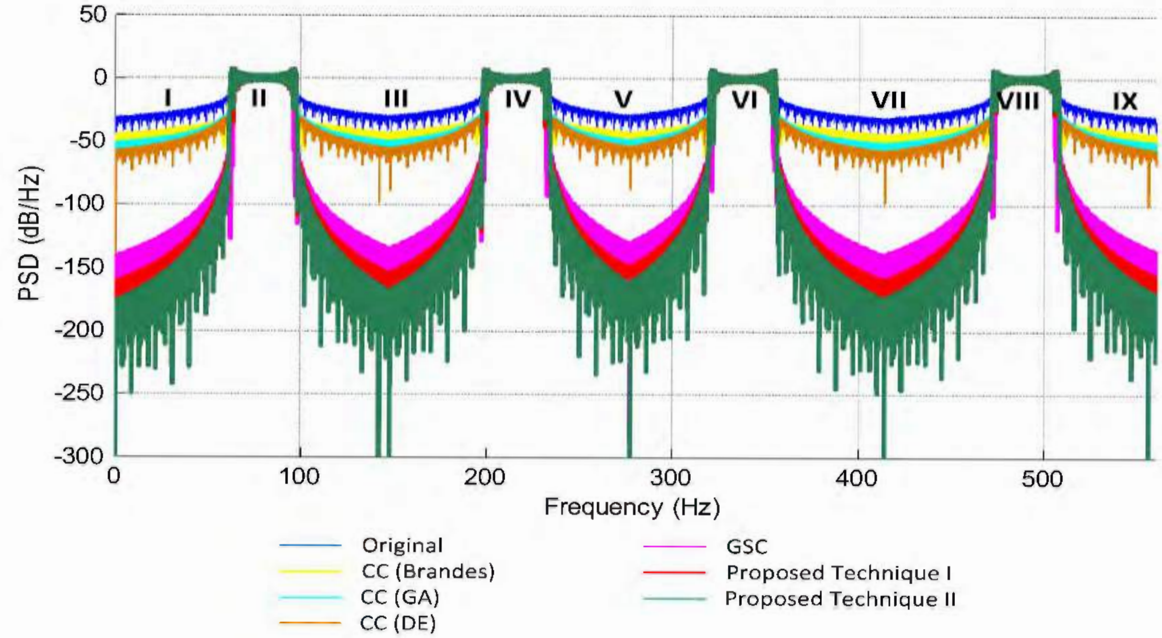

Figure 6. 20 The PSD performance comparison between proposed techniques I and II with the other techniques; Case III

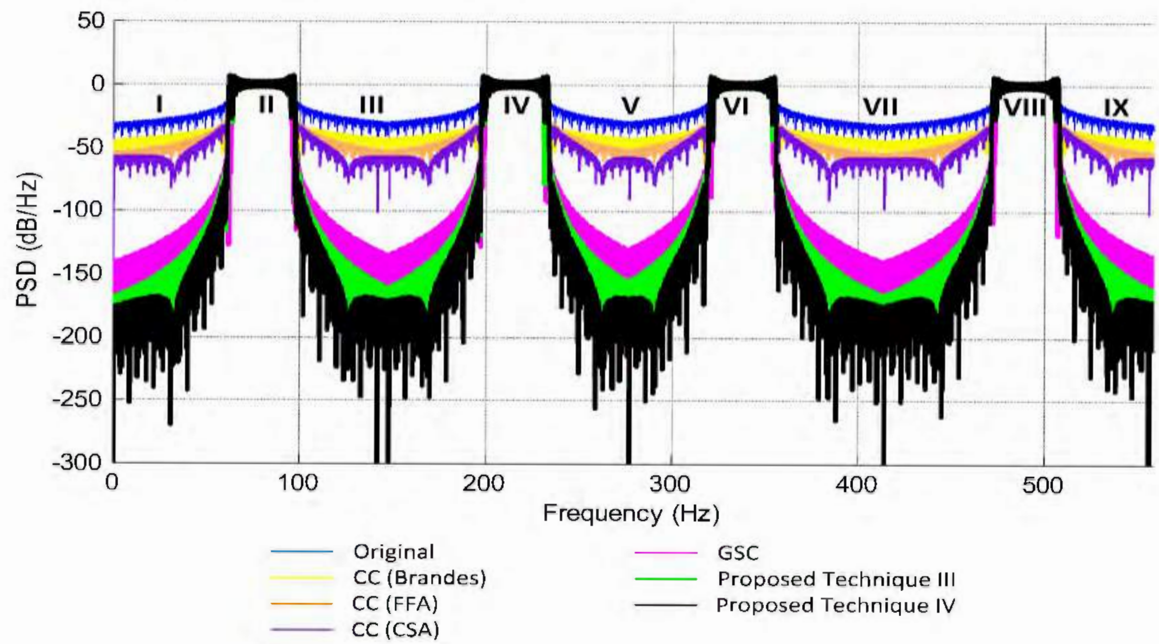

Figure 6. 21 The PSD performance comparison between proposed techniques III and IV with the other techniques; Case III

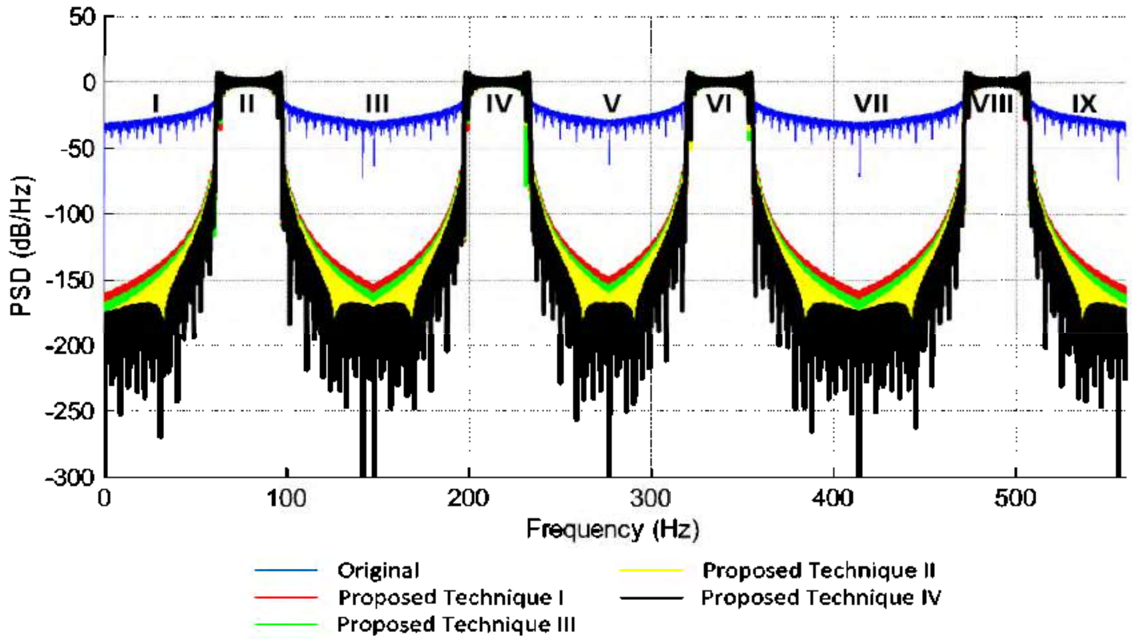

Figure 6. 22 The PSD performance comparison of the proposed techniques; Case III

6.3.1.4 Case IV

In this case, the bandwidth of the spectral white holes detected by CR is considered as unequal represented as II, IV, VI and VIII which is considered to be utilized by four different SUs. The spacing between these spectral white holes I, III, V, VII and IX are considered to be of equal bandwidth and is in possession of different PUs. SU*s* operating in white hole II divides the bandwidth into 16 subcarriers, SU operating in white hole IV divides the bandwidth into 32 subcarriers, SU operating in white hole VI divides the bandwidth into 64 subcarriers and SU operating in white hole VIII divides the bandwidth into 128 subcarriers, each modulated with BPSK with normalized power equal to 1. Figures 6.23 – 6.25 show that the proposed techniques are effective and reliable in such a spectrum sharing scenario, get significant reduction of sidelobes in comparison with the current techniques.

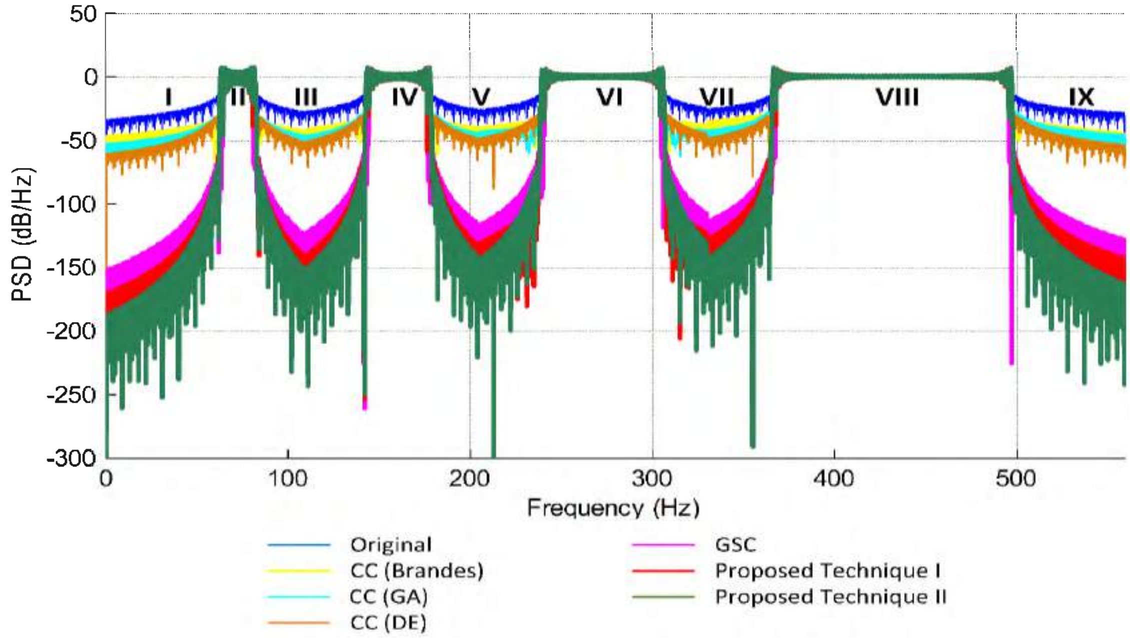

Figure 6. 23 The PSD performance comparison between proposed techniques I and II with the other techniques; Case IV

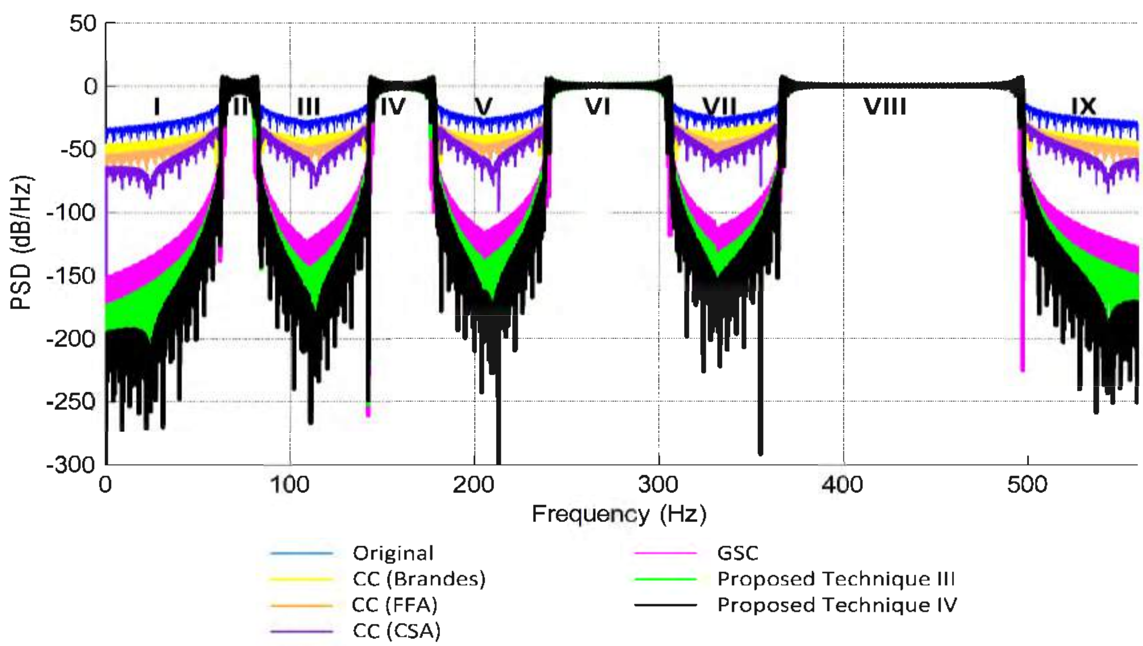

Figure 6. 24 The PSD performance comparison between proposed techniques III and IV with the other techniques; Case IV

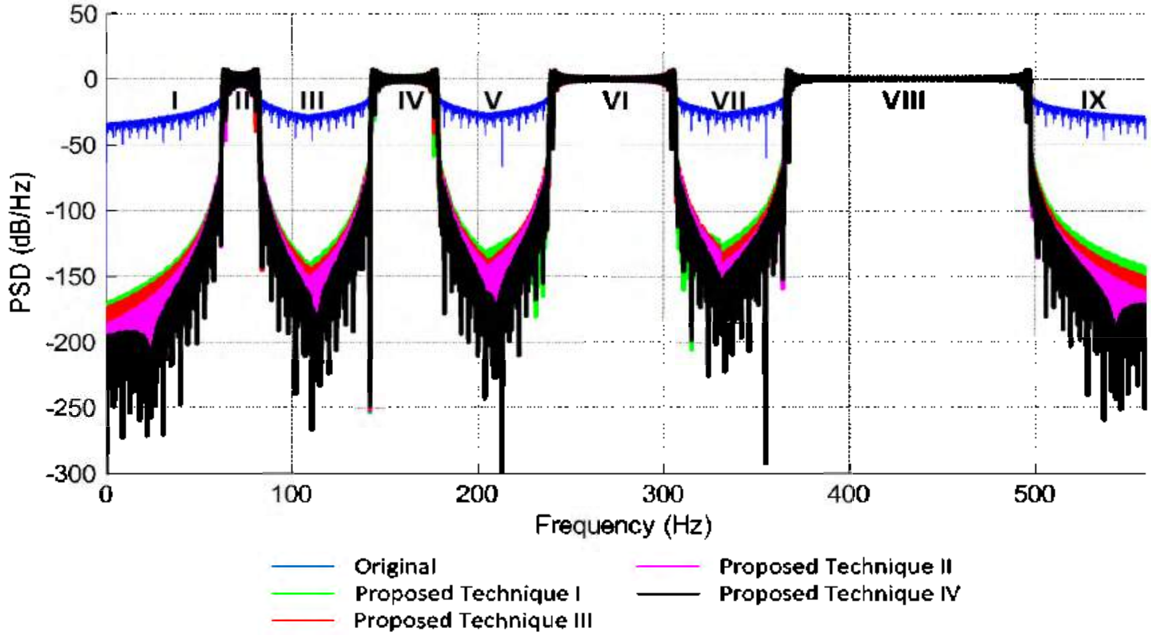

Figure 6. 25 The PSD performance comparison of proposed techniques; Case IV

6.3.1.5 Case V

In this scenario, our spectral white spaces are considered to be detected by CR, represented by II, IV, VI and VIII, have unequal bandwidth occupied by four different SUs. Spacing I, III, V, VII and IX between the spectral white spaces are also considered to be of unequal bandwidth. SUs operating in spectral white space II divide the bandwidth into 16 subcarriers, operating in spectral white space IV divide the bandwidth into 32 subcarriers, operating in spectral white space VI divide the bandwidth into 64 subcarriers while SU operating in spectral white space VI divide the bandwidth into128 subcarriers, modulated with BPSK with normalized power equal to 1. The performance of our proposed techniques for that scenario compared with the current techniques is given in Figures. 6.26 – 6.28, which show that the proposed scheme outclasses all the existing techniques and gets significant reduction.

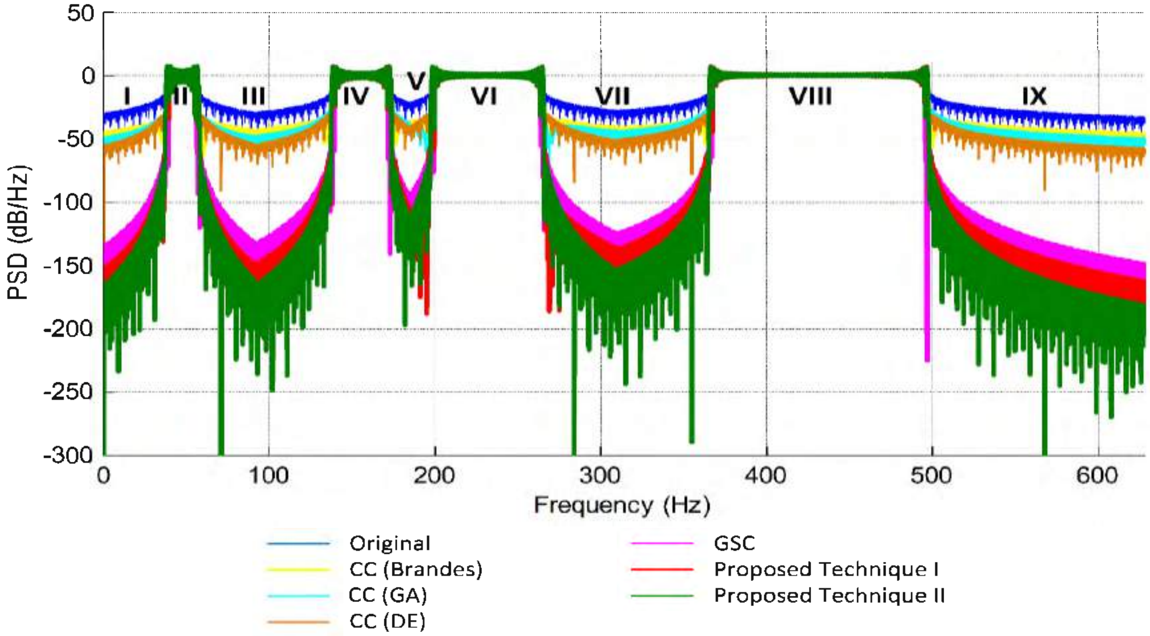

Figure 6. 26 The PSD performance comparison between proposed techniques I and II with the other techniques; Case V

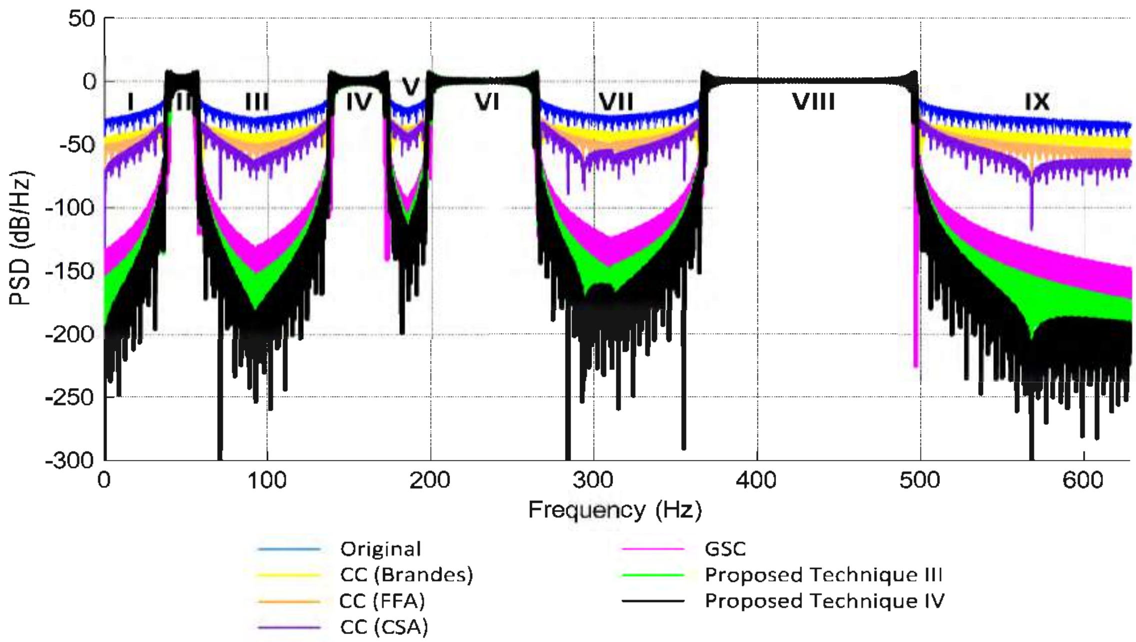

Figure 6. 27 The PSD performance comparison between proposed techniques III and IV with the other techniques; Case V

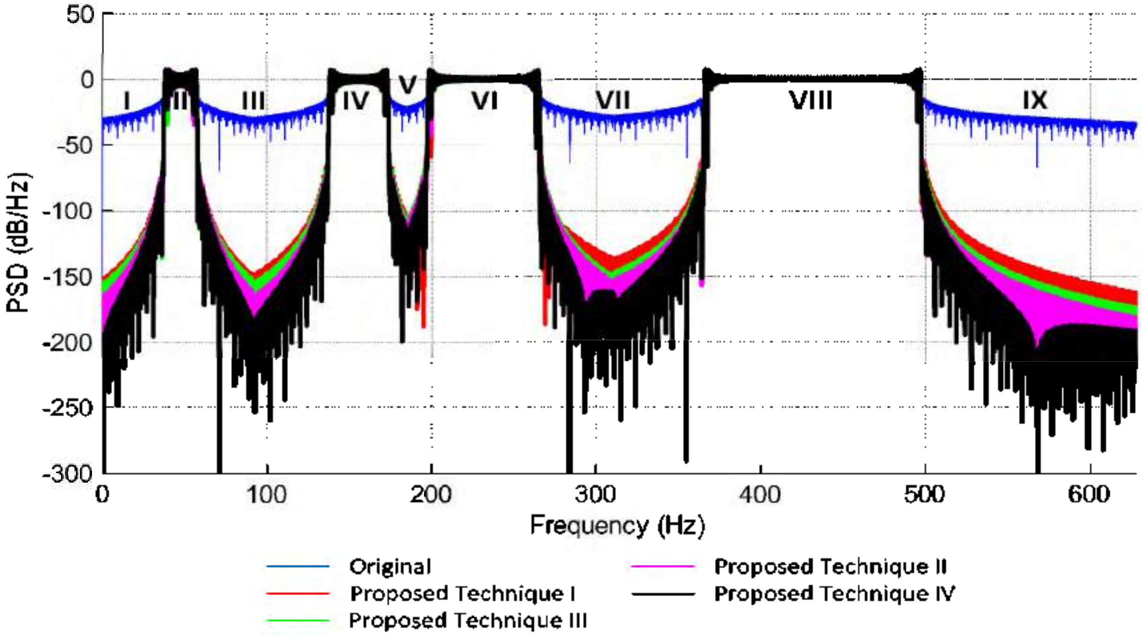

Figure 6. 28 The PSD performance comparison of the proposed techniques; Case V

6.4 Conclusion

In this chapter, we present an OFDM framework that has a capability of describing any OOB radiation reduction technique, no matter whether we are applying a single or multiple techniques. In this framework according to the location where the OOB radiation reduction techniques are employed, these are divided into three groups, which are Symbol mapping, precoding and time domain methods. Based on this OFDM framework, eight, two level OOB radiation reduction techniques are proposed, which are divided into two major groups: The first one is the combination of our proposed technique GSC with four different existing technique including CC by Brandes, CC by Pagadarai, ACC and ANCC. The second one is the combination of our proposed techniques discussed in chapter 4 and 5 i.e. combination of GSC with CC (GA), combination of GSC with CC (FFA), combination of GSC with CC (DE) and combination of GSC with CC (CSA). The purpose of combining different techniques is, to take advantages of the individual techniques for further enhancing the suppression of sidelobes. The strength and reliability of the proposed techniques are shown via computer simulations in different types of spectrum sharing scenarios, which show that the proposed techniques get far better reduction of OOB radiation as compared to the existing techniques.

Chapter 7

Conclusion and Future Work

7.1 Conclusion

In order to prevail the problem of spectrum shortage, request for more bandwidth and higher data rates, competency of spectrum has to be improved. An encouraging methodology is the coexistence of two or more users operating in the same frequency band without disrupting each other. Multicarrier communication techniques have been acknowledged as promising applicants as it has an ability of occupying the available spectral holes in an efficient manner. The most common multicarrier technique is OFDM, presented as a best candidate for this purpose.

The major issue in the successful coexistence between different users is the mutual interference between the users that arrises due to the high sidelobes of the subcarriers of OFDM. The objective of our dissertation is to efficiently reduce the sidelobes of OFDM to keep the interference between the users at a minimum possible level.

This dissertation is divided into three parts: In the first part, we have proposed different heuristic algorithms namely GA, FFA, DE and CSA that uses our proposed Fitness function for the calculation of amplitudes of main lobe of CCs, which are used to suppress the sidelobes. The effectiveness of our proposed algorithms are shown via extensive simulations by considering five different spectrum scenario and shows that better reduction of sidelobes are achieved as compared to the existing techniques.

In the second part, we present a novel technique based on a GSC for the reduction of sidelobes. The upper branch of the GSC consists of a weight vector designed by multiple constraints to preserve the desired portion of the input signal. The lower branch has a blocking matrix that blocks the desired portion and preserves the undesired portion (the sidelobes) of the input signal, followed by an adaptive weight vector. The adaptive weight vector adjusts the amplitudes of the undesired portion (the sidelobes) so that when the signal from the lower branch is subtracted from the signal from the upper branch, it results in cancellation of the sidelobes of the input signal. The effectiveness and strength of the proposed technique is verified through extensive simulations. The proposed technique produces competitive results in terms of sidelobe reduction as compared to the existing techniques.

The aim of the third part of this dissertation was further improvement in the reduction of sidelobes. For that, we proposed combination of different techniques that are categorized into two groups: First one is the combination of our proposed technique GSC with the techniques found in the literature including CC (Brandes), CC (Pagadarai), ACC and ANCC. Second one is the combination of our proposed techniques with each other, i.e. combination of GSC with CC (GA), CC (DE), CC (FFA) and CC (CSA). Again the effectiveness of these combined techniques are shown with the help of extensive simulations that shows that effective suppression of sidelobes are achieved.

7.2 Future work

Future direction for extending the work of this dissertation are as under.

1. Spectrum sensing in cognitive radio networks is challenged by several sources of uncertainty ranging from channel randomness to device level and network-level

uncertainties. Since spectrum sensing should perform robustly even under worst case conditions, such uncertainties usually have implications in terms of the required detection sensitivity. Under channel fading or shadowing, a low received signal strength does not necessarily imply that the primary system is located out of the secondary user's interference range, as the primary signal may be experiencing a deep fade or being heavily shadowed by obstacles. Therefore, spectrum sensing is challenged by such channel uncertainty since cognitive radios have to be more sensitive to distinguish a faded or shadowed primary signal from a white space. Under severe fading, a single cognitive radio relying on local sensing may be unable to achieve this increased sensitivity since the required sensing time may exceed the sensing period. By proper combination of local signal processing, user-level cooperation among cognitive radios, and system-level coordination among different cognitive radio networks. Research on spectrum sensing thus far has mainly focused on meeting the regulatory requirements for reliable sensing. An important venue for further research, can be explored is the interplay of spectrum sensing and higher-layer functionalities to enhance the end user's perceived QoS. In this respect one can outline some of the major cross-layer trade-offs involved in spectrum sensing.

2. Today's wireless networks are characterized by a fixed spectrum assignment policy. However, a large portion of the assigned spectrum is used sporadically and geographical variations in the utilization of assigned spectrum ranges from 15 to 85% with a high variance in time. The limited available spectrum and the inefficiency in the spectrum usage necessitate a new communication paradigm to exploit the existing wireless spectrum opportunistically. This new networking paradigm is referred to as NeXt Generation (xG) Networks as well as Dynamic Spectrum Access (DSA) and cognitive radio networks. The

influence of these functions on the performance of the upper layer protocols such as routing and transport can be investigated and open research issues in these areas.

3. CR networks can provide high bandwidth to mobile users via heterogeneous wireless architectures and dynamic spectrum access techniques. However, CR networks impose challenges due to the fluctuating nature of the available spectrum, as well as the diverse QoS requirements of various applications. Spectrum management functions can address these challenges for the realization of this new network paradigm. To provide a better understanding of CR networks, one can present recent developments and open research issues in spectrum management in CR networks. More specifically, one can focus the discussion on the development of CR networks that require no modification of existing networks. The four main challenges of spectrum management can be discussed: spectrum sensing, spectrum decision, spectrum sharing and spectrum mobility.
4. The spectrum sensing issues in the CR networks of opportunistic unlicensed spectrum access can be investigated. The cognitive radios can perform a communication using the incumbent user spectrum band without the interference caused by the cognitive radio users. In this case, the cognitive radios must know the real-time radio environments of the incumbent user spectrum band using the spectrum sensing, beacon signals, and geo-location database access. Then he can provide spectrum sensing issues which include the sensing techniques, the regulatory requirements, the analysis of DTV detection threshold, and main considerations associated with the spectrum sensing design in cognitive radio systems. Also, design trade-offs can be introduced in order to optimize the sensing parameters such as sensing time and sensing complexity.

5. Protection of interference on the primary system is the key requirement for deployment of a CR system. Typically, spectrum sensing is interleaved in the transmission process of a secondary user to detect the return of primary user for quick evacuation, resulting in frequent stopping of transmission. A novel method of agile spectrum evacuation can be introduced that ensures continuous transmission by the secondary user until the primary user actually returns. The sensing process can go on simultaneously by a dedicated set of users working in a cooperative manner. The proposed method can be evaluated under fading and shadowing conditions and better interference protection and improved utilization of RF spectrum can thus be obtained.
6. The CR technology allows a group of potential users to identify and access available spectrum resources provided that the interference to the users for whom the band has been licensed is kept below a prescribed level. However, this research area is at a very immature stage because various research challenges have to be addressed and solved. An overview of some research issues for CR networks can be presented. Specifically, one can present some research and development in CR networks with focus on: information-theoretic aspects, spectrum sensing, link adaptation, advance transceiver design and admission control. One can also discuss some important research problems related to these specific topics that needs to be addressed before deployment of CR systems in practice
7. One critical issue in dynamic spectrum access of CR networks is the analysis of interference caused by SUs. Most of the current works focus on mitigating the aggregated interference effects of SUs at PUs in the physical layer. However, the interference is also dynamically related to the communication behaviors between PUs and SUs. The interference caused by SUs in the MAC layer can be analyzed by taking into account the

dynamic behaviors between PUs and SUs. Based on the ON-OFF primary channel state model, one can derive the close-form expressions for the probability of interference caused by SUs and quantify the interference effect in two scenarios: slotted secondary network and non-slotted secondary network. It can also be discussed how to control SUs' access behaviour such that the normal communication of PUs can be guaranteed. Finally, simulation results can be shown to verify the effectiveness of the analysis.

8. Currently, the radio spectrum is beginning to be crowded due to the rapid growth of wireless technologies this century. However, many studies show that the major licensed bands, such as those allocated for television broadcasting, amateur radio, paging, etc. are underutilized and some of the remaining bands are heavily used. This fact leads to spectrum wastage. Therefore, new techniques are needed to take advantage of the spectrum opportunities causing a reasonable level of interference in the licensed bands. Hence, CR has become an important research topic in these last years since it tries to take advantage of the unused spectrum by the licensed users. In addition to spectrum sensing algorithms, sharing protocols, policies, among other things, the interference management has become an important topic in CR in order to manage and fulfil the regulatory constraints. The management of interference is, unquestionably, required to treat and quantify all the interference produced by the unlicensed users at the licensed receivers. In order to manage this interference, the secondary users must be able to adjust their parameters to fulfil these constraints. An overview of CR and interference management can be presented. Several quantitative and performance criteria can be studied as well, in order to illustrate the effect that the different parameters produce on the interference in the licensed bands.

References

[1] J. Mitola III and G. Q. Maguire Jr, "Cognitive radio: making software radios more personal," *Personal Communications, IEEE*, vol. 6, no. 4, pp. 13–18, 1999.

[2] S. Brandes, I. Cosovic, and M. Schnell, "Reduction of out-of-band radiation in OFDM systems by insertion of cancellation carriers," *IEEE communications letters*, vol. 10, no. 6, pp. 420–422, 2006.

[3] S. Brandes, I. Cosovic, and M. Schnell, "Reduction of out-of-band radiation in OFDM based overlay systems," in *First IEEE International Symposium on New Frontiers in Dynamic Spectrum Access Networks, 2005. DySPAN 2005.*, 2005, pp. 662–665.

[4] S. Pagadarai, R. Rajbanshi, A. M. Wyglinski, and G. J. Minden, "Sidelobe suppression for OFDM-based cognitive radios using constellation expansion," in *Wireless Communications and Networking Conference, 2008. WCNC 2008. IEEE*, 2008, pp. 888–893.

[5] A. Selim, I. Macaluso, and L. Doyle, "Efficient sidelobe suppression for OFDM systems using advanced cancellation carriers," in *Communications (ICC), 2013 IEEE International Conference on*, 2013, pp. 4687–4692.

[6] F. R. B. Lopes and J. S. G. Panaro, "OFDM sidelobe suppression combining active and null cancellation carriers in the guard bands," in *Microwave & Optoelectronics Conference (IMOC), 2013 SBMO/IEEE MTT-S International*, 2013, pp. 1–5.

[7] M. A. McHenry and D. McCloskey, "Spectrum Occupancy Measurements: Chicago, Illinois, November 16-18, 2005. Shared Spectrum Company," Technical report, RPRT, 2005.

[8] T. Erpek, K. Steadman, and D. Jones, "Spectrum occupancy measurements: Dublin, Ireland," April 16-18, 2007. Technical Report, Shared Spectrum Company Nov 2007. Available at: http://www. sharedspectrum. com, RPRT, 2007.

[9] T. A. Weiss and F. K. Jondral, "Spectrum pooling: an innovative strategy for the

enhancement of spectrum efficiency," *IEEE Communications Magazine*, vol. 42, no. 3, pp. S8-14, 2004.

[10] M. Calabrese, "Use it or Share it: Unlocking the Vast Wasteland of Fallow Spectrum," 2011.

[11] J. Zander, "Radio resource management in future wireless networks: requirements and limitations," *IEEE Communications magazine*, vol. 35, no. 8, pp. 30–36, 1997.

[12] E. M. Noam, "Taking the next step beyond spectrum auctions: open spectrum access," *IEEE Communications Magazine*, vol. 33, no. 12, pp. 66–73, 1995.

[13] S. Sengupta and M. Chatterjee, "Designing auction mechanisms for dynamic spectrum access," *Mobile Networks and Applications*, vol. 13, no. 5, pp. 498–515, 2008.

[14] S. P. T. Force, "Spectrum policy task force report et docket no. 02-135," *US Federal Communications Commission*, 2002.

[15] F. C. C. S. P. T. Force, "FCC Report of the Spectrum Efficiency Working Group, November 2002." 2009.

[16] M. H. Rehmani, *Cognitive Radio Sensor Networks: Applications, Architectures, and Challenges: Applications, Architectures, and Challenges*. IGI Global, 2014.

[17] M. Bkassiny, Y. Li, and S. K. Jayaweera, "A survey on machine-learning techniques in cognitive radios," *IEEE Communications Surveys & Tutorials*, vol. 15, no. 3, pp. 1136–1159, 2013.

[18] K. Kumar, A. Prakash, and R. Tripathi, "Spectrum handoff in cognitive radio networks: A classification and comprehensive survey," *Journal of Network and Computer Applications*, vol. 61, pp. 161–188, 2016.

[19] J. Mitola and G. Q. Maguire, "Cognitive radio: making software radios more personal," *IEEE personal communications*, vol. 6, no. 4, pp. 13–18, 1999.

[20] J. Mitola, "Cognitive radio for flexible mobile multimedia communications," in *Mobile*

Multimedia Communications, 1999.(MoMuC'99) 1999 IEEE International Workshop on, 1999, pp. 3–10.

[21] S. Haykin, "Cognitive radio: brain-empowered wireless communications," *IEEE journal on selected areas in communications*, vol. 23, no. 2, pp. 201–220, 2005.

[22] S. Haykin, D. J. Thomson, and J. H. Reed, "Spectrum sensing for cognitive radio," *Proceedings of the IEEE*, vol. 97, no. 5, pp. 849–877, 2009.

[23] E. Axell, G. Leus, E. G. Larsson, and H. V. Poor, "Spectrum sensing for cognitive radio: State-of-the-art and recent advances," *IEEE Signal Processing Magazine*, vol. 29, no. 3, pp. 101–116, 2012.

[24] W. Wang, "Spectrum sensing for cognitive radio," in *2009 Third International Symposium on Intelligent Information Technology Application Workshops*, 2009.

[25] B. Wang and K. J. R. Liu, "Advances in cognitive radio networks: A survey," *IEEE Journal of selected topics in signal processing*, vol. 5, no. 1, pp. 5–23, 2011.

[26] K.-C. Chen, Y.-J. Peng, N. Prasad, Y.-C. Liang, and S. Sun, "Cognitive radio network architecture: part I--general structure," in *Proceedings of the 2nd international conference on Ubiquitous information management and communication*, 2008, pp. 114–119.

[27] K.-C. Chen, Y.-J. Peng, N. Prasad, Y.-C. Liang, and S. Sun, "Cognitive radio network architecture: part II--trusted network layer structure," in *Proceedings of the 2nd international conference on Ubiquitous information management and communication*, 2008, pp. 120–124.

[28] J. Mitola, "Cognitive radio architecture evolution," *Proceedings of the IEEE*, vol. 97, no. 4, pp. 626–641, 2009.

[29] R. W. Chang and R. Gibby, "A theoretical study of performance of an orthogonal multiplexing data transmission scheme," *IEEE Transactions on Communication Technology*, vol. 16, no. 4, pp. 529–540, 1968.

[30] B. Saltzberg, “Performance of an efficient parallel data transmission system,” *IEEE Transactions on Communication Technology*, vol. 15, no. 6, pp. 805–811, 1967.

[31] R. van Nee and R. Prasad, *OFDM for wireless multimedia communications*. Artech House, Inc., 2000.

[32] S. Weinstein and P. Ebert, “Data transmission by frequency-division multiplexing using the discrete Fourier transform,” *IEEE transactions on communication technology*, vol. 19, no. 5, pp. 628–634, 1971.

[33] P. Layer, “specifications: High-speed Physical Layer in the 5GHz Band,” *IEEE Std*, vol. 802, 1999.

[34] J. A. C. Bingham, “Multicarrier modulation for data transmission: An idea whose time has come,” *IEEE Communications magazine*, vol. 28, no. 5, pp. 5–14, 1990.

[35] I. Recommendation, “G. 992.1: Asymmetric digital subscriber line (ADSL) transceivers,” *ITU-T, June*, 1999.

[36] I. ITU-T, “Recommendation G. 992.1: Asymmetric Digital Subscriber Line (ADSL) Transceivers.” July, 1999.

[37] B. Farhang-Boroujeny and R. Kempter, “Multicarrier communication techniques for spectrum sensing and communication in cognitive radios,” *IEEE Communications Magazine*, vol. 46, no. 4, pp. 80–85, 2008.

[38] I. Budiarjo, H. Nikookar, and L. P. Ligthart, “Cognitive radio modulation techniques,” *IEEE Signal Processing Magazine,* vol. 25, no. 6, pp. 24–34, 2008.

[39] J. G. Proakis and M. Salehi, *Salehi Digital Communications*. New York, NY: McGraw-Hill, 2008.

[40] A. Goldsmith, *Wireless communications*. Cambridge university press, 2005.

[41] D. Cabric and R. W. Brodersen, “Physical layer design issues unique to cognitive radio systems,” in *2005 IEEE 16th International Symposium on Personal, Indoor and Mobile*

Radio Communications, 2005, vol. 2, pp. 759–763.

[42] H. Tang, "Some physical layer issues of wide-band cognitive radio systems," in *First IEEE International Symposium on New Frontiers in Dynamic Spectrum Access Networks, 2005. DySPAN 2005.*, 2005, pp. 151–159.

[43] U. Berthold, F. K. Jondral, S. Brandes, and M. Schnell, "OFDM-based overlay systems: A promising approach for enhancing spectral efficiency [Topics in radio communications]," *IEEE Communications Magazine*, vol. 45, no. 12, pp. 52–58, 2007.

[44] Y. Zhang and C. Leung, "Resource allocation for non-real-time services in OFDM-based cognitive radio systems," *IEEE Communications Letters*, vol. 13, no. 1, pp. 16–18, 2009.

[45] T. A. Weiss, "A diversity approach for the detection of idle spectral resources in spectrum pooling systems," in *Proc. of 48th International Scientific Colloquium, Sept. 2003*, 2003.

[46] J. Hillenbrand, T. A. Weiss, and F. K. Jondral, "Calculation of detection and false alarm probabilities in spectrum pooling systems," *IEEE Communications letters*, vol. 9, no. 4, pp. 349–351, 2005.

[47] U. Berthold and F. K. Jondral, "Guidelines for designing OFDM overlay systems," in *First IEEE International Symposium on New Frontiers in Dynamic Spectrum Access Networks, 2005. DySPAN 2005.*, 2005, pp. 626–629.

[48] A. Vahlin and N. Holte, "Optimal finite duration pulses for OFDM," *IEEE Transactions on Communications*, vol. 44, no. 1, pp. 10–14, 1996.

[49] H. Nikookar and R. Prasad, "Optimal waveform design for multicarrier transmission through a multipath channel," in *Vehicular Technology Conference, 1997, IEEE 47th*, 1997, vol. 3, pp. 1812–1816.

[50] J. Luo, W. Keusgen, and A. Kortke, "Optimization of time domain windowing and guardband size for cellular OFDM systems," in *Vehicular Technology Conference, 2008. VTC 2008-Fall. IEEE 68th*, 2008, pp. 1–5.

[51] T. Weiss, J. Hillenbrand, A. Krohn, and F. K. Jondral, “Mutual interference in OFDM-based spectrum pooling systems,” in *Vehicular Technology Conference, 2004. VTC 2004-Spring. 2004 IEEE 59th*, 2004, vol. 4, pp. 1873–1877.

[52] M. S. El-Saadany, A. F. Shalash, and M. Abdallah, “Revisiting active cancellation carriers for shaping the spectrum of OFDM-based cognitive radios,” in *Sarnoff Symposium, 2009. SARNOFF’09. IEEE*, 2009, pp. 1–5.

[53] M. Gudmundson and P.-O. Anderson, “Adjacent channel interference in an OFDM system,” in *Vehicular Technology Conference, 1996. Mobile Technology for the Human Race., IEEE 46th*, 1996, vol. 2, pp. 918–922.

[54] H. Nikookar and R. Prasad, “Waveshaping of multicarrier signal for data transmission over wireless channels,” in *Universal Personal Communications Record, 1997. Conference Record., 1997 IEEE 6th International Conference on*, 1997, pp. 173–177.

[55] A. Sahin and H. Arslan, “Edge windowing for OFDM based systems,” *Communications Letters, IEEE*, vol. 15, no. 11, pp. 1208–1211, 2011.

[56] H. A. Mahmoud and H. Arslan, “Sidelobe suppression in OFDM-based spectrum sharing systems using adaptive symbol transition,” *IEEE Communications Letters*, vol. 12, no. 2, pp. 133–135, 2008.

[57] H. Yamaguchi, “Active interference cancellation technique for MB-OFDM cognitive radio,” in *Microwave Conference, 2004. 34th European*, 2004, vol. 2, pp. 1105–1108.

[58] Z. Wang, D. Qu, T. Jiang, and Y. He, “Spectral sculpting for OFDM based opportunistic spectrum access by extended active interference cancellation,” in *Global Telecommunications Conference, 2008. IEEE GLOBECOM 2008. IEEE*, 2008, pp. 1–5.

[59] D. Qu, Z. Wang, and T. Jiang, “Extended active interference cancellation for sidelobe suppression in cognitive radio OFDM systems with cyclic prefix,” *Vehicular Technology, IEEE Transactions on*, vol. 59, no. 4, pp. 1689–1695, 2010.

[60] I. Cosovic, S. Brandes, and M. Schnell, “Subcarrier weighting: a method for sidelobe

suppression in OFDM systems," *IEEE Communications Letters,* vol. 10, no. 6, pp. 444–446, 2006.

[61] A. Selim and L. Doyle, "Real-time sidelobe suppression for OFDM systems using advanced subcarrier weighting," in *Wireless Communications and Networking Conference (WCNC), 2013 IEEE*, 2013, pp. 4043–4047.

[62] I. Cosovic and T. Mazzoni, "Suppression of sidelobes in OFDM systems by multiple-choice sequences," *European transactions on telecommunications,* vol. 17, no. 6, pp. 623–630, 2006.

[63] D. Li, X. Dai, and H. Zhang, "Sidelobe suppression in NC-OFDM systems using constellation adjustment," *IEEE Communications Letters,* vol. 13, no. 5, pp. 327–329, 2009.

[64] A. Selim, B. Ozgul, and L. Doyle, "Efficient sidelobe suppression for OFDM systems with peak-to-average power ratio reduction," in *Dynamic Spectrum Access Networks (DYSPAN), 2012 IEEE International Symposium on*, 2012, pp. 510–516.

[65] S. Brandes, I. Cosovic, and M. Schnell, "Sidelobe suppression in OFDM systems by insertion of cancellation carriers," in *Vehicular Technology Conference, 2005. VTC-2005-Fall. 2005 IEEE 62nd,* 2005, vol. 1, pp. 152–156.

[66] S. Pagadarai, A. M. Wyglinski, and R. Rajbanshi, "A sub-optimal sidelobe suppression technique for OFDM-based cognitive radios," in *Military Communications Conference, 2008. MILCOM 2008. IEEE,* 2008, pp. 1–6.

[67] Z. Yuan, S. Pagadarai, and A. M. Wyglinski, "Cancellation carrier technique using genetic algorithm for OFDM sidelobe suppression," in *Military Communications Conference, 2008. MILCOM 2008. IEEE*, 2008, pp. 1–5.

[68] M. Ma, X. Huang, B. Jiao, and Y. J. Guo, "Optimal orthogonal precoding for power leakage suppression in DFT-based systems," *IEEE Transactions on Communications,* vol. 59, no. 3, pp. 844–853, 2011.

[69] X. Zhou, G. Y. Li, and G. Sun, "Multiuser spectral precoding for OFDM-based cognitive

radio systems," *IEEE Journal on Selected Areas in Communications*, vol. 31, no. 3, pp. 345–352, 2013.

[70] X. Zhou, G. Y. Li, and G. Sun, "Multiuser spectral precoding for ofdm-based cognitive radios," in *Global Telecommunications Conference (GLOBECOM 2011), 2011 IEEE*, 2011, pp. 1–5.

[71] R. Xu and M. Chen, "A precoding scheme for DFT-based OFDM to suppress sidelobes," *IEEE Communications Letters*, vol. 13, no. 10, pp. 776–778, 2009.

[72] J. van de Beek, "Orthogonal multiplexing in a subspace of frequency well-localized signals," *IEEE Communications Letters*, vol. 14, no. 10, pp. 882–884, 2010.

[73] J. Van De Beek and F. Berggren, "N-continuous ofdm," *IEEE Communications Letters*, vol. 13, no. 1, pp. 1–3, 2009.

[74] J. Van De Beek, "Sculpting the multicarrier spectrum: a novel projection precoder," *IEEE Communications Letters*, vol. 13, no. 12, pp. 881–883, 2009.

[75] A. Pandey, P. Muneer, and S. M. Sameer, "Two level precoding scheme for out of band radiation reduction in multiuser OFDM based cognitive radio," in *2014 International Conference on Signal Processing and Communications (SPCOM)*, 2014, pp. 1–5.

[76] Z. You, J. Fang, and I.-T. Lu, "Combination of spectral and SVD precodings for out-of-band leakage suppression," in *Systems, Applications and Technology Conference (LISAT), 2013 IEEE Long Island*, 2013, pp. 1–6.

[77] D. B. Fogel and L. J. Fogel, "Using evolutionary programming to schedule tasks on a suite of heterogeneous computers," *Computers & Operations Research*, vol. 23, no. 6, pp. 527–534, 1996.

[78] P. J. Angeline, G. M. Saunders, and J. B. Pollack, "An evolutionary algorithm that constructs recurrent neural networks," *IEEE transactions on Neural Networks*, vol. 5, no. 1, pp. 54–65, 1994.

[79] S. B. Haffner and A. V Sebald, “Computer-aided design of fuzzy HVAC controllers using evolutionary programming,” in *Proc. 2nd Annu. Conf. on Evolutionary Programming*, 1993, pp. 98–107.

[80] D. Dasgupta and Z. Michalewicz, *Evolutionary algorithms in engineering applications*. Springer Science & Business Media, 2013.

[81] M. C. Bhuvaneswari, *Application of Evolutionary Algorithms for Multi-objective Optimization in VLSI and Embedded Systems*. Springer, 2015.

[82] G. G. Pascual, R. E. Lopez-Herrejon, M. Pinto, L. Fuentes, and A. Egyed, “Applying multiobjective evolutionary algorithms to dynamic software product lines for reconfiguring mobile applications,” *Journal of Systems and Software*, vol. 103, pp. 392–411, 2015.

[83] H.-P. Schwefel, “Evolution and optimum seeking. Sixth-generation computer technology series.” Wiley, New York, 1995.

[84] M. Pelikan, “NK landscapes, problem difficulty, and hybrid evolutionary algorithms,” in *Proceedings of the 12th annual conference on Genetic and evolutionary computation*, 2010, pp. 665–672.

[85] C. Blum and A. Roli, “Hybrid metaheuristics: an introduction,” in *Hybrid Metaheuristics*, Springer, 2008, pp. 1–30.

[86] D. S. Touretzky, J. L. Elman, and T. J. Sejnowski, *Connectionist models: proceedings of the 1990 summer school*. Morgan Kaufmann, 2014.

[87] D. B. Fogel, “The Advantages of Evolutionary Computation.,” in *BCEC*, 1997, pp. 1–11.

[88] J. Reed, R. Toombs, and N. A. Barricelli, “Simulation of biological evolution and machine learning: I. Selection of self-reproducing numeric patterns by data processing machines, effects of hereditary control, mutation type and crossing,” *Journal of theoretical biology*, vol. 17, no. 3, pp. 319–342, 1967.

[89] A. E. Eiben and J. E. Smith, *Introduction to evolutionary computing*, vol. 53. Springer,

2003.

[90] D. Ashlock, *Evolutionary computation for modeling and optimization*. Springer Science & Business Media, 2006.

[91] J. Hollad, *Adaptation in Natural and Artificial Systems*. University of Michigan Press, 1995.

[92] J. H. Holland, *Adaptation in natural and artificial systems: an introductory analysis with applications to biology, control, and artificial intelligence.* U Michigan Press, 1975.

[93] D. B. Fogel, *Evolutionary computation: the fossil record*. Wiley-IEEE Press, 1998.

[94] J. B. Grimbleby, "Hybrid genetic algorithms for analogue network synthesis," in *Proceedings of the 1999 Congress on Evolutionary Computation-CEC99*, 1999, vol. 3, pp. 1781–1787.

[95] U. Maulik, "Analysis of gene microarray data in a soft computing framework," *Applied Soft Computing*, vol. 11, no. 6, pp. 4152–4160, 2011.

[96] L. M. O. Queiroz and C. Lyra, "Adaptive hybrid genetic algorithm for technical loss reduction in distribution networks under variable demands," *IEEE Transactions on Power Systems*, vol. 24, no. 1, pp. 445–453, 2009.

[97] B. Addad, S. Amari, and J.-J. Lesage, "Genetic algorithms for delays evaluation in networked automation systems," *Engineering Applications of Artificial Intelligence*, vol. 24, no. 3, pp. 485–490, 2011.

[98] P. Aarabi, "Genetic sensor selection enhanced independent component analysis and its applications to speech recognition," in *Proceedings of the 5th IEEE Workshop on Nonlinear Signal and Information Processing*, 2001.

[99] F. Zaman, I. M. Qureshi, A. Naveed, J. A. Khan, and R. M. Asif Zahoor, "Amplitude and directional of arrival estimation: comparison between different techniques," *Progress in Electromagnetics Research B*, vol. 39, pp. 319–335, 2012.

[100] F. Zaman, I. M. Qureshi, A. Naveed, and Z. U. Khan, "Joint estimation of amplitude,

direction of arrival and range of near field sources using memetic computing," *Progress in Electromagnetics Research C*, vol. 31, pp. 199–213, 2012.

[101] S. U. Khan, I. M. Qureshi, F. Zaman, and A. Naveed, "Null placement and sidelobe suppression in failed array using symmetrical element failure technique and hybrid heuristic computation," *Progress in Electromagnetics Research B*, vol. 52, pp. 165–184, 2013.

[102] C. Blum and X. Li, "Swarm intelligence in optimization," in *Swarm Intelligence*, Springer, 2008, pp. 43–85.

[103] M. Beekman, G. A. Sword, and S. J. Simpson, "Biological foundations of swarm intelligence," in *Swarm intelligence*, Springer, 2008, pp. 3–41.

[104] G. Beni and J. Wang, "Swarm intelligence in cellular robotic systems," in *Robots and Biological Systems: Towards a New Bionics?*, Springer, 1993, pp. 703–712.

[105] X.-S. Yang, *Nature-inspired metaheuristic algorithms*. Luniver press, 2010.

[106] M. A. Zaman and A. Matin, "Nonuniformly spaced linear antenna array design using firefly algorithm," *International Journal of Microwave Science and Technology*, vol. 2012, 2012.

[107] A. Chatterjee, G. K. Mahanti, and A. Chatterjee, "Design of a fully digital controlled reconfigurable switched beam concentric ring array antenna using firefly and particle swarm optimization algorithm," *Progress In Electromagnetics Research B*, vol. 36, pp. 113–131, 2012.

[108] B. Basu and G. K. Mahanti, "Fire fly and artificial bees colony algorithm for synthesis of scanned and broadside linear array antenna," *Progress In Electromagnetics Research B*, vol. 32, pp. 169–190, 2011.

[109] H. Banati and M. Bajaj, "Fire fly based feature selection approach," *IJCSI International Journal of Computer Science Issues*, vol. 8, no. 4, 2011.

[110] S. Kazemzadeh Azad, "Optimum design of structures using an improved firefly algorithm," *Iran University of Science & Technology*, vol. 1, no. 2, pp. 327–340, 2011.

[111] A. H. Gandomi, X.-S. Yang, S. Talatahari, and A. H. Alavi, “Firefly algorithm with chaos,” *Communications in Nonlinear Science and Numerical Simulation*, vol. 18, no. 1, pp. 89–98, 2013.

[112] J. Senthilnath, S. N. Omkar, and V. Mani, “Clustering using firefly algorithm: performance study,” *Swarm and Evolutionary Computation*, vol. 1, no. 3, pp. 164–171, 2011.

[113] S. U. Khan, I. M. Qureshi, F. Zaman, A. Basit, and W. Khan, “Application of firefly algorithm to fault finding in linear arrays antenna,” *World Applied Sciences Journal*, vol. 26, no. 2, pp. 232–238, 2013.

[114] X.-S. Yang, “Firefly algorithm, stochastic test functions and design optimisation,” *International Journal of Bio-Inspired Computation*, vol. 2, no. 2, pp. 78–84, 2010.

[115] M. Sayadi, R. Ramezanian, and N. Ghaffari-Nasab, “A discrete firefly meta-heuristic with local search for makespan minimization in permutation flow shop scheduling problems,” *International Journal of Industrial Engineering Computations*, vol. 1, no. 1, pp. 1–10, 2010.

[116] M.-H. Horng, “Vector quantization using the firefly algorithm for image compression,” *Expert Systems with Applications*, vol. 39, no. 1, pp. 1078–1091, 2012.

[117] M.-H. Horng, Y.-X. Lee, M.-C. Lee, and R.-J. Liou, “Firefly metaheuristic algorithm for training the radial basis function network for data classification and disease diagnosis,” *Theory and new applications of swarm intelligence*, vol. 4, no. 7, pp. 115–132, 2012.

[118] T. Hassanzadeh, H. Vojodi, and A. M. E. Moghadam, “An image segmentation approach based on maximum variance intra-cluster method and firefly algorithm,” in *Natural computation (icnc), 2011 seventh international conference on*, 2011, vol. 3, pp. 1817–1821.

[119] T. Apostolopoulos and A. Vlachos, “Application of the firefly algorithm for solving the economic emissions load dispatch problem,” *International Journal of Combinatorics*, vol. 2011, 2010.

[120] X.-S. Yang, “Firefly algorithms for multimodal optimization,” in *International Symposium on Stochastic Algorithms*, 2009, pp. 169–178.

[121] R. Storn and K. Price, “Differential evolution–a simple and efficient heuristic for global optimization over continuous spaces,” *Journal of global optimization*, vol. 11, no. 4, pp. 341–359, 1997.

[122] K. Price, R. M. Storn, and J. A. Lampinen, *Differential evolution: a practical approach to global optimization*. Springer Science & Business Media, 2006.

[123] Y. A. Sheikh, F. Zaman, I. M. Qureshi, and M. Atique-ur-Rehman, “Amplitude and direction of arrival estimation using differential evolution,” in *Emerging Technologies (ICET), 2012 International Conference on*, 2012, pp. 1–4.

[124] R. Joshi and A. C. Sanderson, “Minimal representation multisensor fusion using differential evolution,” *IEEE Transactions on Systems, Man, and Cybernetics-Part A: Systems and Humans*, vol. 29, no. 1, pp. 63–76, 1999.

[125] S. Das and A. Konar, “Two-dimensional IIR filter design with modern search heuristics: A comparative study,” *International Journal of Computational Intelligence and Applications*, vol. 6, no. 3, pp. 329–355, 2006.

[126] C. M. C. Roque, P. Martins, A. J. M. Ferreira, and R. M. N. Jorge, “Differential evolution for free vibration optimization of functionally graded nano beams,” *Composite Structures*, 2016.

[127] F. Lezama, G. Castañón, A. M. Sarmiento, and I. B. Martins, “Differential evolution optimization applied to the routing and spectrum allocation problem in flexgrid optical networks,” *Photonic Network Communications*, vol. 31, no. 1, pp. 129–146, 2016.

[128] E. N. Dragoi and S. Curteanu, “The use of differential evolution algorithm for solving chemical engineering problems,” *Reviews in Chemical Engineering*, vol. 32, no. 2, pp. 149–180, 2016.

[129] M. Prauzek, P. Krömer, J. Rodway, and P. Musilek, “Differential evolution of fuzzy controller for environmentally-powered wireless sensors,” *Applied Soft Computing*, vol. 48, pp. 193–206, 2016.

[130] L. J. Fogel, “Autonomous automata,” *Industrial Research*, vol. 4, no. 2, pp. 14–19, 1962.

[131] I. Zelinka and J. Lampinen, “On stagnation of the differential evolution algorithm,” in *Proceedings of Mendel, 6th International Mendel Conference on Soft Computing*, 2000.

[132] X.-S. Yang and S. Deb, “Cuckoo search via Lévy flights,” in *Nature & Biologically Inspired Computing, 2009. NaBIC 2009. World Congress on*, 2009, pp. 210–214.

[133] M. Kumar and T. K. Rawat, “Optimal design of FIR fractional order differentiator using cuckoo search algorithm,” *Expert Systems with Applications*, vol. 42, no. 7, pp. 3433–3449, 2015.

[134] V. Stojanovic, N. Nedic, D. Prsic, L. Dubonjic, and V. Djordjevic, “Application of cuckoo search algorithm to constrained control problem of a parallel robot platform,” *The International Journal of Advanced Manufacturing Technology*, pp. 1–11, 2016.

[135] X.-S. Yang and S. Deb, “Cuckoo Search for Optimization and Computational Intelligence,” 2015.

[136] N. J. Navimipour and F. S. Milani, “Task scheduling in the cloud computing based on the cuckoo search algorithm,” *International Journal of Modeling and Optimization*, vol. 5, no. 1, p. 44, 2015.

[137] S. U. Khan, I. M. Qureshi, B. Shoaib, and A. Basit, “Correction of faulty pattern using cuckoo search algorithm and symmetrical element failure technique along with distance adjustment between the antenna array,” in *2015 12th International Bhurban Conference on Applied Sciences and Technology (IBCAST)*, 2015, pp. 633–636.

[138] R. B. Payne, M. D. Sorenson, and K. Klitz, “The cuckoos, vol. 15.” Oxford University Press, Oxford, 2005.

[139] C. T. Brown, L. S. Liebovitch, and R. Glendon, “Lévy flights in Dobe Ju/’hoansi foraging patterns,” *Human Ecology*, vol. 35, no. 1, pp. 129–138, 2007.

[140] I. Pavlyukevich, “Lévy flights, non-local search and simulated annealing,” *Journal of*

Computational Physics, vol. 226, no. 2, pp. 1830–1844, 2007.

[141] A. M. Reynolds and M. A. Frye, “Free-flight odor tracking in Drosophila is consistent with an optimal intermittent scale-free search,” *PloS one*, vol. 2, no. 4, p. e354, 2007.

[142] L. Flights, “Related Topics in Physics, edited by MF Shlesinger, GM Zaslavsky, and U. Frisch,” *Lecture Notes in Physics (Springer-Verlag, Berlin, 1995)*, 1995.

[143] M. F. Shlesinger, “Mathematical physics: Search research,” *Nature*, vol. 443, no. 7109, pp. 281–282, 2006.

[144] P. Barthelemy, J. Bertolotti, and D. S. Wiersma, “A Lévy flight for light,” *Nature*, vol. 453, no. 7194, pp. 495–498, 2008.